Oxidative DNA damage following *in vivo* exposure to Benzo(a)pyrene in the testis, lung and liver of wild type and Ogg1-deficient mice

Silje Lied

Master thesis in Toxicology

Department of Toxicology and Ecophysiology

Institute of Biology

UNIVERSITETET I OSLO

August 2010

Acknowledgements

Jeg velger å skrive dette på norsk, siden det føles mer personlig og alle som skal takkes kan lese norsk.

Arbeidet er gjort ved avdeling for Kjemikalietoksikologi, divisjonen er Miljø Medisin, ved Nasjonalt Folkehelseinstitutt, Oslo. Mine hovedveiledere har vært Ann-Karin Olsen PhD og Nur Duale PhD, ved siden av disse har også Gunnar Brunborg PhD vært veileder. Som veileder på Universitetet i Oslo har jeg hatt professor Steinar Øvrebø PhD fra avdelingen Toksikologi og Økotofysiologi på Biologis Institutt.

Jeg vil gi aller størst takk til Ann-Karin Olsen og Nur Duale for all hjelpen disse to årene. Ann-Karin Olsen du har presset og inspirert meg til å jobbe og gjøre mitt beste hele tiden, Nur Duale du har alltid tatt seg tid til meg og alle mine spørsmål og problemer uansett hvor travel du har vært. Tusen takk begge to!

Takk til Gunnar Brunborg for at jeg fikk komme og gjøre denne oppgaven hos deg, og takk for tilbakemeldinger og råd underveis.

Jeg vil også takke alle medarbeidere på MIKT for to fine år, dere har tatt godt vare på meg. Da vil jeg spesielt takke Anne Graupner for å være min sol på tunge dager og for passe på at jeg jobber med det jeg skal. Jeg vil også takke Daniel Minh Pham for hjelp med laboratoriearbeid da mine to armer ikke strakk til.

Også mange mange takk til mannen min Hans Øyvind Lied for all støtte og hjelp med annet praktisk arbeid sånn at jeg har hatt mulighet og tid til å fullføre denne oppgaven. Jeg hadde ikke klart dette uten deg!

Table of contents

Abstract

In the industrial communities of today there is reason for concern for the reproductive health of the male, due to decreasing sperm quality and increased incidences of testicular cancer. Norway and Denmark have the highest incidence rates of testicular cancer in the world. There has traditionally been more focus on the maternal contribution for infertility and defects on the offspring compared to the paternal contribution. The genetic constitution of the offspring depends on the integrity of both the paternal (sperm) and the maternal (oocyte) genomes. When the integrity of the paternal genome is challenged it may lead to serious conditions; Oxidative damage in human sperm correlates with poor sperm quality and reduced fecundity (ability to conceive children). Couples undergoing assisted fertilisation have lower success rates when the father is a smoker, and there is epidemiological data suggesting that children of smoking fathers have a higher risk of developing cancer. One component of cigarette smoke, Benzo(a)pyrene (BaP), induce bulky DNA adducts and also is believed to cause oxidised base damage through generation of reactive oxygen species (ROS).

BaP is a polycyclic aromatic hydrocarbon (PAH) that has been studied extensively. PAHs are an ubiquitous class of environmental contaminants. We are exposed to PAHs on a daily basis from food, burning of fossil fuels, forest fire, tobacco smoke and diesel exhaust. This exposure to humans qualifies for extensive studies to achieve a good understanding of the possible negative effects on humans.

BaP-exposure leads to induction of DNA damage that may be removed via DNA repair. We have previously shown that human testicular cells exhibit poor repair of oxidative damage such as 8-oxoG, compared to rodents. We, and others, have also shown that male germ cells exhibit a low NER function for several bulky DNA adducts, including BPDE-adducts. These findings indicate that male germ cells, particularly human, may be particularly sensitive for exposure to certain environmental agents and that care should be taken in extrapolating results from rodents to man. The use of repair deficient mice, such as *Ogg1*$^{-/-}$ mice, thus mimics the repair capacity of human male germ cells and allows more relevant analyses of the possible genotoxic effects of environmental agents.

In this study a small increase in oxidative damage was observed in the testis at Day 31 following BaP-exposure of *Ogg1*$^{-/-}$ mice. The increased levels of oxidative damage were most evident in haploid round spermatids. Oxidative damage was also induced in the somatic tissues investigated in *Ogg1*$^{-/-}$ mice; at Day 31 a small increase was observed in the liver whereas in the lung a more pronounced induction was detected, with increases at both Day 17 and Day 31 after exposure. No increases in oxidative damage were observed in *Ogg1*$^{+/+}$ mice in any of the tissues investigated. NADP/NADPH-ratios declined following BaP-exposure in line with the DNA damage levels observed. The expression of *Cyp1a1* and *Akr1a4* was studied, with induction of *Cyp1a1* at Day 1 following exposure in all tissues examined of both genotypes. The constitutive expression of *Akr1a4* was significantly higher than *Cyp1a1* in all the tissues. *Akr1a4* was induced following BaP-exposure in the testis at Day 17 in *Ogg1*$^{+/+}$ mice whereas the induction on the lung was more apparent, it occurred in both genotypes and took place at earlier time points following BaP-exposure. The decline in NADP/NADPH-ratios and expression levels of *Cyp1a1* and *Akr1a4* correspond well with the oxidative DNA damage levels observed.

We conclude that exposure to BaP *in vivo* do induce oxidative damage. We provide solid evidence for its induction on the lung whereas the indications that oxidative damage is induced in male germ cells or in the liver are still unresolved.

Abbreviations

8-oxoG	7,8-dihydro-8-oxodeoxyguanosine
AhR	Aryl hydrocarbon receptor
AhRR	Aryl hydrocarbon receptor repressor
Akr	Aldo-keto reductase
AP sites	Apurinic/apyrimidinic sites
ARNT	AhR nuclear translocator
BaP	Benzo(a)pyrene
BER	Base excision repair
BK	Best Keeper
BPDE	7,8-dihydro-9,10-epoxy-7,8,9,10tetrahydrobenzo(a)pyrene
BSA	Bovine Serum albumin
CP	Crossing point
CSA and CSB	Cockayne syndrome factors A and B
CT	Cycle treshold
CTL	Control (untreated)
Cyp	Cytochrome P450
dH2O	Distilled water
DMSO	Dimethyl sulphoxide
DNA	Deoxyribonucleic acid
ds	Double stranded
E.coli	Escherichia coli
EDTA	Ethylenediaminetetraacetic acid
ERCC1	Excision repair cross complementing group 1 protein
FEN1	Flap endonuclease
Fpg	Formamidopyrimidine-DNA glycosylase
Fpg-ss	Formamidpyrimidine-DNA glycosylase-sensitive site
G	Guanine
GGR	Global genome repair
HAP1	Human AP endonuclease 1
hHR23B	Human homologue of yeast RAD23B
HKG	Housekeeping gene
i.p.	Intraperitoneal
KO	Knock out
LD50	Lethald dose (50%)
LigI	DNA ligase I
LigIII	DNA ligase III
miRNA	MicroRNA
MIQUE	Minimum Information for Publication of Quantitative Real-Time PCR Experiments
NADP	Nicotinamide adenine dinucleotide phosphate
NADPH	Nicotinamide adenine dinucleotide phosphate
NER	Nucleotide excision repair
NTP	Non template control
OD	Optical Density
Ogg1	8-oxoguanine-DNA glycosylase

PAH	Polycyclic aromatic hydrocarbon
PBS	Phosphate buffer solution
PCNA	Proliferating cell nuclear antigen
PCR	Polymerase chain reaction
Polβ	DNA polymerase beta
Polδ/ε	DNA polymerase delta/epsilon
Polδ-ε	DNA polymerase δ-ε
RFC	Replication factor C
RNA	Ribonucleic acid
RNA pol II	RNA polymerase II
ROS	Reactive oxygen species
RPA	Replication protein A
RT	Reverse transcription
RT-PCR	Real time polymerase chain reaction
RDML	Real-Time PCR Data Markup Language
SD	Standard deviation
SE	Standard error
ss	Single stranded
T 1/2	Half life time
TCDD	2,3,7,8 –tetrakloridbenzo-para-dioxin
TCR	Trancription-coupled repair
TFIIH	General transcription factor IIH
WT	Wild type
XPA-G	Xeroderma pigmentosum complementation group A-G
XRCC1	X-ray cross complementing protein 1
XRE	Xenobiotic response element

1. Introduction

1.1 General background

Today in the industrial world there is reason for concern about the male reproductive health since the sperm count and quality is declining and the incidence of testicular cancer is increasing (Moline *et al.*, 2000). Men in Norway and Denmark have the highest incidence rates of testicular cancer in the world (Adami *et al.*, 1994; Jacobsen *et al.*, 2006; Richiardi *et al.*, 2004). Traditionally there has been more focus on the maternal than the paternal genome with respect to their contribution to infertility, early embryo loss and defects on the offspring. The genetic constitution of the offspring depends on the integrity of the genomes of both the sperm cell and the egg DNA (Olsen *et al.*, 2005). In USA approximately 15% (2008) of couples experience some difficulties to conceive, and in roughly 50% of the infertile couples, the male factor is partially responsible for the failure to conceive (Jarow and Zirkin 2005). Men that smoke have lower success rates in assisted reproduction procedures (Zitzmann *et al.*, 2003). Sperm from smokers exhibit more DNA damaged compared to sperm from non-smokers (Sipinen *et al.*, 2010).

In this thesis we have investigated effects of in vivo exposure to a mutagenic compound that humans are exposed on a daily basis: Benzo(a)pyrene (BaP). BaP is a ubiquitous polycyclic aromatic hydrocarbon (PAH). Epidemiological studies have shown that paternal exposure to PAHs increase the risk of childhood cancer in their offspring (Boffetta *et al.*, 2000; Cordier *et al.*, 1997; Lee *et al.*, 2009). The main area of research in our laboratory is male reproductive toxicology hence the main focus in this thesis will be on effects on male germ cells. Selected somatic tissues (liver and lung) are studied for comparison due to their role in BaP metabolism (liver, Chapter 1.3), and since they are target organs for BaP-mediated carcinogenesis (lung).

In a previous study (denoted: Study 1) we had indications of a small, but statistically significant increase in oxidative DNA lesions in male germ cells following *in vivo* exposure to BaP of mice lacking the repair enzyme 8-oxoguanine-DNA glycosylase (*Ogg1*;(Meier 2008)). Scientific research is based on the ability to reproduce results by using different

methods, reiterating experiments, using new personal or alternative laboratories. The increased level of oxidative damage observed in the previous study (Study 1;(Meier2008)) was based on a limited number of experimental animals and the induction was significant but marginal. In the current study we include a higher number of mice to have more robust data; other somatic tissues are studied, as well as new relevant endpoints.

1.1.1 Aims

The main aim is to determine whether exposure to environmental mutagens *in vivo* compromises the DNA integrity of male germ cells. We use a mouse model to mimic the reduced repair capacity of oxidative purines characteristic of humans (Olsen *et al.,* 2003), i.e. a mouse line deficient in an enzyme involved in the repair of oxidative DNA damage (*Ogg1*$^{-/-}$) and its concurrent wild type (*Ogg1*$^{+/+}$). Moreover, besides mimicking the repair capacity of human male germ cells, oxidative DNA damage will accumulate in every tissue of the *Ogg1*$^{-/-}$ model making it possible to clarify the role of oxidative DNA damage following exposure to BaP. Special focus is on elucidating the possible effects of BaP-exposure on the genotoxic effects in male germ cells.

Our aims are:

1) Reproduce a previous experiment, Study 1;(Meier2008).

2) Investigate whether *in vivo* exposure of *Ogg1*$^{-/-}$ and *Ogg1*$^{+/+}$ mice to BaP leads to induction of oxidative damage in the testis, liver and lung.

3) Establish the presence of NADPH and investigate the temporal change in NADP/NADPH-rates in the testis, liver and lung of *Ogg1*$^{-/-}$ and *Ogg1*$^{+/+}$ mice after exposure to BaP to explore the potential for generating reactive oxygen species (ROS) due to futile redox reactions during BaP-metabolism.

4) Investigate the temporal expression patterns of central genes involved in BaP-metabolism (*Cyp1a1* and *Akr1a4*) in the testis, liver and lung of *Ogg1*$^{-/-}$ and *Ogg1*$^{+/+}$ mice following BaP-exposure *in vivo*.

1.2 Benzo(a)pyrene

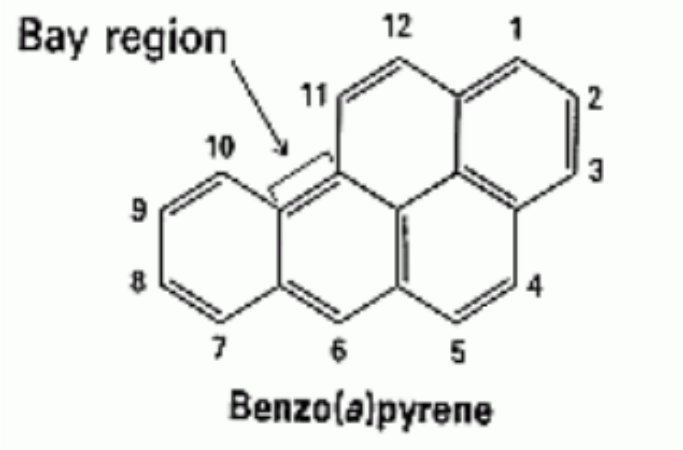

Figure 1.1 Benzo(a)pyrene. The chemical structure of BaP, numbered by the UPAC system, showing the sterically hindered bay region.

BaP is a PAH that has been extensively studied (Casarett *et al.*, 2008). PAHs constitute a ubiquitous class of environmental contaminants. They enter the environment through several routes, including burning of fossil fuels, forest fire, tobacco smoke and diesel exhaust. PAHs can also be found in high levels in charcoal broiled food. The major route of exposure for humans are inhalation, consumption of contaminated food and water (Ramesh *et al.*, 2004). PAHs are carcinogenic and mutagenic, BaP is categorised as an IARC group 1 (carcinogenic to humans), it was previously categorised in group 2B (possibly carcinogenic to humans), but recently (actually still in progress) it has been upgraded "*based on mechanistic and other relevant data*" (IARC 2010). In addition to this, PAHs have also been found to be potent immunosuppressant's (Casarett *et al.*, 2008). One of the most studied PAHs is BaP. We want to study BaP, because humans are exposed to it on almost a daily base (3 mg/day in USA, according to Environmental Protection Agency, (Stedeford *et al.*, 2001)) through several routs of exposure (air/food) and *in vitro* studies have shown that BaP generates ROS which leads to oxidative damage to DNA (Briede *et al.*, 2004; Gallagher *et al.*, 1993; Park *et al.*, 2008b; Park *et al.*, 2006b; Penning *et al.*, 1996).

Tobacco smoke is an important source of exposure to BaP. Levels of 11 ng of BaP per cigarette were found in mainstream smoke and 103 ng per cigarette in side stream smoke have been reported (WHO 1998). For smokers this is a significant contribution to the exposure to BaP. There has also been found high amount of DNA damage in sperm from

smokers (Sipinen *et al.*, 2010; Zenzes *et al.*, 1999a), and there are evidences of transmission of DNA adducts from spermatozoa to embryos (Zenzes *et al.*, 1999b).

1.2.1 Metabolism

When xenobiotica enter a cell the metabolism has evolved to detoxify and eliminate the xenobiotica. BaP, and all other PAHs, is hydrophobic and through metabolism the hydrophilic property of the xenobiotic is elevated and excretion is thereby facilitated. In general, metabolic conversions of xenobiotica either detoxify or activate the xenobiotica. BaP is activated to its ultimate carcinogen metabolite, 7,8-dihydro-9,10-epoxy-7,8,9,10tetrahydrobenzo(a)pyrene (BPDE), by metabolism.

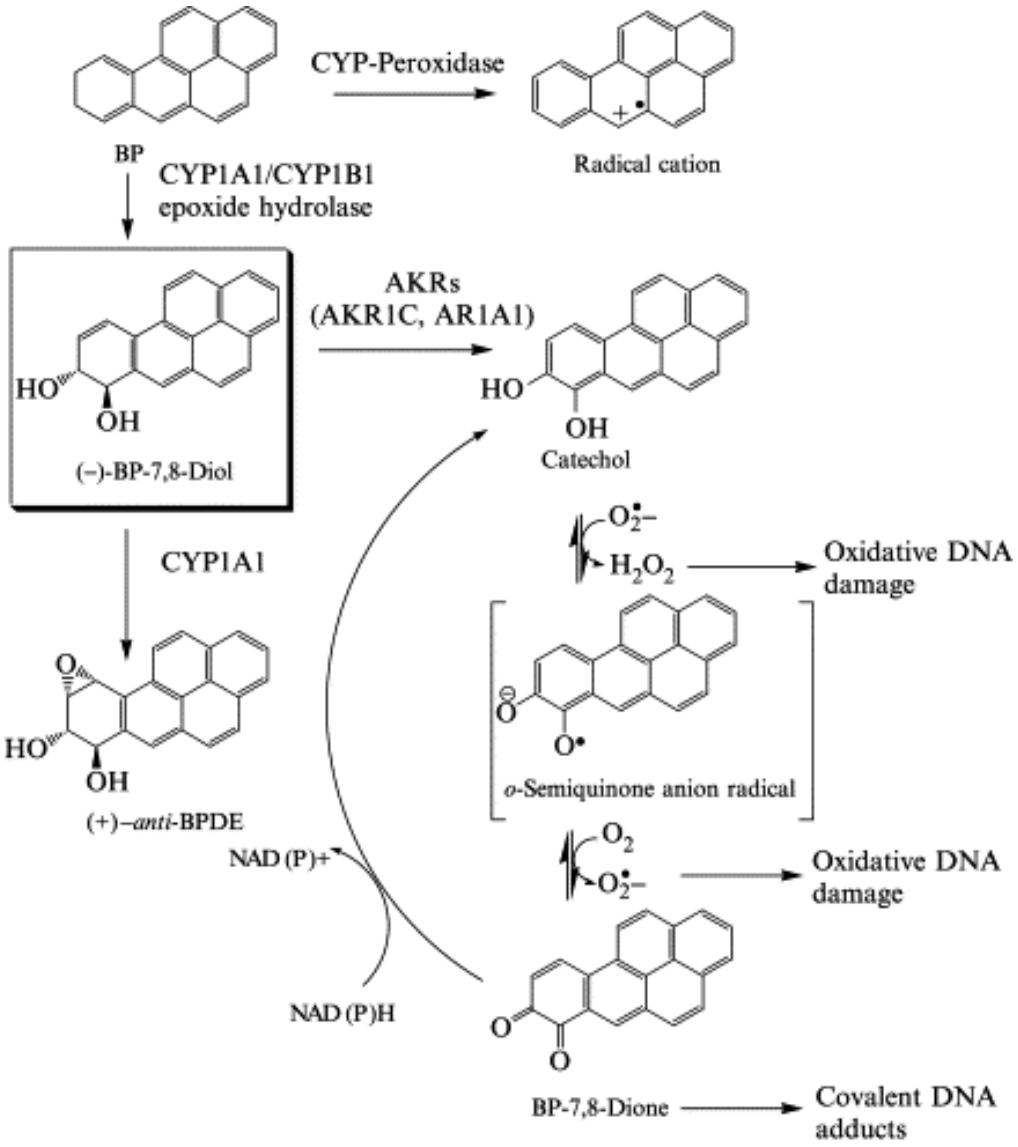

Figure 1.2: The metabolism of BaP (Penning 2004). Detailed information is presented in the text.

Metabolism of BaP, and other PAHs, occurs in most tissues, and through several pathways. The ultimate carcinogen is a diol epoxide of BaP (BPDE). BPDE is formed by three consecutive enzymatic reactions (Casarett *et al.*, 2008; Sims *et al.*, 1974), and arises through one of the three major activation routes (Figure 1.2; (Penning2004)). The metabolic activation to BPDE represents a minor pathway, suggested by Leadon et al. (1988) who found the amount of total indirect damage induced exposure to BaP greatly exceeds that of total direct adduct formation, and these adducts are efficiently removed by the nucleotide excision repair (NER) (Chapter 1.2.3.1) pathway. Indirect damage to DNA via the generation of ROS may occur through another pathway, producing quinones (Leadon *et al.*, 1988; Stedeford *et al.*, 2001).

A BaP radical cation is formed via one route by the peroxidase activity of Cytochrome P450 superfamily (Cyp), a one electron mediated oxidation. This BaP-radical have potential to induce DNA adducts, but it is probably not long-lived enough to cause DNA damage in living cells (Cavalieri and Rogan 1995).

In the other two routes BaP is first converted into BaP-7,8-oxide by *CYP1A1*/*CYP1B1*, which is further metabolized by epoxide hydrolase to yield a *trans*-dihydrodiol ((-)-BaP-7,8-diol) (Penning2004). Only (-)-BaP-7,8-diol is formed *in vivo* (Gelboin 1980) and it is the substrate for two further subpathways for BaP metabolism. The (-)-BP-7,8-diol may undergo a second epoxidation by *CYP1A1*, *-1A2* or *-1B1* to yield 7,8-dihydroxy-9,10-epoxy-7,8,9,10-tetrahydroBaP ((+)-anti-BPDE), that readily forms adducts with DNA (mainly (+)-*anti*-BPDE-N^2-dGuo adducts) (Xue and Warshawsky 2005). The epoxide is located at the sterically hindered bay region of BaP where epoxide hydrolase does not easily react. Alternatively (-)-BP-7,8-diol may undergo a $NADP^+$-dependent oxidation catalyzed by enzymes in the aldo-keto reductase (*Akr*) superfamily, via a catechol and an *o*-semiquinone anion radical to yield the corresponding reactive and redox-active *o*-quinone (BaP-7,8-dione) (Penning2004). This *o*-quinone can then either undergo a reduction in the presence of a reducing cofactor, such as NADPH, back to catechol, or form covalent DNA adducts. Each time the catechol is reformed it may be reoxidised by molecular oxygen to form reactive oxygen species (ROS) like superoxid anion (O_2^-), hydroxyl radical (OH) and hydrogen peroxidase (H_2O_2) until it is fully oxidised to *o*-quinone. This may establish a futile redox

cycle that generates ROS. In the absence of redox-cycling conditions, such as the presence of NADPH and $CuCl_2$, less ROS-mediated oxidative damage will occur (Park *et al.*, 2006a). ROS may oxidise the bases in DNA and one major lesion formed is the product of oxidised guanines, 8-oxoG. During BaP-metabolism aryl hydrocarbon receptor (AhR) facilitates damage to DNA formed by PAH *o*-quinones by acting as a carrier of quinones into the nucleus and concentrating them there, where they can form oxidative DNA damage in the form of DNA strand breaks or lesions like 8-oxoG (Park *et al.*, 2009).

1.2.2 DNA damage

DNA in human cells is subject to approximately 20,000 lesions every day due to normal metabolism alone. These lesions arise from endogenous and environmental agents which attack cellular DNA. For endogenous factors DNA is susceptible to temperature, pH, chemical compounds, oxidation, deaminations, spontaneous hydrolysis and to errors introduced during replication. Examples of environmental factors are ionising irradiation, UV irradiation, chemical agents, cross-linking agents, intercalating agents and electrophilic reactants. There are several types of DNA damage, single- and double strand breaks, cross-links (both between bases in the DNA and between bases and proteins), damage to the sugar-phosphate backbone, and chemical alterations of DNA bases or covalent binding of metabolites to the DNA bases, also called DNA adducts (Casarett *et al.*, 2008). In this thesis the focus is on oxidative DNA base alterations induced by ROS.

1.2.2.1 Oxidative DNA damage

ROS is a major source of oxidative damage. The most common ROS are superoxide anion (O_2^-), hydroxyl radical (OH) and hydrogen peroxidase (H_2O_2). ROS react with DNA but also with other macromolecules such as proteins and lipids. The major intracellular source of ROS is electron leakage from the cellular respiration process in the mitochondria. Peroxisomal metabolism, lipid peroxidation and enzymatic synthesis of nitric oxide also contribute. Extracellular sources that can lead to ROS include ionising and near-UV radiation, heat, various drugs and redox cycling compounds, as well as inflammation caused by various endogenous and environmental agents (Casarett *et al.*, 2008).

One of the major oxidative lesion in the genome is the mutagenic 8-oxoG (figure 1.3) (Hsu *et al.*, 2004). All bases can be oxidised, but guanine has the lowest redox potential and is therefore the most prone to be oxidised (Kovacic and Wakelin 2001). When the DNA polymerases encounter an 8-oxoG during replication adenine is frequently misincorporated instead of cytosine (figure 1.3). This results in a guanine to thymine (G to T) transversion mutation, which is a commonly observed somatic mutation associated with cancer (Hsu *et al.*, 2004). In lung cancer the pattern of mutations in *p53* are predominantly G to T transformations (Holstein *et al.* 1991).

Numerous approaches and attempts have been made to quantify intracellular levels of 8-oxoG (De Iuliis *et al.*, 2009; Devi *et al.*, 2008; Gallagher *et al.*, 1993; Mangal *et al.*, 2009; Park *et al.*, 2009; Penning *et al.*, 1996; Quinn and Penning 2008; Rosenquist *et al.*, 1997; Stedeford *et al.*, 2001; Zenzes *et al.*, 1999a).The estimations have reported levels of 8-oxoG with at least 10 times differences according to the different methods used. The challenge is that DNA is readily oxidised and the methods used themselves generate 8-oxoG (Gedik and Collins 2005). Anyhow, estimations using the comet assay have suggested background levels of 8-oxoG in normal human cells as approximately one per 10^6 guanine (Collins 2005; Gedik and Collins2005).

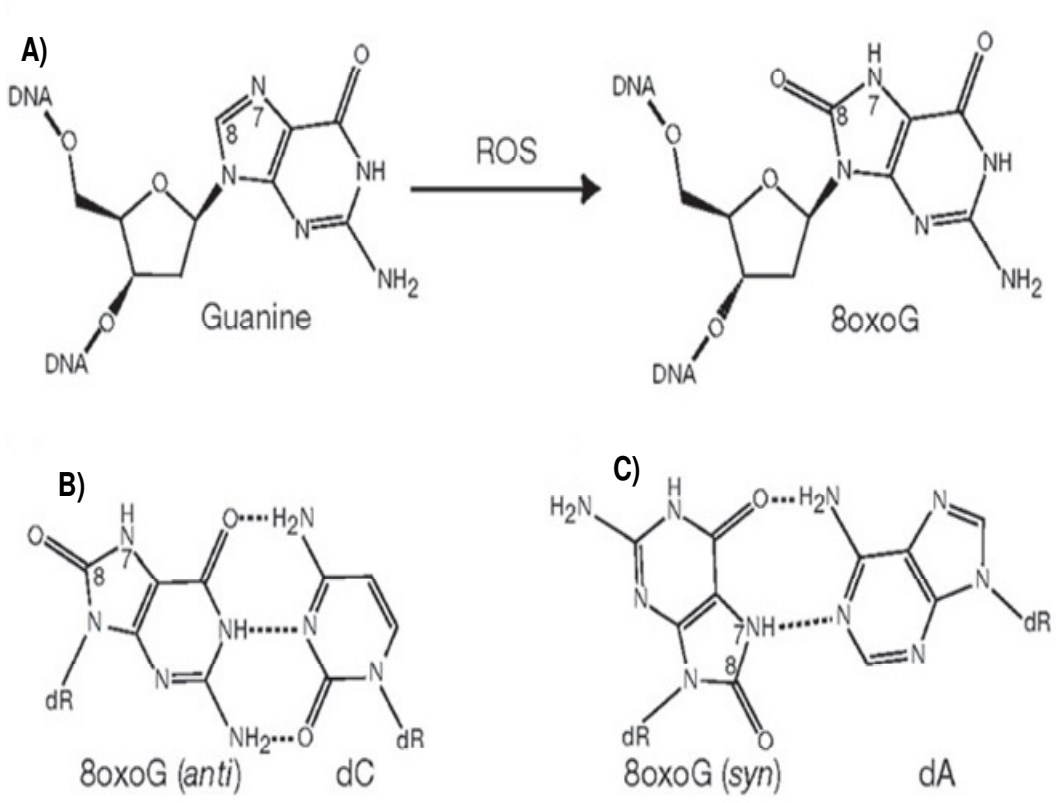

Figure 1.3: Base pairing properties of 8-oxoG. **A**) Oxidation of guanine to 8-oxoG at C8-position by ROS. **B**) 8-oxoG base paired with cytosine, the normal *anti* conformation form a stable Watson-Crick base pair with three hydrogen bonds. **C**) 8-oxoG base pared with adenine in the *syn* conformation forming a stable Hogsteen mispair with two hydrogen bonds. Figure from Hsu et al. (2004).

1.2.3 Repair

There are several ways to defend a cell against damage to the DNA. First, there are agents that directly prevent damage to the DNA, such as detoxifying peptides, protein or antioxidants. Second, there are repair mechanisms that remove and replace DNA lesions. Third, cells might enter cell cycle-arrest, to repair damage and stop replication of damaged template. And finally, when the cells exhibit extensive DNA damage they may be eliminated by apoptosis, to prevent accumulation of mutations (Olsen *et al.*, 2005).

Chemically modified DNA bases, or DNA adducts are typically removed via excision repair (Casarett *et al.*, 2008). There are two major pathways of excision repair; nucleotide excision repair (NER) and base excision repair (BER)(Olsen *et al.*, 2005).

1.2.3.1 Nucleotide excision repair (NER)

NER (Figure 1.4) is believed to be the most relevant repair mechanism for bulky DNA adducts, such as BPDE-DNA adducts (Rechkunova and Lavrik 2010). Defects in repair genes involved in NER are associated with very high cancer risk (Cleaver 1989).

As depicted in figure 1.4 the DNA adducts are first recognized and verified followed by incision on both sides of the adducted DNA strand. *De novo* DNA synthesis occurs replacing the excised DNA strand followed by DNA ligation (Rechkunova and Lavrik2010). Two subpathways exist; global genomic repair (GGR), which repair the entire genome, and transcription-coupled repair (TCR) that removes DNA lesions that block RNA synthesis in actively transcribed genes. In total 25 or more proteins are involved in NER. GGR is initiated by binding of XPC-hHR23B to disrupted base pairs. During TCR, lesions that block the RNA polymerase are detected, and the polymerase is displaced, making the DNA lesion accessible for repair; this requires at least two TCR-specific factors: Cockayne syndrome factors (CSA and CSB). A multi-protein complex that includes the two helicases xeroderma pigmentosum complementation group B and D (XPB and XPD) unwinds about 30 base pairs surrounding the DNA lesion. The subsequent steps of GGR and TCR are believed to be identical. GGR is also found to be able to repair oxidative DNA damage, like 8-oxoG (Osterod *et al.*, 2002; Sunesen *et al.*, 2002). This might be the backup repair mechanism in *Ogg1* deficient mice, but this pathway may not be functional in humans which have impaired NER capacity in the testis (Brunborg *et al.*, 1995; Olsen *et al.*, 2003).

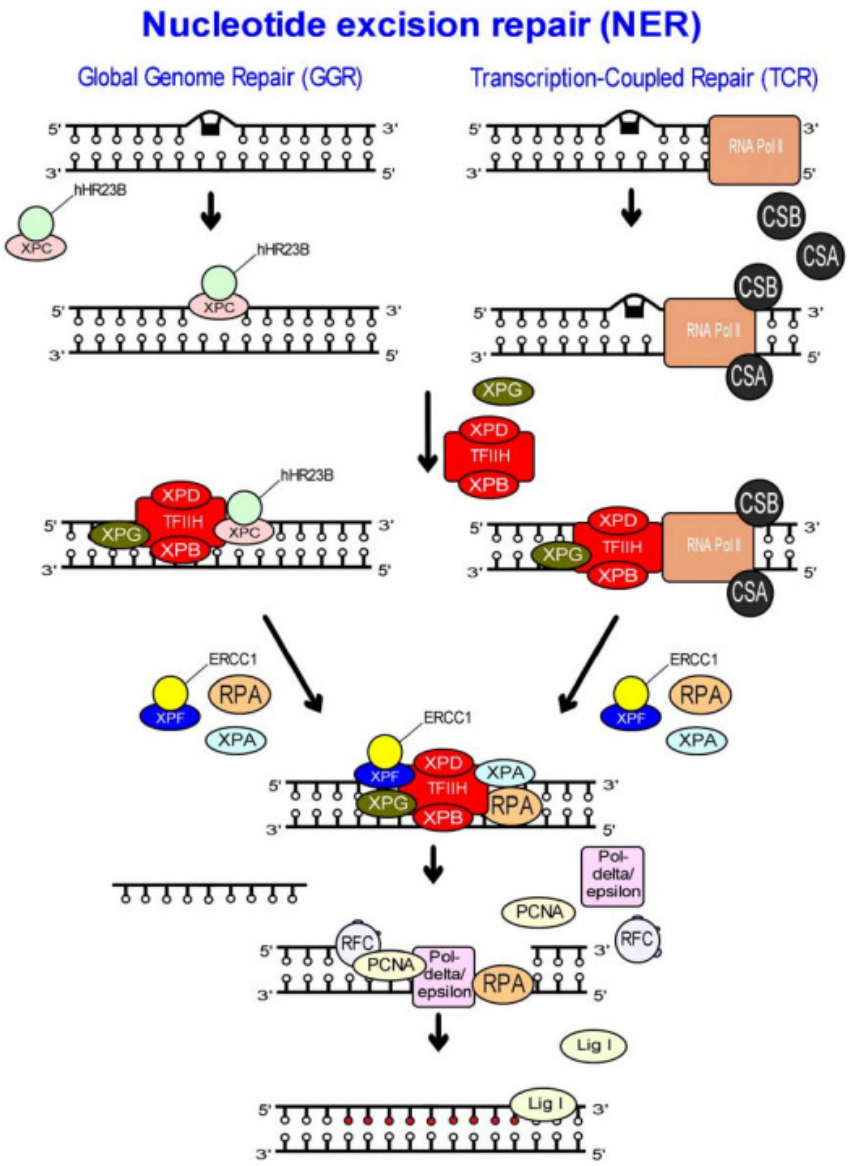

Figure 1.4: The NER pathway, for repair of bulky DNA adducts. See text for description of the pathway. Abbreviations: XPA-G, xeroderma pigmentosum complementation group A-G; hHR23B, human homologue of yeast RAD23B; RNA pol II, RNA polymerase II; CSA and CSB, Cocayne syndrome factors A and B; TFIIH, general transcription factor IIH; ERCC1, excision repair cross complementing group 1 protein; RPA, replication protein A; PCNA proliferating cell nuclear antigen; RFC, replication factor C; Polδ/ε, DNA polymerase delta/epsilon; Lig1, DNA ligase 1. Figure from (Olsen *et al.*, 2005).

1.2.3.2 Base excision repair (BER)

The major pathway for repairing aberrant DNA bases induced by endogenous and exogenous agents is BER (Figure 1.5), including ROS-induced DNA lesions like 8-oxoG (Klungland and Bjelland 2007). As first reported by Thomas Lindahl in 1974 (Lindahl 1974), BER is initiated by the release of an altered base by a DNA glycosylase via hydrolytic cleavage of

the N-C1' glycosylic bond between the base and deoxyribose, forming a baseless apurinic/apyrimidinic (AP) site. Each DNA glycosylase recognises a specific set of aberrant DNA bases, and recognise and excise aberrant bases without requiring that the lesions cause major structural change in DNA (Olsen *et al.*, 2005). The excision of the base generates apurinic/apyrimidinic sites (AP-sites) followed by endonuclease cleavage, re-synthesis and DNA ligation. Similar to NER, BER probably remove lesions that inhibit transcription, such as 8-oxoG, partly using the same enzymes as in NER-TCR (Olsen *et al.*, 2005).

There are mono-functional and bi-functional DNA glycosylases; the mono-functional DNA glycosylases only removes the damaged base, whereas bi-functional DNA glycosylases cleaves the AP sites. In mammalian, eleven different DNA glycosylases are described and we will have the focus on those who remove oxidative DNA lesions: Human MutY homologue (MYH), which removes adenine basepaired with 8-oxoG; Thymine glycol-DNA glycosylase 1 (NTH1), which removes oxidised pyrimidines and 2,6-diamino-4-hydroxy-5-formamidopyrimidine (FaPyG) lesions; Nei-like protein (NEIL1 and NEIL2), which removes 8-oxoG, oxidised pyrimidines, FaPyG and FaPyA; and the main DNA glycosylase in eukaryotes for removal of 8-oxoG is 8-oxoguanine-DNA glycosylase (Ogg1), which removes 8-oxoG basepaired with C, and FaPyG lesions creating an AP site (Aburatani *et al.*, 1997; Lu *et al.*, 1997; Radicella *et al.*, 1997; Rosenquist *et al.*, 1997). In humans the OGG1 is located on the short arm of chromosome 3, a region which is commonly deleted in cancers (Lu *et al.*, 1997). Ogg1 is a bifunctional enzyme and is extremely specific: it is able to remove 8-oxoG basepaired with C and therefore has to distinguish between 8-oxoG and the vast majority of normal bases (Klungland and Bjelland2007).

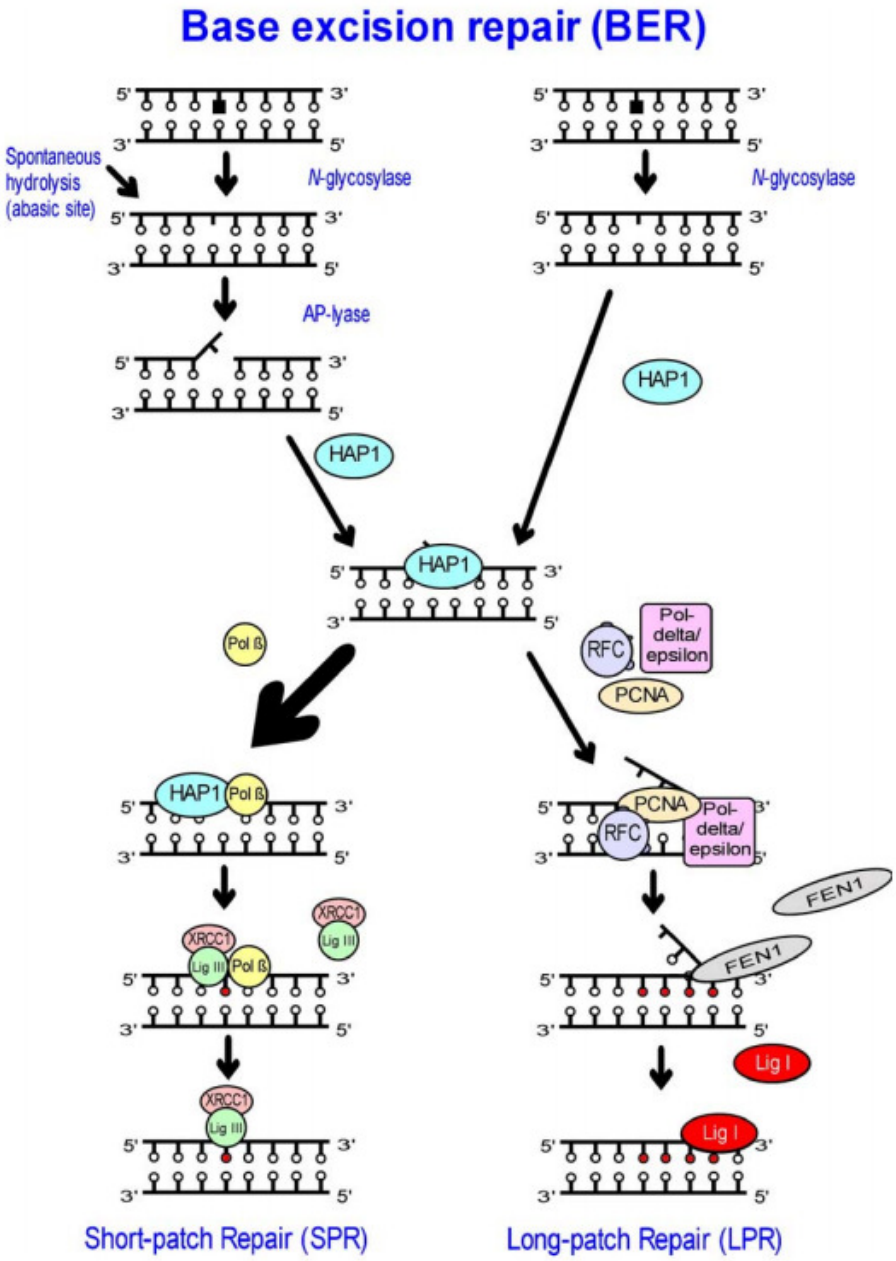

Figure 1.5: The BER pathway. See explanation in the text. Abbreviations: HAP1, human AP endonuclease 1; Polβ, DNA polymerase beta; XRCC1, X-ray cross complementing protein 1; LigIII, DNA ligase III; PCNA, proliferating cell nuclear antigen; RFC, replication factor C; Polδ-ε, DNA polymerase δ-ε; FEN1, Flap endonuclease; Lig1, DNA ligase 1. The figure is modified by Olsen et al. (2005) from (Ide and Kotera 2004).

Relevant to this thesis is the observation of limited repair of 8-oxoG in human testicular cells compared to efficient repair in rodent spermatogenic cells (Olsen *et al.*, 2003; Olsen *et al.*, 2005). A very high level of *Ogg1* mRNA is reported in mouse testis mRNA (Rosenquist *et al.*, 1997), whereas in human tissues, including the testis OGG1 mRNA is ubiquitously expresses and the expression in testis varies markedly between individuals, in conclusion the

human germ cells may be more sensitive than rodents to DNA oxidation (Olsen *et al.*, 2005). This is one of the major reasons why *Ogg1*$^{-/-}$ mice are used as a model in this work. Moreover the activity of *Ogg1* has been reported to be inhibited in protein extracts from lung tissue of rats after an acute treatment to BaP (Stedeford *et al.*, 2001).

Formamidopyrimidine-DNA glycosylase (Fpg, from *E. coli*) is a bacterial DNA glycosylase that recognise oxidative DNA damage, such as 8-oxoG, the bacterial homologue to OGG1. It is a bifunctional DNA glycosylase cleaving the DNA strand at the site of the DNA damage, and thereby allow the detection of specific DNA lesions in the comet assay (Collins *et al.*, 2008) enhancing the sensitivity of this assay.

1.3 Organs

1.3.1 Testis

In the testicle sperm cells and steroid hormones such as testosterone are produced. The testis is physically enclosed by a capsule (tunica albuginea), and display two major compartments: the intertubular/interstitial compartment and the seminiferous tubule compartment.

The intertubular compartment contains the blood and lymphatic vessels. This is where the Leydig cells are found, which are the major source of androgen, testosterone and other steroids (Russel *et al.*, 1990). There are studies showing that exposure to BaP decrease the level of testosterone (Archibong *et al.*, 2008), and a reduction in testis weight (Archibong *et al.*, 2008; Ramesh *et al.*, 2008). Both studies suggest that exposure to BaP contribute to reduced testicular and spermatogenic functions in rats. Reduced testis weight may also arise due to increased cell death which may occur as a consequence of extensive DNA damage. In this thesis we investigate whether BaP give rise to oxidative damage in testicular cells. BaP induce somatic mutations, and *de novo* germ line mutations in sperm originating from BaP-exposed stem cell spermatogonia (Olsen et al., 2010).

The seminiferous tubules contain the male germ cells and the Sertoli cells, and this is where spermatogenesis takes place (Figure 1.5).

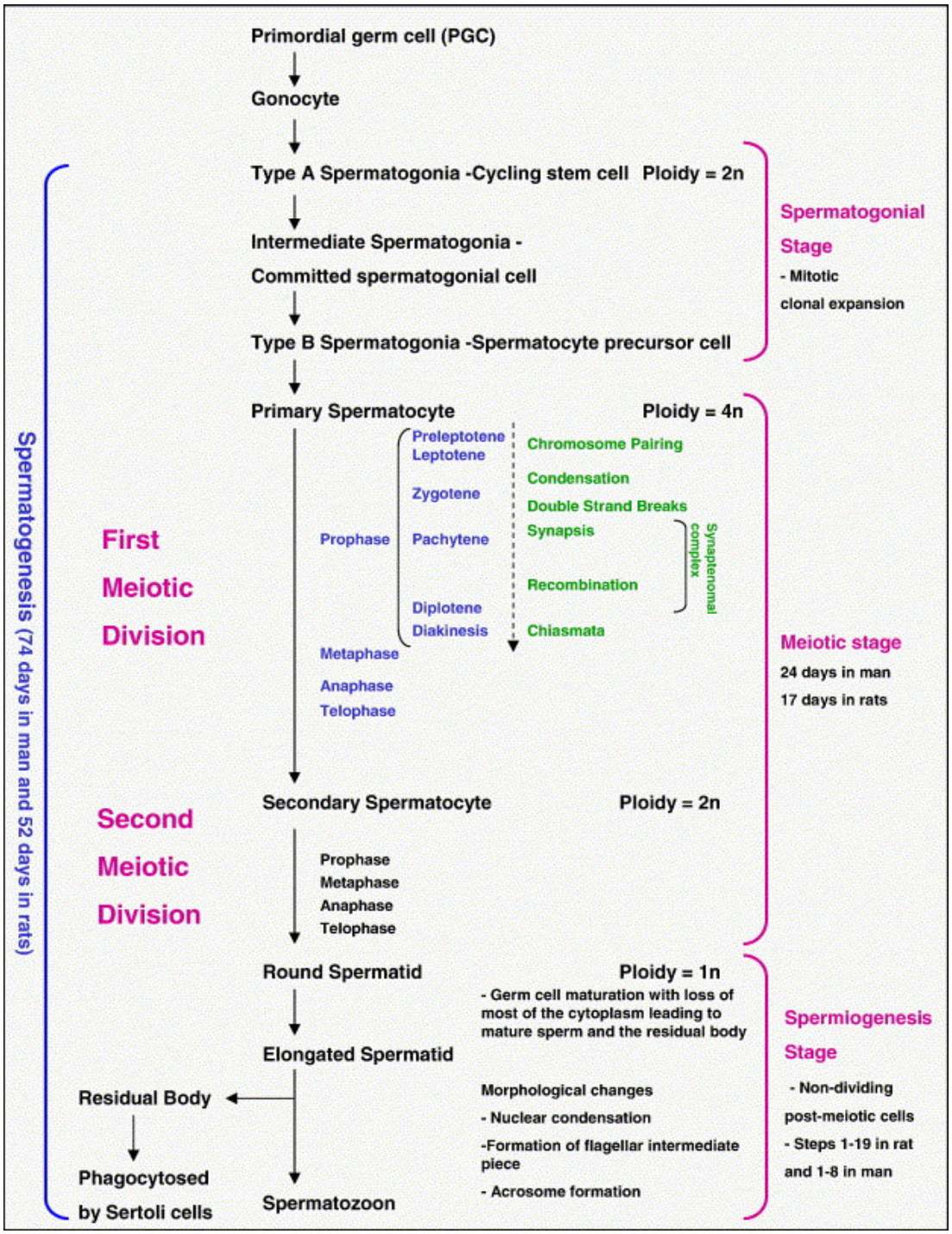

Figure 1.6: Spermatogenesis (Olsen *et al.*, 2005). Spermatogenesis can be divided into three phases; the spermatogonial, the meiotic and the spermiogenesis stages. The spermatogonial phase starts with a division of spermatogonial stem cells into two daughter cells, one of which enter the process of spermatogenesis, while the other remains as a stem cell. This is the period of active replicative DNA synthesis producing different types of spermatogonia. The number of cell divisions varies from with species, but ultimately type B spermatogonia give rise to tetraploid primary spermatocytes. During the first part of the meiotic stage, genetic recombination takes place after which the first reduction division gives rise to secondary diploid spermatocytes, and subsequently the second reduction division results in haploid round spermatids. During spermatogenesis the nuclei are condensed and teh cells transformed into mature spermatozoa (Holstein *et al.*, 2003; Olsen *et al.*, 2005). In mice spermatogenesis lasts 35 days.

The general organisation of the spermatogenesis is essentially the same in all mammals and can be divided into three phases: the spermatogonial phase, the meiotic phase and spermiogenesis (Olsen *et al.*, 2005). The vulnerability for DNA damage change varies with the stage of spermatogenesis and the agent (Adler 1996) Olsen et al., 2001, 2003, 2005, 2010), and BaP related DNA damage are observed at all stages of the spermatogenesis (Olsen *et al.*, 2010; Verhofstad *et al.*, 2010b). DNA repair is deficient in the post-meiotic stages, the spermatids lack DNA repair (NER) and DNA damage persist in the sperm to fertilisation (Jansen et al., 2001)(Olsen *et al.*, 2003; Olsen *et al.*, 2010; Verhofstad *et al.*, 2010b). In the comet assay used extensively in this thesis the majority of the scored cells are round spermatids.

DNA damage in the male germ line has been linked to a variety of adverse clinical effects, including impaired fertility, increased incidence of miscarriage, and enhanced risk of diseases in offspring (Aitken *et al.*, 2009; Aitken and De Iuliis 2010; Zenzes *et al.*, 1999b). Smoking has been shown to induce increased levels of oxidative DNA damage, such as 8-oxoG, in human sperm, abnormal sperm and reduced fecundity (Zenzes *et al.*, 1999a; Zitzmann *et al.*, 2003). The origin of DNA damage could, in principle, involve: abortive apoptosis initiated post meiotically, unresolved strand breaks borne during spermiogenesis or oxidative stress. This has been proposed as the three major mechanisms for the formation of DNA damage in sperm and DNA damage may arise from combinations of all three (Aitken and De Iuliis2010). It is suggested by Aitken et al (2010) that oxidative stress is one of the major contributors to DNA damage in sperm. Mitochondrial DNA is extra vulnerable to free radical attack because it is essentially unprotected, compared to DNA in the nuclei (Sawyer *et al.*, 2001). Sperm nuclear DNA on the other hand is tightly packed with protamines that are further stabilised by inter- and intra-molecular disulphide bonds (Aitken and De Iuliis2010; Sawyer *et al.*, 2001). Even though DNA is tightly packed in the sperm free radicals can attack DNA and form DNA adducts which may ultimately result in DNA strand breaks. 8-oxoG, the major oxidized base damage induced by ROS, is found in high levels in spermatozoa of infertile patients (Kodama *et al.*, 1997). It is also reported that 8-oxoG is highly correlated with DNA strand breaks in human spermatozoa (Aitken and De Iuliis2010).

1.3.2 Liver

The liver maintain the metabolic homeostasis in the body, it extracts ingested nutrients, vitamins, metals, drugs and also environmental toxicants, like PAHs, from the blood for catabolism, storage and/or excretion into the bile (Casarett *et al.*, 2008).

In vitro studies with human hepatoma HepG2 cells showed a statistically significant decreased cell viability and increased catalase activity following BaP exposure (Briede *et al.*, 2004; Park *et al.*, 2006b), finding increased levels of oxidative DNA damage. ROS and PAH may cause oxidative DNA damage and DNA adducts. Park and coworkers observed increased levels of DNA strand breaks using the comet assay following BaP exposure (Park *et al.*, 2006b).

In vivo studies with BaP and liver have also been conducted (Briede *et al.*, 2004; Ramesh *et al.*, 2004; Stedeford *et al.*, 2001). Male rats were exposed to BaP, 20 mg/kg i.p. two times a day for up to five days (Stedeford *et al.*, 2001), and organ specific differences in removal of 8-oxoG were investigated in liver, lung and kidney. The capacity to remove 8-oxoG for the liver, and kidney, remained at baseline for all time points analyzed. *Ogg1* protein levels were also measured in this study, finding that liver has the highest level of *Ogg1* compared to lung (possesses 95% of the level) and kidney (possess 44.5% of the level. The amount of *Ogg1* in the liver was constant at all times measured in this experiment (24hr, 72hr and 120hr). Briede et al. (2004) observed indication of ROS formation but a decrease in 8-oxoG in liver (and lung) of rats after exposure to BaP, suggesting a possible induction of DNA repair mechanism.

DNA damage is thus induced in liver cells *in vitro*, but is such lesions induced after *in vivo* exposure to BaP? The *Ogg1*$^{-/-}$ model is useful to measure a potential accumulation of such DNA damage

1.3.3 Lung

The lung is highly exposed to BaP through pollution from cars and especially tobacco smoke, it is estimated that 85-90% of all lung cancer is observed in individuals that smoke (Edwards *et al.*, 2005). BaP is shown to give rise to oxidative damage in the lungs (Briede *et al.*, 2004), regardless of the route of exposure (Stedeford *et al.*, 2001). Water solubility is a

critical factor determining how deeply a toxicant will penetrate the lungs (Casarett *et al.*, 2008). PAHs are lipophilic compounds and BaP; which is almost insoluble in water, will be able to penetrate deeply into the lung and easily cross membranes and enter the cells. Studies have shown that BaP is rapidly taken up in the lung and transferred into the blood, and also considerable recycled back to the lung (Bevan and Weyand 1988).

The lung also contains most of the enzymes involved in the xenobiotic biotransformation that has been identified in other tissues (Casarett *et al.*, 2008), but the content of CYP in lung tissue is lower compared to other tissues (Casarett *et al.*, 2008) and this may favour the peroxidative pathway (figures 1.2, 1.8) giving rise to increased production of *o*-quinone metabolites. *In vitro* studies have demonstrated that lung tissue has a high capacity to form quinones (Bevan and Weyand1988; Stedeford *et al.*, 2001; Weyand and Bevan 1986). One *in vitro* study found evidence for the involvement of the *Akr* pathway (Figure 1.2, 1.8) in the metabolism of BaP in human lung A549 cells (Park *et al.*, 2008b) confirming that lung cells form quinones from BaP. Studies have shown that submicromloar concentrations of PAH quinones causes G to T transversion in *p53* cDNA, but only when the quinones were allowed to redox in the presence of both NADPH and $CuCl_2$ (Park *et al.*, 2008a). In lung cancer the most unambiguous signature is that the pattern of mutations in *p53* is predominantly G to T transformation (Hollstein *et al.*, 1991; Park *et al.*, 2008a). Oxidative damage in lung cells formed by BaP might therefore very well give rice to mutations on *p53* and cancer, and because of this the lung is also a very important and interesting organ to investigate in this thesis.

1.4 BaP-metabolism genes selected for gene expression studies

1.4.1 Cytochrome P450 (CYP)

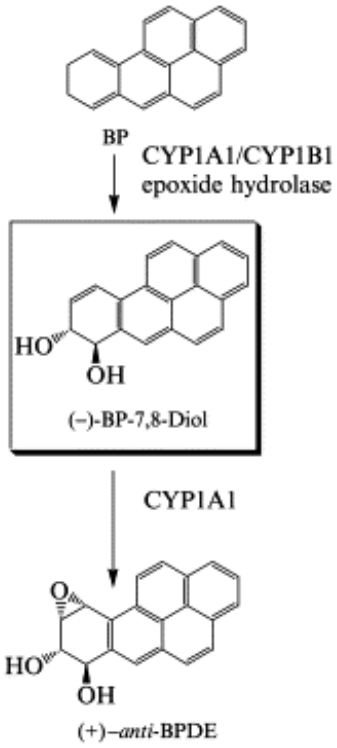

Figure 1.7: The CYP pathway of BaP metabolism, from figure 1.2.

During the metabolism of BaP (Figure 1.7) CYP and especially *Cyp1a1* is important in the activation of BaP, it is a part the first step in the metabolism (Figure 1.2) and it creates BPDE which forms a stable adduct with DNA (Figure 1.7) (Penning *et al.*, 1996).

BaP and its quinone metabolites are relatively potent ligands of the aryl hydrocarbon receptor (AhR). It binds to AhR and translocates into the nucleus in association with the AhR nuclear translocator (ARNT) (Park *et al.*, 2009). The AhR-ARNT heterodimer binds to DNA sequences called Xenobiotic response elements (XRE). This direct binding of the heterodimer to the XRE leads to induction of *Cyp1a1* (Hankinson 2005; Yauk *et al.*, 2010). AhR and ARNT is found to be expressed ubiquitously in adult human tissues, with relatively high levels of both in lung (Yamamoto *et al.*, 2004). Earlier findings in our lab by Håland *et*

al. (Håland 2005) report a higher expression of AhR in testis of mice than liver, a reduction following BaP exposure was also reported. Same reduction has also been reported by (Roman *et al.*, 1998) after exposure to 2,3,7,8 –tetrakloridbenzo-para-dioxin (TCDD), which also is a ligand for AhR. This reduction corresponds with AhR being translocated to cytoplasma and degraded after ligand-binding. In human tissues the level of AhR is reported to be similar in testis and liver, and higher in lung and the level of ARNT to be higher in testis than liver, but even higher in lung tissue (Yamamoto *et al.*, 2004). Yamamoto *et al.* also found an extremely high expression of aryl hydrocarbon receptor repressor (AhRR) in human testis.

Yauk et al. (2010) found a significant increase of the expression of *Cyp1a1* gene in the liver after giving BaP orally to male mice. High levels of mRNA may not necessarily correlate with protein quantity or activity. It has been suggested that members of the CYP superfamily may be regulated by microRNA (miRNA) (Hudder and Novak 2008; Yauk *et al.*, 2010), but Yauk et al. (2010) found in their study that hepatic miRNAs exhibit minimal direct response to AHR agonists.

In this thesis the expression of *Cyp1a1* gene was studied following *in vivo* BaP exposure. In Study 1;(Meier2008), the *Cyp1a1* gene expression was induced in liver and testis following BaP exposure *in vivo*. In the same work other CYP (*Cyp1a2* and *Cyp1b1*) genes were also investigated, however these two genes were only induced in the liver and not in the testis. Besides repeating the previous experiment, the expression of *Cyp1a1* gene upon BaP exposure can be used as positive control in this study.

1.4.2 Aldo-Keto Reductases

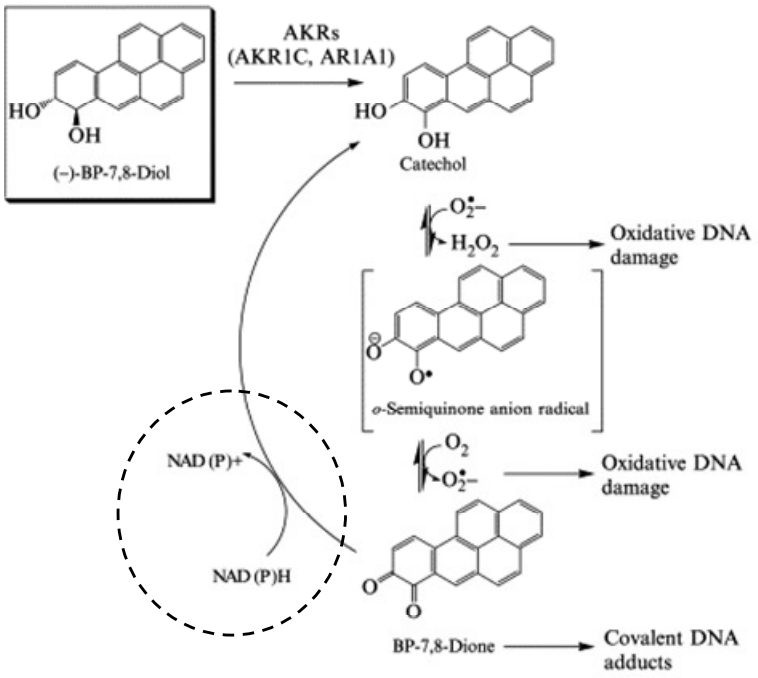

Figure 1.8: The AKR pathway of BaP metabolism, from figure 1.2. NADPH reduces the quinone back to catechol establishing a futile cycle creating ROS.

AKRs are generally monomeric reduced nicotinamide adenine dinucleotide phosphate (NAD(P)H) –linked oxidoreductases. These enzymes convert carbonyl-containing substrates to alcohols; aldehydes to primary alcohols and ketones are converted to secondary alcohols. These enzymes thus play a central role in the metabolism of endogenous substrates, drugs, xenobiotics and carcinogens and are likely to be as important as the CYP superfamily in dealing with toxic insults (Penning2004). Several AKRs have been implicated in carcinogen metabolism: these include the dihydrodiol dehydrogenases that oxidize PAH *trans*-dihydrodiols to reactive and redox-active *o*-quinones, a pathway that creates ROS, relevant for BaP (figure 1.8). Quinones are also ligands for AhR (chapter 1.4.1).

In this thesis we studied the expression of *Akr1a4*, which is one of several AKR enzymes involved in BaP metabolism, following *in vivo* BaP exposure to the mice. *Akr1a4* is the mouse homolog to human AKR1A1, which is present in all tissues examined, including the testis (Barski *et al.*, 1999). AKR1A1 takes part in BaP metabolism (Figure 1.2) (Penning2004). The expression of *Akr1a4* has previously been investigated in Study

1;(Meier2008), observing a modest change in the *Akr1a4* gene expression both in the liver and the testis. The constitutive expression of *Akr1a4* was however high compared to different CYP gene expression.

2. Materials and Methods

All solutions and chemicals used in this study are listed in Appendix A.

2.1 Benzo(a)pyrene

BaP is both toxic and carcinogenic and carful handling is necessary. The dissolving of BaP was done in ventilation cabinets and safety masks and gloves were used.

2.1.1 Dissolving BaP in corn oil

BaP is a lipophilic compound and almost unsolvable in water. Corn oil is commonly used for solving BaP, and has previously been used in our lab.

Procedure:

1.) BaP was weighed in a glass, and corn oil was added. We prepared a stock solution of 7.5 mg BaP/ml corn oil.

2.) The bottle was placed in a shaking water bath at 37˚C, for one hour to dissolve.

3.) The remaining unsolved BaP was solved by using a magnetic stirrer for another hour.

4.) The stock solution (BaP-corn oil) was placed in bottles covered with aluminium foil and stored in a container in a dry, dark and ventilated security cabinet, at room temperature.

2.1.2 Exposing of mice

BaP is dissolved in corn oil and is exposed in the mice by intra peritoneal (i.p.) injection. We used nine to eleven weeks old male mice (Chapter 2.2.1). Injection was according to bodyweight, the mice weighed about 21-25 g and were injected with 0.4-0.5 ml BaP-corn oil, and the dose of BaP was 150 mg BaP/kg bodyweight.

Control mice were treated with corn oil (oil) or not treated at all (CTL).

The mice were kept in separate cages, or cages with mice exposed to the same treatment, until sacrificing hence one, three, five, ten, seventeen and thirty-one days after exposure.

The experiment design is shown in table 2.1, with the number of animals sacrificed at each time point:

Table 2.1: Experiment design.

Mice-genotype	Treatment	Days after expusure 0	1	3	5	10	17	31
$Ogg1^{-/-}$	CTL	6						
	Oil					2	3	1
	BaP		3	3	3	2	3	1
$Ogg1^{+/+}$	CTL	6						
	Oil					2	3	1
	BaP		3	3	3	2	3	1

Showing how many mice were killed at the different days after exposure.

After we had the results from this we added extra animals at 10 days, see more about this in Appendix B.

2.2 Mice

2.2.1 Breeding

Ogg1$^{-/-}$ null mice in a mixed background of C57BL/6 and 129SV were generated by Klungland and co-workers (Klungland *et al.*, 1999) and kindly given to us. The *Ogg1*$^{-/-}$ mice were crossed with Big Blue® C57BL/6 homozygous mice purchased from Stratagene (La Jolla, California, USA). The *Ogg1*$^{-/-}$ mice were backcrossed for 9 generations with Big Blue C57BL/6 mice to achieve isogenic strains with identical background (C57BL/6). Littermate intercrossing of heterozygotes performed maintenance of the mouse line. Homozygotic mice were bred for experiments. The mice used for this study were of generation 4-6 after backcrossing. The genotypes of the mice were identified by conventional PCR genotyping.

Breeding and care were performed at the Norwegian Institute of Public Health, Oslo, Norway. Breeding trios contained one male and two females, the females were from the same litter. Litters were separated after 17 days; males and females were housed separately. The mice were housed in air flow IVC racks (Thoren Maxi-Miser System) or filter cabinets (Scantainer, Scanbur BK AS, Nittedal, Norway) in plastic disposable cages on Nestpack (Datesand Ltd., Manchester, UK) bedding. The room had 12-hour light/dark cycle, 6-10 air changes per hour, controlled humidity (55±5%) and temperature (19-23˚C). Water and diet were given *ad libitum*. The mice were given a breeding/maintenance diet (2018SX Teklad Global 18% Protein Extruded Rodent Diet, Harland Teklad, Madison, Wisconsin, USA). The males used in this study were 9-11 weeks old. Both *Ogg1*$^{-/-}$ Big Blue (OBKO/KO) and *Ogg1*$^{+/+}$ Big Blue (OBWT/WT) male mice were used.

2.2.2 Sacrifice of mice and harvesting of organs

The mice were sacrificed at different times after exposure to BaP. Some mice were sacrificed at day 0, no exposure, and after one, three, five, ten, seventeen and thirty-one days (Figure 2.1).

The mice were sacrificed mostly by breaking the neck or using CO_2. The mice that were sacrificed after 17 days were sacrificed with CO_2, because then you find more blood in the heart and it makes it easier to get more blood. Blood was drawn from the heart, and checked for inflammatory agents. The organs used were liver, lung, testis, cauda and caput. Most of the liver, lung and testis were quickly frozen with dry ice and stored at - 80˚C. One small piece of the liver and half of the lung and testis were used for the comet assay, and other small pieces were used to measure NADPH/NADP.

2.3 Isolation of nuclei.

The method used to isolate nuclei from tissue was developed in our lab by Brunborg (Brunborg *et al.*, 1988). This isolating method is called the squeezing method and was developed for isolating nuclei from tissues as lung, liver, testis, brain and kidney. In order to squeeze the tissue, a small cylindrical tube with a stainless steel screen of 0.4 nm fitted inside is used. First the tissue is cut to small pieces and putted in the tube, and squeezed through the

screen with a modified plastic plunger (similar to the one you use in a syringe). The method is easy and quick, so it is possible to use it for a large scale *in vivo* animal study. Tissue used in this study was fresh, and we used lung, liver and testis. Fresh tissues were taken from only two animals at a time to make the time from sacrificing, squeezing and until cells are moulded in the gel as short as possible.

2.3.1 Procedure

The buffer and tissue were kept on ice. Lung, testis and liver were kept cold on PBS, before putting them in the Merchant buffer.

1.) A small piece of the liver was used, about 0.5 cm in diameters. Half a lung was used; this is needed to get enough cells/nuclei for the comet assay. The testis was taken out of the capsule and one half was squeezed.

2.) The tissue was put in 1 ml Merchant buffer and cut into small pieces.

3.) Then transferred into the squeeze-unit, sometimes we had to add a little bit more Merchant buffer to get all the tissue, and squeezed through the screen by pressing the plunge a couple of times.

4.) The suspension was filtered through a 100 µm nylon filter and centrifuged at 290g for 5min at 4˚C.

5.) The pellet was resuspended in 4 ml Merchant buffer. Pilot studies showed that this gave the right amount of nuclei for the comet assay (about 1.3 x 10^6 nuclei/ml).

The nuclei suspension was used immediately for the comet assay and the left over were centrifuged and frozen at – 80˚C.

2.4 The comet assay

The comet assay, or the single-cell electrophoresis assay –which explain more about what it is, has now been used for over 20 years. The assay has moved from being the main focus of investigation to now being an analytical tool that is well known and used in several areas

(McArt *et al.*, 2009). This is a versatile and sensitive method for measuring single- and double-strand DNA breaks (Collins *et al.*, 2008).

The main objective in this thesis was to study the possible induction of oxidative damage in cells from the testis, liver, lung following exposure to BaP. The use of *Ogg1*-deficient mice served two purposes: First, the *Ogg1*$^{-/-}$ mouse line functions as a model for human testicular cells mimicking the repair capacity for oxidative DNA lesions (Olsen et al., 2003). Second, oxidative DNA damage induced in cells of *Ogg1*$^{-/-}$ mice will not be repaired efficiently and will probably accumulate in any tissue and thereby increase the potential for detecting such DNA lesions that are rapidly repaired in wild type mice. In order to measure oxidative DNA lesions we used the comet assay, this assay is extensively used in our lab (Bjorge *et al.*, 1996; Collins2005; Collins *et al.*, 2008; Hansen *et al.*, 2010; Olsen *et al.*, 2001; Olsen *et al.*, 2003; Sipinen *et al.*, 2010).

In this assay cells are fixed in agarose, lysis of cells and unwinding the DNA, before electrophoresis. Than the negatively charged DNA will wander to the positive pole and make a tail. Intact DNA will remain in the so-called head so the more brake in the DNA the longer the tail will be.

In this thesis a modified version is used. The cells will be exposed with Fpg enzyme, a repair enzyme from *E. coli* (David-Cordonnier *et al.*, 2001), before doing electrophoresis. This enzyme recognises damage caused by oxidative stress, oxidised purines like 8-oxoG, and cuts the DNA. Another recent modification is the use of Gelbond® films instead of glass slides. This is more effective because 12 agarose gels (or more) are moulded on the hydrophilic side, instead of only three gels per glass slide (Shaposhnikov *et al.*, 2010). The films can also be stored for a longer period before and after scoring when it is fixed with ethanol and dried.

2.4.1 Procedure

Every step was performed in dim light. Low melting agarose (0.75%) was prepared and kept at 37˚C. Lysis solution and electrophoresis buffer were prepared and kept at 4˚C.

Eight technical replicates of every organ used from each mouse were made: four that got Fpg-enzyme treatment, and four as controls.

1.) The nuclei suspension, from chapter 2.3, was mixed with agarose (1:10) and 60 µl were moulded on the films. There are 12 agarose-gels on every film, and the agarose solution was moulded on the film with help of a casting frame. The film was on a cold metal plate to speed up the moulding.

2.) After moulding, the films were put into lysis solution over night.

3.) The next day the films were rinsed in dH_2O and then placed in enzyme reaction buffer, first for ten minutes and afterwards for fifty minutes. This step was at 4˚C.

4.) While the films are in enzyme reaction buffer another enzyme reaction buffer solution with 0.2 mg/ml BSA is heated to 37˚C. In half of this, crude Fpg was added, giving a concentration of 1µg/ml, before placing the films in the solution for one hour.

5.) After incubation for one hour the films were placed in electrophoresis buffer (pH 13.2) for washing first for 5 minutes, and afterwards unwinding for 35 minutes in a fresh buffer, both in 4˚C.

6.) Gel electrophoresis for 20 minutes. The electric source was a car-battery with 25V, and 1.5 l of the electrophoresis buffer.

7.) Neutralising for to times 5 minutes in neutralisation buffer.

8.) Rinsing the films in dH_2O for about 1 minute.

9.) After rinsing, the films were placed in absolute ethanol for 5 minutes and then in fresh absolute ethanol for 1 hour 30 minutes to fix the gels. After this the films were dried over night, and stored in a CD-folder until coloured and scored. The films can be stored like this, dark, dry and at room temperature for months.

10.) Colouring and scoring of the films: The films were stained using 20µl – 30µl SYBER® Gold (1000x stock in DMSO) in 25 ml TE-buffer and shaked for 20 - 30 minutes. The colouring is supposed to be saturated, so if the comets look likes donuts they have not been coloured enough, and if so they can be coloured again. If not scored at once, the films were stored moist and cold. After scoring the films were air-dried and stored dry at room temperature.

2.4.2 Scoring of comets

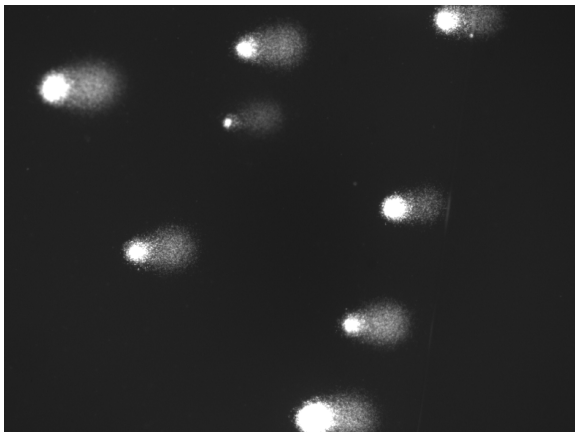

Figure 2.1: Comets from lung cells.

For scoring the comets the software called “Comet assay IV” (Perceptive Instruments) was used.

SYBR Gold binds to DNA and emits fluorescence. The operator selected the comets, without selectively avoiding certain comets. The operator only knew if the gels were treated with enzyme or not, she did not know if the samples were from a mouse treated with BaP.

The tail intensity is measured from the middle of the head to the end of the tail (see figure 2.1). Usually the software finds the middle of the head, but it is possible for the operator to edit the line from where the tail is measured. This happens mostly if the cell has a lot of damage, because then it is difficult to distinguish between head and tail.

2.5 Measuring $NADP^+$ and NADPH

One of the three major routs of activation of BaP (Figure 1.8) is that catechol undergoes a $NADP^+$-dependent oxidation catalyzed by AKRs to yield an *o*-quinone. This reaction will give rise to oxidative damage. After the oxidation the *o*-quinone can then undergo a reduction in the presence of a reducing cofactor, such as NADPH which is an essential cofactor in the *in vitro* microsomal metabolism of BaP (Sadowski *et al.*, 1985), back to catechol, or *o*-quinone can form covalent DNA adducts. By measuring $NADP^+$ and NADPH we can see if NADPH is present in the cell and making this reaction possible and the

relationship between them can tell us about what happens in the cells. NADPH has been shown, by indirect measuring, to be a rate limiting factor in mixed function oxidase activity in the whole liver perfusion system (Sadowski *et al.*, 1985).

To measure the NADP/NADPH ratio we used the kit: EnzyChrom^{TM} $NADP^+$/NADPH Assay Kit, from BioAssay Systems. This kit measures the concentration of $NADP^+$/NADPH in cell or tissue extract.

Fresh lung, liver and testis tissues were used from both *Ogg1*$^{-/-}$ and *Ogg1*$^{+/+}$ mice, but some extracts were frozen down at -80˚C after step two in the procedure.

2.5.1 Procedure

The procedure was done after the description from material safety data sheet in the kit, with some small adjustments.

1.) Liver, lung and testis were taken out of the mice and put in PBS.

2.) Sample: ≈ 20 mg from the tissue: liver and lung were used. Half a testis was cut with Evensens-cut and 20-100 µl were taken (according to the standard curve). This was homogenised in a 1,5 ml eppendorf tube with either 100 µl NADP extraction buffer, for NADP determination, or NADPH extraction buffer for NADPH determination.

3.) The extract was heated on 60˚C for 5 min. Then 20 µl assay buffer were added, and 100 µl of the opposite extraction buffer (NADP or NADPH). Two separate samples from each tissue were used to measure both NADP and NADPH.

4.) Calibration curve: 500 µl were prepared by mixing 5 µl 1 mM Standard and 495 µl distilled water. To make a curve, we diluted the standard as shown in the table.

Table 2.2: The mixtures for the standard curve.

No	Premix + H_2O	Volume (µl)	[NADP] (µM)
1	100 µl + 0 µl	100	**10**
2	80 µl + 20 µl	100	**8**
3	60 µl + 40 µl	100	**6**
4	40 µl + 60 µl	100	**4**
5	30 µl + 70 µl	100	**3**
6	20 µl + 80 µl	100	**2**
7	10 µl + 90 µl	100	**1**
8	0 µl + 100 µl	100	**0**

40 µl of the standards were put in to a clear bottom 96-well plate. We did not do this every time, because we used the relationship between NADP/NADPH and not the total concentration. But it was used some times to see if we got the curve and that the reaction was working.

5.) Reagent: For each well of reaction this working reagent was prepared. 50 µl assay buffer was mixed with 1 µl enzyme, 10 µl glucose, 14 µl PMS and 14 µl MTT. This was kept out of the light, and made freshly every time.

6.) 40 µl from the tissue samples were put into the 96-well plate.

7.) 80 µl of the Working Reagent were put quickly into each well with samples and standards.

8.) The optical density (OD) was measured at time zero, at 570 nm, and again after incubating for 30 minutes at room temperature, without light.

2.6 Gene expression analysis by quantitative real time PCR (RT-qPCR)

2.6.1 RNA extraction

RNA was isolated from the following tissue; liver, lung and testis, from mice exposed to BaP, oil and untreated CTLs. The tissues were prepared (see chapter 2.2.2) and stored at -80 until use.

RNA isolation was done according to GenElute™ Mammalian Total RNA Miniprep Kit (Sigma-Aldrich) with some modifications; tissues were homogenized by the Precellys®24 (Bertin Technologies), a machine designed to lyse and homogenize biological samples, according to manufacture recommended use. We used 2 ml tubes containing CK14 small ceramic beads, for homogenization of soft animal tissue.

It was important to not let the tissue thaw before coming in contact with the Lysis Solution, so it was kept and cut on dry ice before putting it into the solution. This prevents RNA degradation.

2.6.1.1 Procedure

All steps were carried out at room temperature.

1.) Tissue homogenization

a.) Up to 40 mg of tissue per preparation could be used. The tissue was kept on dry ice.

b.) The tissue was transferred into a tube containing 500 µl of Lysis Solution and 2-MercaptoEthanol mixture and ~ 200 beads of type CK14.

c.) The tissue was homogenized using the Precellys®24 at 5000 rpm for 2x20sec. This homogenized tissue might be stored at -70 ˚C for several months.

d.) The homogenized tissue was pipetted into a GenElute Filtration Column and centrifuged at maximum speed (~14 100 g) for 2 minutes. The filtered lysate was used further and the filtration column was discarded.

e.) 500 µl of 70% ethanol solution was added to the lysate and vortexed to prepare for binding of RNA to a binding column.

2.) RNA isolation

f.) Up to 700 µl, at one time, of the ethanol containing lysate were pipetted into a GeneElute Binding Column and centrifuged at maximum speed for 15 seconds.

g.) The flow-through was discarded and the rest, up to 700 µl, of the ethanol containing lysate was added and centrifuged at maximum speed for 15 seconds.

h.) The flow-through was discarded.

i.) First column wash: 500 µl of Wash Solution 1 was pipetted into the column and centrifuged at maximum speed for 15 seconds.

j.) Second column wash: The binding column was transferred into a fresh 2 ml collection tube. The other collection tube was discarded with the flow-through. 500 µl of Wash Solution 2, diluted with ethanol, was pipetted into the binding column in the fresh collection tube and centrifuged at maximum speed for 15 seconds. Collecting tube was retained but the flow-through was discarded.

k.) Third column wash: For the second time 500 µl of Wash Solution 2 were pipetted into the column and centrifuged at maximum speed for 2 minutes. Or more if the binding column was not dry.

l.) Elute RNA: The binding column was transferred into a fresh 2 ml collection tube. 50 µl of the Elution Solution was pipetted into the binding column and centrifuged at maximum speed for 1 minute.

Quantification and purity of total RNA were measured using the NanoDrop™ 1000 Spectrophotometer (Thermo Scientific) (see 2.6.1.2).

2.6.1.2 RNA quality and quantity assessment

RNA quality and quantity was evaluated by NanoDrop Spectrophotometry. The samples were measured according to the manual of the NanoDrop1000 software. RNA and DNA

absorb at 260 nm, this software estimate the concentration according to the absorbance at 260 nm (Figure 2.2). Proteins and phenols absorb light at 280, other contaminants like carbohydrates, salts and also phenols absorb light at 230 nm. The ratio 260/280 and 260/230 of absorbance is calculated, giving the purity of the samples. A 260/280 ratio of around 1.8 for DNA and 2.0 for RNA indicates pure samples and a 260/230 ratio below 2.0 indicates contaminants.

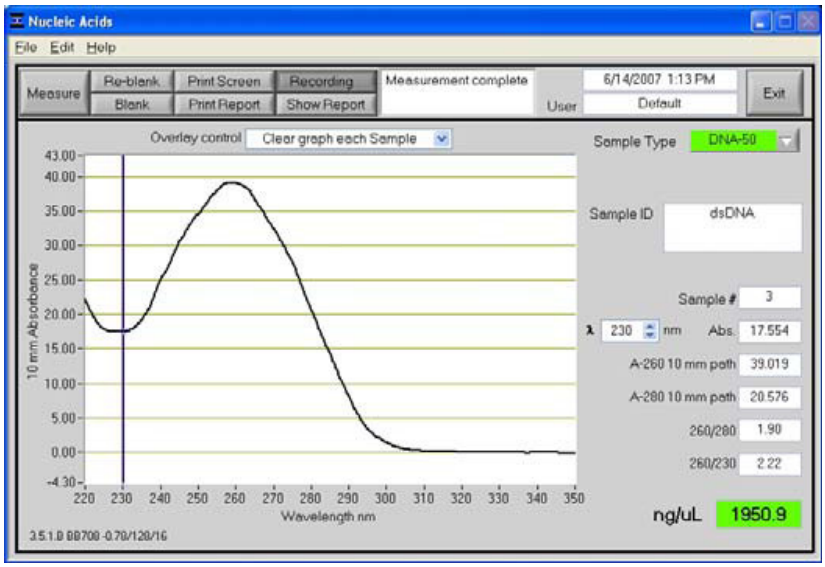

Figure 2.2: The absorbance at 260 nm for DNA, picture from NanoDrop1000 software manual.

1.) The system was initiated with a distilled water sample.

2.) In the computer program ”RNA-40” was chosen for RNA samples, “DNA-50” for DNA samples and “other-39” for cDNA.

3.) A blank measurement was conducted using 2 µl distilled water.

4.) 2.0 µl of each sample were used for the measurement.

5.) The system measures the absorbance at 260 nm and 280 nm and gave directly the concentration of the sample in ng/µl.

6.) Afterwards the Sample Retention System was cleaned with distilled water.

2.6.2 Reverse transcription

Reverse transcription of the isolated totalRNA (see 2.6.1) to cDNA was done using the High-Capacity cDNA Reverse Transcription Kits (Applied Biosystems) according to manufacture recommendation. The Kit uses a random primer scheme for initiating cDNA synthesis. The RT reaction can also be carried out using oligo-dT or gene specific primers. We choose to use the random primers because it came with the Kit. Random primers are capable of priming cDNA synthesis at many points along the RNA template. Priming at many points simultaneously ensures the efficiency of the cDNA and that the whole sequence of interest is synthesised.

2.6.2.1 Procedure

To avoid RNA degradation, samples were kept on ice during the procedure.

1.) Total RNA (1 µg) was synthesised to cDNA using a 96-well reaction plate. The remaining RNA was stored at -80˚C.

2.) The mastermix was prepared according to the kit (Table 2.3).

Table 2.3: cDNA mastermix reaction set up.

Component	Volume (µl) reaction kit (without RNase inhibitor)
10x RT Buffer	**2.0**
25x dNTP Mix (100mM)	**0.8**
10x RT Random Primers	**2.0**
MultiScribe™ Reverse Transcriptase	**1.0**
Nuclease-free H_2O	**4.2**
Total per reaction	**10.0**

3.) 10 µl Mastermix were added to each well with diluted RNA, for a total volume of 20 µl in the 96-well reaction plate.

4.) The 96-well plate was centrifuged briefly to remove air bubbles and to spin down the content.

5.) The cDNA synthesis was done with the following thermal cycle, program shown in table 2.4:

Table 2.4: The thermal cycler program.

	Step 1	**Step 2**	**Step 3**	**Step 4**
Temperature	25˚C	37˚C	85˚C	4˚C
Time	10 min	120 min	5 sec	∞

6.) The synthesised cDNA were quantified by NanoDrop^{TM} 1000 Spectrophotometer as described in chapter 2.6.1.2

7.) cDNA was stored at -20˚C until use, avoiding thawing and freezing.

8.) cDNA was thawed and water (1-9 µl) was added to some of the samples so that all of them would have the same concentration of cDNA.

2.6.3 Real-time PCR

The principle behind the real-time PCR (RT-PCR) methode is essentially the same as original PCR (also called end point PCR), developed by Kary Mullis and co-workers in the mid 1980s. (Kubista *et al.*, 2006; Saiki *et al.*, 1992). Instead of having to amplify the samples first to generate a large number of identical copies and then analyzing them with RT-PCR the generated data is collected every cycle "in real time". PCR is still performed in a DNA template, in this case cDNA; this can be single or double-stranded. Primers are also needed, they have to flank the DNA sequence to be amplified, dNTPs, the rest we need is a heat stable polymerase and magnesium ions in the buffer. At first high temperature will melt and separate the strands and opening up for the primers. It is important that the melting fully separate the strands, if not they will quickly reanneal when the heat sinks. Then several cycles of high temperature follows for separating, and lower for the primers to get to the strands and start amplifying.

The difference with RT-PCR is that it also needs a fluorescent reporter that binds to the product formed and reports its presence by fluorescence and reflects the amount of product formed. Fluorescence is used for detection in real-time PCR. There are several dyes available, both sequence specific probes and non-specific labels (Kubista *et al.*, 2006). For this experiment the dye SYBR green (SG) is used. This has virtually no fluorescence when it is free in solution and becomes brightly fluorescent when it binds to DNA (Kubista *et al.*, 2006). SG can bind to both single stranded DNA (ss-DNA) and double stranded (ds), but is about 11 fold lower with ss-DNA (Zipper *et al.*, 2004), therefore the fluorescence will increase with the amount of ds-DNA. It is sequence non-specific and binds to the minor grove in DNA, and will detect both the gene we are looking for and also undesired primer-dimer products. During the first cycles the signal is weak and cannot be distinguished from the background, but after a while as the product accumulates the signal will increase exponentially until it runs out of critical components.

In end-point PCR it says nothing about the initial amount of target molecules; it can only give a positive or negative answer. For real-time PCR the growth curve for the signal reflects on the difference in their initial amount of template molecules. This can be measured by the numbers of cycles needed to reach a threshold line, this number is called the CT (cycle threshold) or CP (crossing point) value (Kubista *et al.*, 2006). Different instrument software use different methods to set the threshold and you can also set a threshold manually. Therefore one gene can have different CT values in different experiments and you cannot compare individual CT values between experiments.

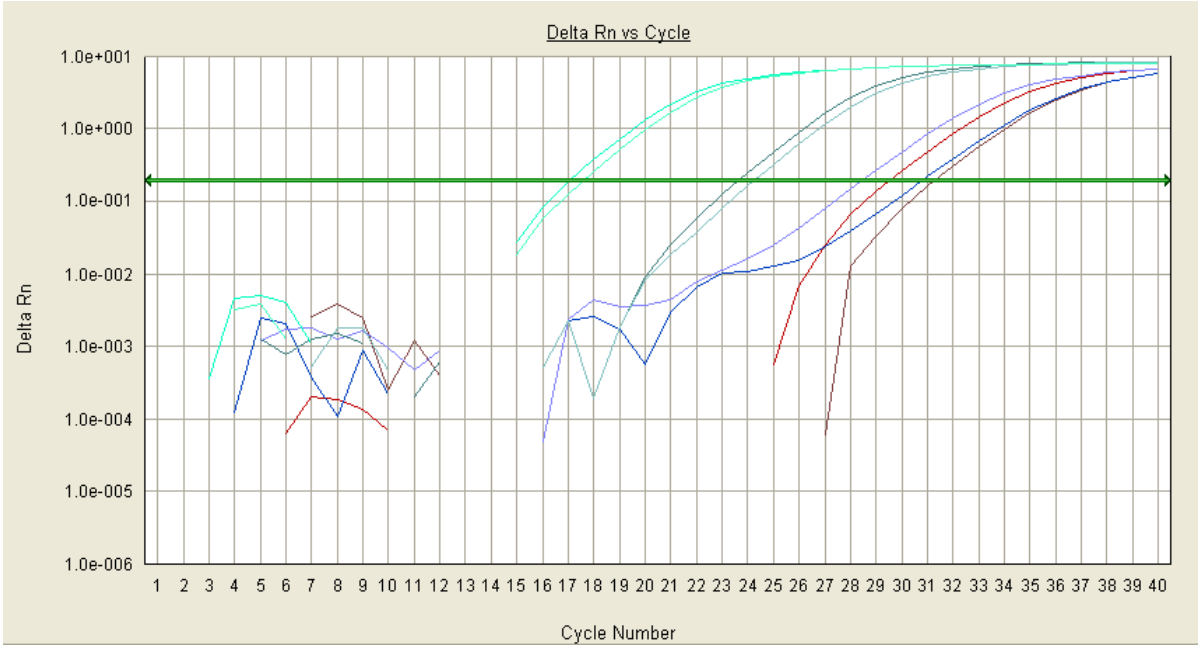

Figure 2.2: The CT value, the number of cycles needed to reach the threshold line.

At the end of the PCR cycles a disassociation-step is added to make a melting curve analysis in order to examine if there are any unwanted products. Shorter (or longer) products will melt at a different temperature.

A) Dissociation curve

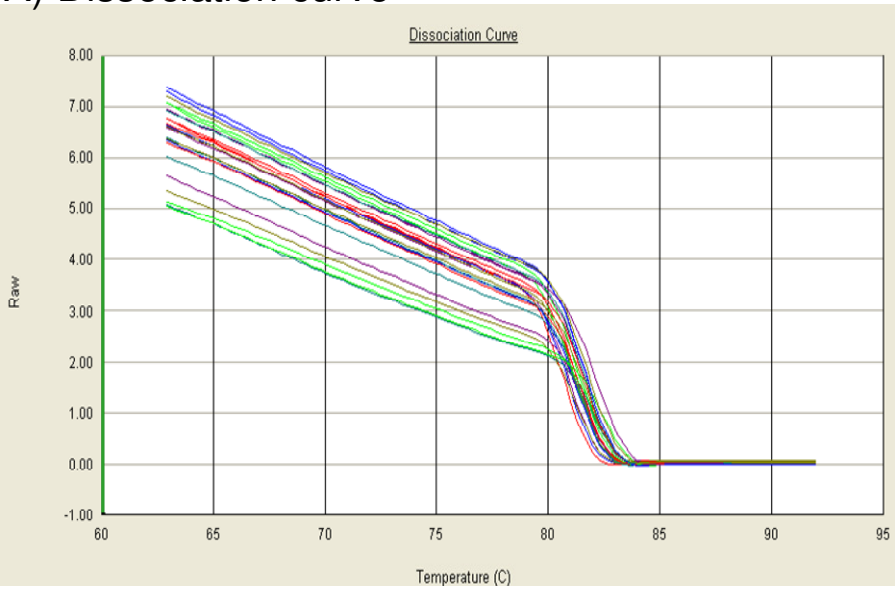

B) Dissociation curve derivative

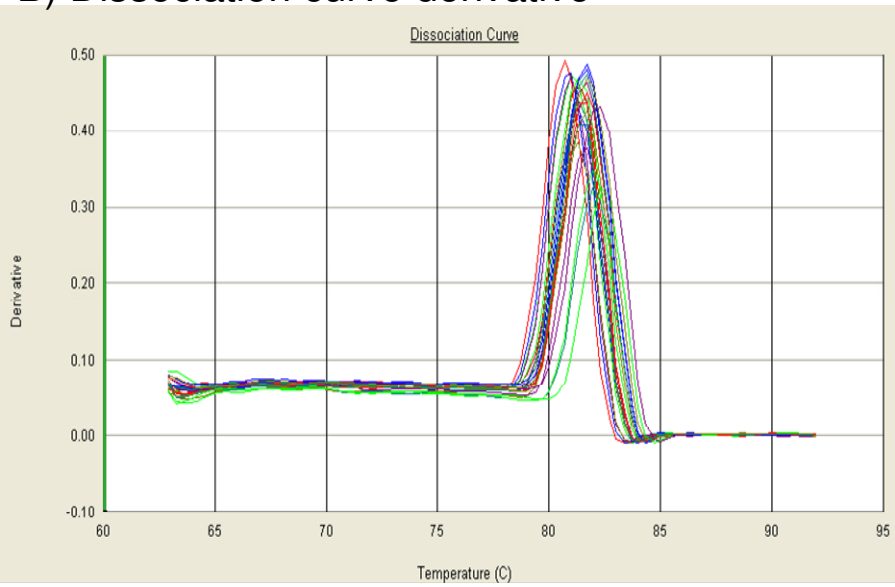

Figure 2.3: Dissociation curve. A: Melting curve for the product. B: The derived of the melting curve.

To avoid unspecific annealing, sequence specific primers are used. We use primers for *Cyp1a1* and *Akr1a4* as well as five housekeeping genes: *18s ribosomal RNA (18s), Actb, Gapdh, Hprt1* and *Rpl13a* (more about housekeeping genes in chapter 2.6.3.2, and 3.3.2).

2.6.3.1 Procedure

The cDNA was kept on ice at all times. The procedure is according to the protocol for the RT^2 Real-Time^{TM} SYBR Green/Rox PCR master mix (SA Biosciences).

A dilution series with the samples from the liver were conducted to find the cDNA dilution appropriate for the selected genes. This ensures that the eventually change of expression of the genes are not lost, as well as having the optimal cDNA concentration for the run. Results showed that a 1:10 dilution was appropriate.

1.) The real-time PCR reaction mixture was prepared as shown in Table 2.5

A 96 well reaction plate was used.

Table 2.5: The real time PCR reaction mixture.

Component	Volume (µl)
Master mix	**12.5**
Primers*	**1.0 / 2.0**
cDNA	**2.0**
ddH_2O	**8.5 / 9.5**
Total volume:	**25.0**

*If 1 or 2 µl of the primers were used depended on the primer and the recommendation from the manufacture, water was added to make a total volume of 25 µl. Primers were diluted in TE-buffer.

The reaction plate was centrifuged briefly for one minute to remove air bubbles and to spin down the content.

2.) The real-time PCR run was on 7500 Fast Real Time PCR System (Applied Biosystems), with following thermal cycle program (Table 2.6):

Table 2.6: Thermal cycle for the real time PCR.

Stage	Duration	Temperature	Cycles
1	10 min	95 ˚C	1
2	15 sec	95 ˚C	40
	1 min	60 ˚C *	
3	15 sec	95˚C	1

* Data collecting step

2.6.3.2 Real time PCR data analysis

Relative quantification is the most widely used technique. It determines the changes in steady-state mRNA levels of a gene across multiple samples and expresses it relative to the levels of an internal contntrol RNA (Duale 2010). The reference genes we are using are housekeeping genes (HKGs). HKGs are used to correct methodological variations during the same run; they are ubiquitously and are thought to be expressed at similar levels in cells. Here we used the BestKeeper (BK) algorithm to evaluate the stability of these HKGs (Pfaffl *et al.*, 2004b).

Normalisation was performed according to the ΔΔCT-method (Livak and Schmittgen 2001). This is the simplest one as it is a direct comparison of CT values between target gene and HKG (or BK as we use). The samples were normalised first to the BK ($\Delta CT = CT_{target} - CT_{BK}$) and then values for the treated samples vs. the control samples were calculated ($\Delta\Delta CT = \Delta CT_{treated} - \Delta CT_{contol}$). For expressing the relative change between treated and control $2^{-\Delta\Delta CT}$ values were calculated, and then the fold change values were log2-transformed.

2.7 Statistics

The data from comet assay were analysed using the nonparametric Mann-Witney *U*-test, because the data were not normally distributed.

For the NADP/NADPH ratio we also used nonparametric test. Nonparametric two related samples test (Wilcoxon Signed Ranks Test) to test for $Ogg1^{-/-}$ and $Ogg1^{+/+}$ genotype differences. Nonparametric two dependent sample test (Mann-Whitney *U*-test) was used to examine the difference between BaP- versus corn oil treated samples.

The gene expression data were analyzed by one-way ANOVA followed by a post hoc Dunnett's test to allow for multiple comparisons, i.e. comparison between treatment groups: ΔCT BaP exposed (CT exposed target gene – CT BK genes) versus ΔCT untreated CTL (CT

untreated control target gene – CT BK genes), and two paired *t*-test was used to check for genotype differences.

Statistical analyses were performed using SPSS software v17 (SPSS Inc., Chicago, IL), and $p < 0.05$ was accepted as statistically significant.

3. Results

3.1 Induction of oxidative DNA damage following *in vivo* exposure to BaP

The mice were treated acutely with one dose of BaP (150 mg/kg bw) or vehicle only (corn oil) by i.p. administration. For the comet assay the sacrifice of the mice occurred at day ten (Day 10), seventeen (Day 17) and thirty-one (Day 31) following the treatment, with main focus on Day 17 since we in Study 1 have observed a low but significant increase in Fpg-sensitive DNA lesions in testicular cells (Meier2008). Three mice per genotype were exposed for sacrifice at Day 17 whereas for Day 10 and Day 31 one mouse of each genotype was included. Four untreated control mice (CTL) of each genotype were also included to establish spontaneous background DNA damage levels. For each tissue four technical replicates were generated in the comet assay (four gels were moulded on the GelBond film per sample) and fifty comets were scored on each technical replicate, giving a total of 200 scored comets for each sample.

In order to specifically address oxidative damage digestion of nuclear DNA with a crude extract of the bifunctional DNA glycosylase/AP-lyase Fpg from *E. coli* was included in the comet assay. Net Fpg-sensitive sites (Fpg-ss) were obtained by subtracting the tail intensity value of the corn oil treated mice from the tail intensity value of the BaP treated mice.

In $Ogg1^{-/-}$ mice the background damage level in untreated CTL mice (Appendix B) was lowest in the testis with 19.8% tail intensity in the KO and 15.1% in WT mice. It was markedly higher in lungs of $Ogg1^{-/-}$ mice with a tail intensity of 50.6% whereas the WT had 22.5% in the lung. The liver had approximately similar levels as the lung, with 48.1% tail intensity in KO and 21.6% in WT.

For the animals exposed to the vehicle (corn oil) and sacrificed at Day 10 unexpectedly high DNA damage levels were recorded. Repeating the experiment with new mice lower levels of DNA damage were measured, but we could still see some effect of oil treatment. This is also the reason for subtracting oil treatment from BaP treatment in the results shown here, raw

data are shown in Appendix B. We could not specifically exclude that the first data of DNA damage had been introduced due to health issues with the individual mice, or as a result of operator errors. The results from Day 10 were thus left out of the dataset due to these unexplainable observations, and are represented in Appendix B.

In the testis no increase in Fpg-ss was observed at Day 17, either in $Ogg1^{-/-}$ mice or in wild type mice (Figure 3.1A). At Day 31, on the other hand, there was a small induction of Fpg-ss in $Ogg1^{-/-}$ mice that were not observed in the wild type. The results from Day 31 were however based on only one mouse per genotype. In the somatic tissues investigated, the liver and lung, oxidative DNA damage was induced *in vivo* as a result of BaP (Figures 3.1B and C). Moreover significant differences in DNA damage levels between genotypes were observed. In the liver of $Ogg1^{+/+}$ mice, the level of Fpg-ss increased at Day 17, after which it declined to the level of untreated mice at Day 31. In liver cells of $Ogg1^{-/-}$ mice, on the other hand, the level of Fpg-ss initially declined below that of untreated mice at Day 17. This difference is statistically significantly different between the genotyes ($p = 0.049$). At Day 31 liver cells showed a ~17% increase above that of untreated CTL mice. In the lung of both $Ogg1^{-/-}$ and $Ogg1^{+/+}$ mice increased levels of Fpg-ss was recorded at Day 17 that declined at Day 31. The lung cells from $Ogg1^{-/-}$ mice showed a higher increase in Fpg-ss that the WT and the difference between them were significantly different with ($p = 0.049$). The level of Fpg-ss declined at Day 31, but not to the level of untreated CTL mice as it did for wild type mice. The differences in damage level in the lung between $Ogg1^{+/+}$ and $Ogg1^{-/-}$ mice were largely similar at Day 17 and at Day 31. The induction of Fpg-ss sites were thus most pronounced in the lung.

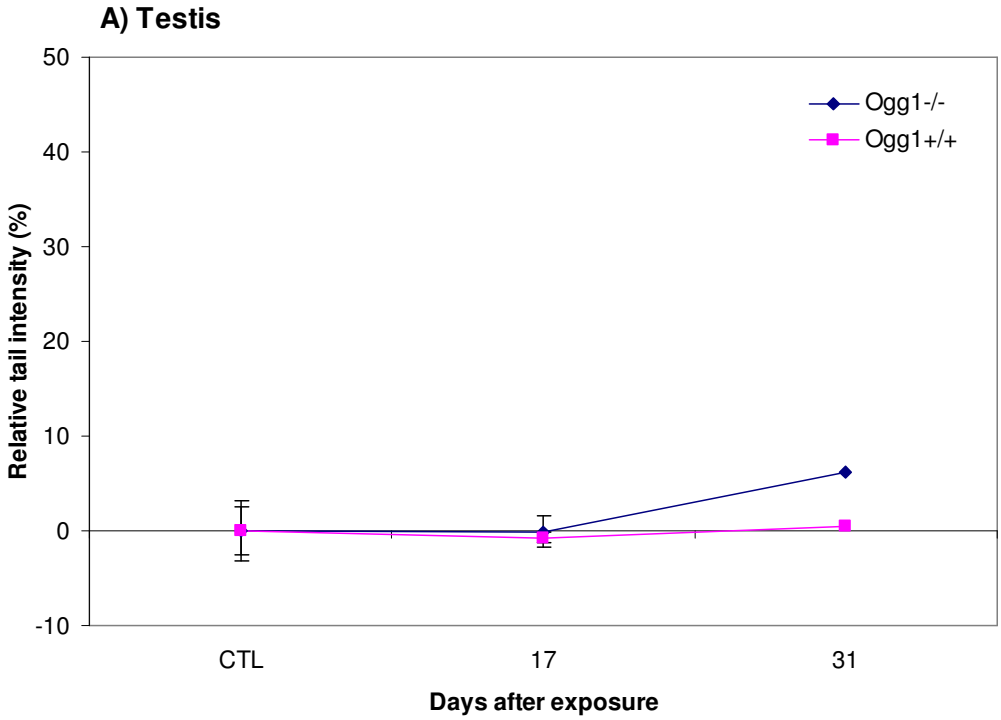
A) Testis
50
40
30
20
10
0
-10
Relative tail intensity (%)
Ogg1-/-
Ogg1+/+
CTL
17
31
Days after exposure

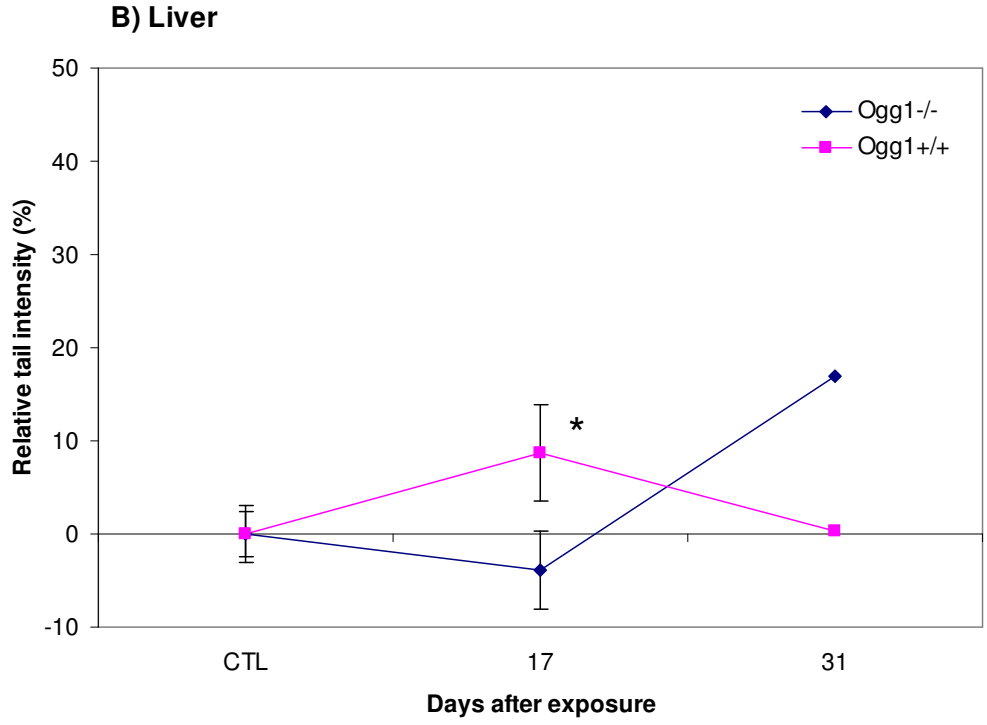
B) Liver
50
40
30
20
10
0
-10
Relative tail intensity (%)
Ogg1-/-
Ogg1+/+
*
CTL
17
31
Days after exposure

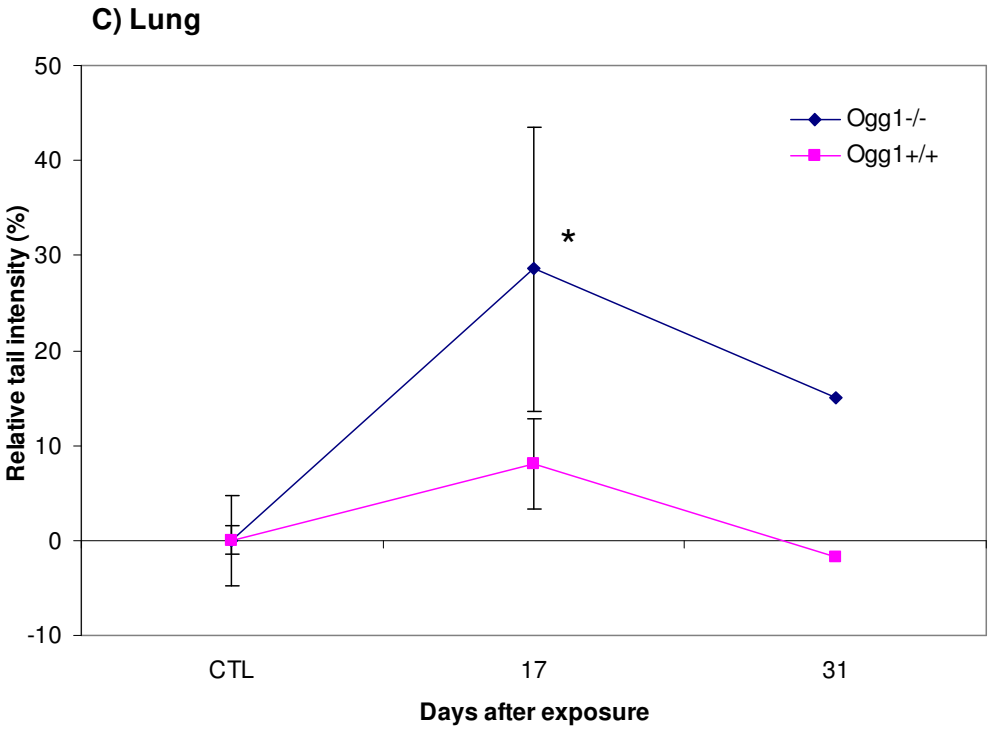

Figure 3.1: Net Fpg-sensitive sites in testis, liver and lung from BaP-exposed mice, measured using the comet assay. Tail intensity (%) of cells from testis (A), liver (B) and lung (C) measured with the comet assay. The y-axis shows the relative tail intensity, after subtracting the tail intensity of the corn oil treated mice from mice exposed to BaP. The x-axis shows day of sacrifice following treatment. These data are based on four untreated CTL animals, three animals per exposure scenario and genotype at Day 17 and one animal per exposure scenario and genotype at Day 31. The average of medians of 200 scored comets per animal ± SE is shown, after subtraction as described above. * Statistical significant differences between genotypes ($p < 0.05$).

When whole tissue cells/nuclei preparations from testis are made by the mechanical squeezing procedure a heterogeneous population of male germ cells of different stages of spermatogenesis and different somatic cells are generated. In comet assays on these samples male germ cells are not distinguished from somatic cells except for the haploid round spermatids due to their lower DNA content identified as total intensity. The comet data can be plotted in a diagram showing the total intensity and the DNA damage level as tail intensity. Using these approach specific results from haploid round spermatids can be obtained. Evaluating results from untreated CTL mice and due to previous experience we found that the haploid round spermatids constitute ~50-60% of the cells scored in the comet assay on testis tissue squeeze cell samples. Based on plotting the results in testis diagrams according to ploidy (total intensity) versus DNA damage (tail intensity) we observed that a

population of the haploid round spermatids at Day 31 following BaP-exposure indeed showed very high damage levels (Circled in Figure 3.2B). In the mice treated with the vehicle (corn oil) only few haploid round spermatids expressed marked levels of Fpg-sensitive sites (Figure 3.2 A). Furthermore, the time from exposure to sacrifice of mice of 31 days imply that the haploid round spermatids present in the testis at the time of sacrifice originated from stem cells spermatogonia at the time of exposure. The results from Day 31 were however restricted to one mouse per exposure scenario and genotype.

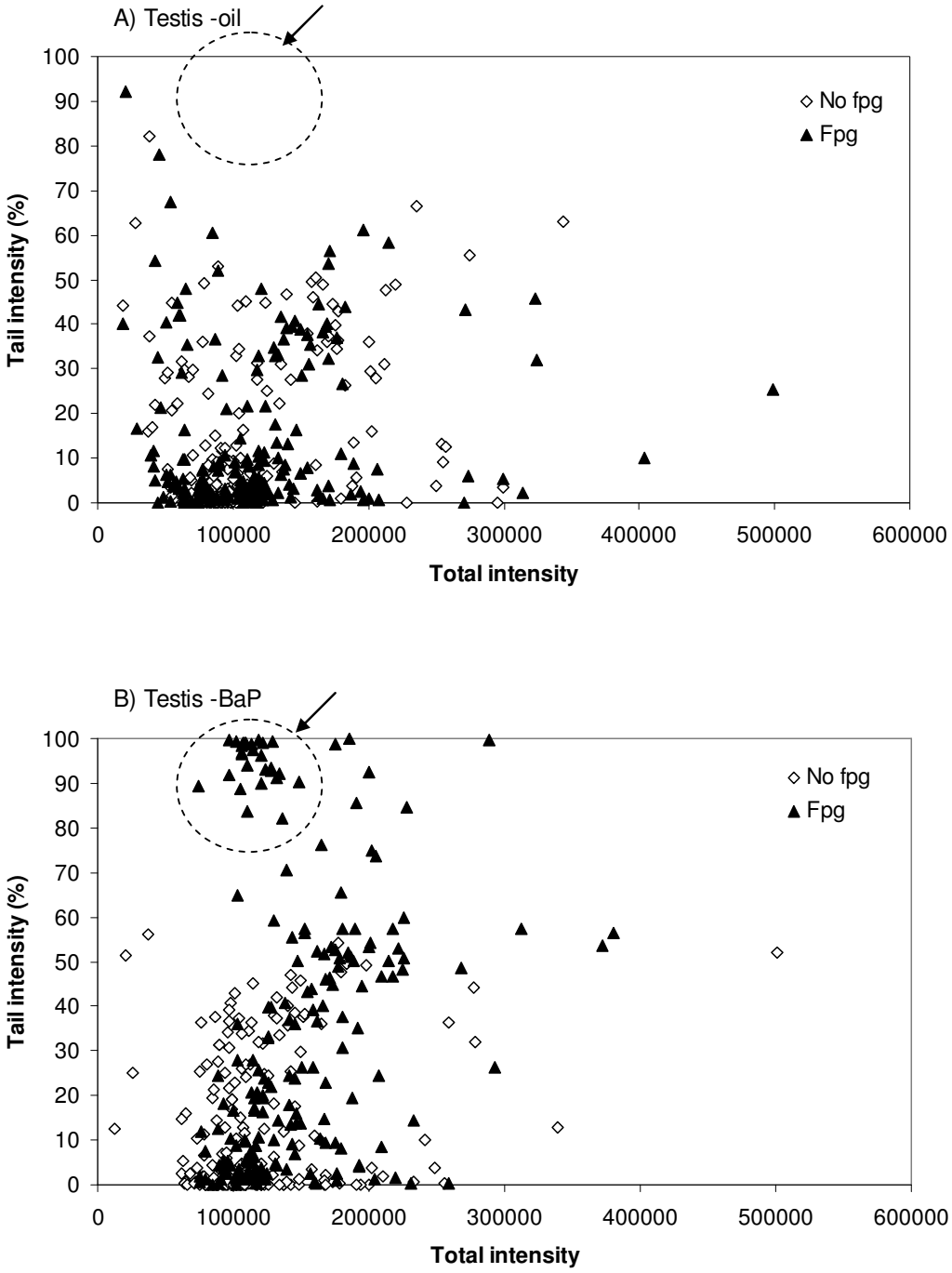

Figure 3.2: Results from comet assays on testis samples presented as DNA damage levels (Tail intensity) as a function of ploidy (Total intensity). Testis samples are from individual *Ogg1*$^{-/-}$ mice treated with oil (A) and BaP (B) sacrificed at Day 31 following treatment. On the x-axis the total intensity for the comets is shown, and on the y-axis the the % tail intensity is shown. Haploid round spermatids are at the left part of the x-axis due to their low DNA content. The circle indicates where heavily damaged haploid round spermatids appear.

.

3.2 The relationship between NADP/NADPH

BaP is first metabolised to (-)-BaP-7,8-diol via Cyp1A1/Cyp1A2 and epoxide hydrolase (see figure 1.2). This metabolite can either be metabolised further by Cyp1A1 to (+)-anti-BPDE or alternatively it can be metabolised by AKRs to a redox-active quinone (BaP-7,8-dione) via a catechol. The *o*-quinone formed can undergo a reduction back to catechol in the presence of a reducing cofactor, like NADPH. Each time the catechol is reformed it may be reoxidised to catechol simultaneously generating ROS via molecular oxygen. This futile redox cycle generates ROS and utilise NADPH. In order for this redox cycle to occur, NADPH must be present in the cell. A decline in the NADPH/NADP-relationship is indicative of consumption of NADPH and is an indication of reiterating redox cycles giving rise to ROS. We measured the NADPH/NADP-relationship in mice exposed to BaP or corn oil that were sacrificed at day one, three, five and seventeen for both genotypes. For WT mice we measured this relationship also in mice sacrificed at Day 10. Two untreated CTL mice of each genotype were used to establish baseline levels of NADPH and NADP.

3.2.1 Standard curve

A standard curve for the amount of NADP was established (Figure 3.2), and we determined the appropriate amounts of tissue extract to be used that had levels of NADP within the range of the standard curve.

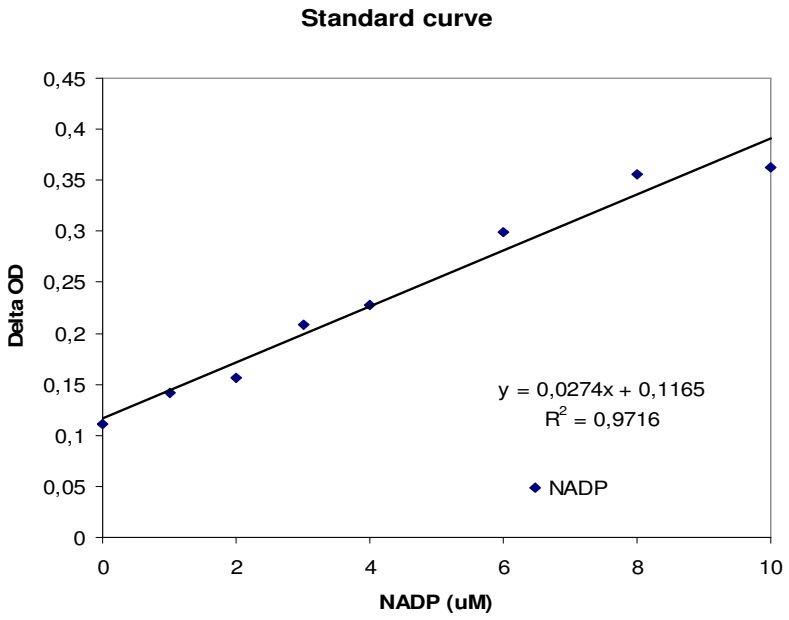

Figure 3.3: The standard curve for NADP. The x-axis shows the concentration of NADP (µM) and the y-axis shows the ΔOD (OD at time 30 minutes minus OD at 0 minutes).

3.2.2 The amount of NADP/NADPH

NADP and NADPH were measured in extracts from half a decapsulated testis (30-40 mg) and from ~20 mg liver or lung tissue from untreated CTL mice. The amounts of NADP and NADPH were lowest in the testis, higher in the lung and highest in liver tissue (Table 3.1). The amounts of NADP and NADPH were stable in the untreated CTL mice described by their low SD.

Table 3.1: Levels of NADP and NADPH in testis, liver and lung tissue for untreated CTL *Ogg1*$^{+/+}$ and *Ogg1*$^{-/-}$ mice

A) Δ OD CTL			
Ogg1-/-	Liver	Lung	Testis
NADP	0.23 ± 0.03*	0.18 ± 0.01	0.09 ± 0.00
NADPH	0.46 ± 0.00	0.22 ± 0.00	0.05 ± 0.00

B) Δ OD CTL			
Ogg1+/+	Liver	Lung	Testis
NADP	0.21 ± 0.07	0.12 ± 0.01	0.09 ± 0.00
NADPH	0.53 ± 0.15	0.19 ± 0.01	0.08 ± 0.01

*mean ΔOD value ± SD for two untreated CTL animals of each genotype.

3.2.3 Relationship between NADP/NADPH

In order for the redox cycle of quinones to occur leading to ROS generation the cell should contain significant amounts of the reducing agents such as NADPH and Cu^{2+}. The NADP/NADPH ratio should therefore ideally start with a very low number that increases as NADPH is being used in the reaction. If NADP/NADPH > 1 there is more NADP than NADPH whereas when NADP/NADPH < 1 there is more NADPH than NAPD, favourable of redox cycling. As the reaction proceed and NADPH is used we would expect the ratios to increase, which was exactly what we found.

In the testis of *Ogg1*$^{-/-}$ mice, the relative amount of NADPH was initially low in untreated controls. The relative amount of NADPH was however markedly reduced at Day 3 following BaP-exposure with higher relative amount than CTL mice at Day 5 after which it returned to the relative amount of CTL mice (Figure 3.4).

In the liver the relative amount of NADPH followed a similar pattern as the testis. The level declined somewhat relative to NADP already at Day 1, with a most pronounced reduction at Day 3, after which it was increased at Day 5 and approached the level of CTL mice and corn oil treated mice at Day 17. The response in the lung did not follow a similar pattern as did the testis and liver. The NADPH level was dramatically reduced at Day 1 (there were no NADPH left in the samples) after which it returned gradually to levels of CTL mice at the subsequent days of analyses.

At Day 17 there were no significant differences between BaP-exposed samples and oil treated ones ($P > 0.05$) in any of the tissues or genotypes. For Day 1-5 there were only one animal in each group, and we could not test for statistical differences.

No significant differences in NADP/NADPH ratios between the genotypes for testis and lung ($P > 0.05$) were observed. In the liver, on the other hand, there were significant differences in NADP/NADPH ratios between *Ogg1*$^{-/-}$ and *Ogg1*$^{+/+}$ samples following BaP treatment ($p = 0.007$)

Ogg1-/- NADP/NADPH			
Days after exposure	Liver	Lung	Testis
CTL	0.49 ± 0.07	0.84 ± 0.03	1.05 ± 0.01
1	1.15 ± 0.33	∞	0.72 ± 0.26
3	4.59 ± 1.77	4.98 ± 1.12	3.81 ± 2.70
5	2.41 ± 1.40	1.20 ± 0.07	0.34 ± 0.19
17	1.30 ± 0.52	1.27	1.10 ± 0.24
17 oil	1.07 ± 0.28	1.04	0.95 ± 0.15

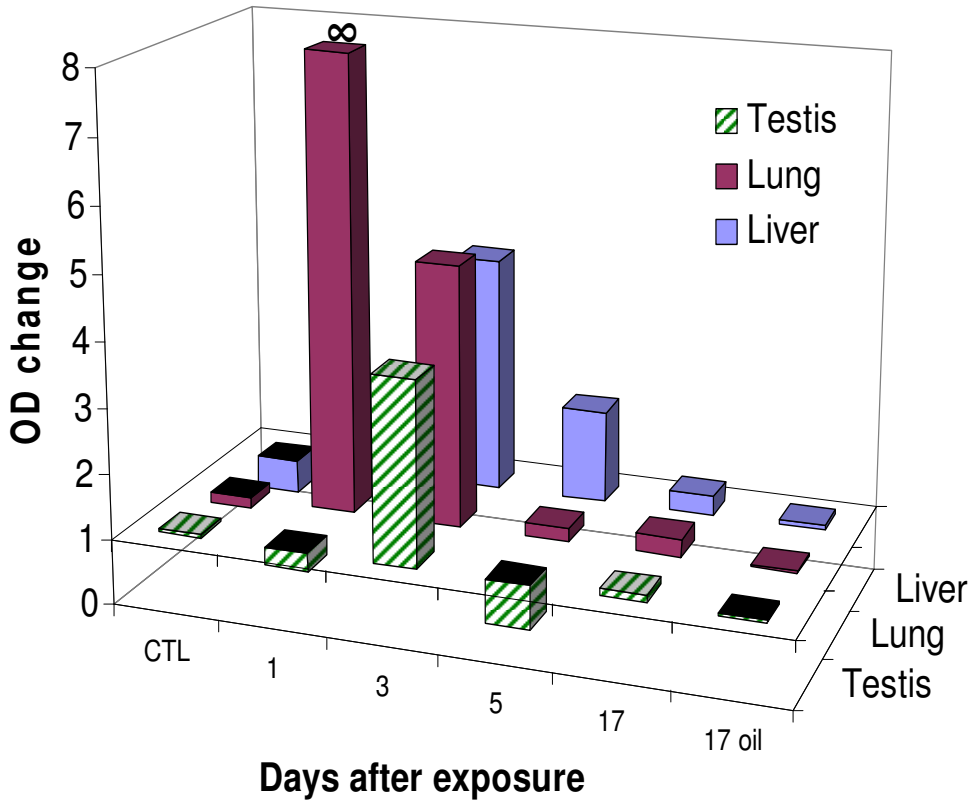

Figure 3.4: Ratios between NADP/NADPH in Ogg1$^{-/-}$ mice. The y-axis shows the ΔOD for NADP divided by the ΔOD for NADPH. The x-axis is categorical and shows the treatment and the day of sacrifice after treatment, single numbers represent mice exposed to BaP. The mean values and SD of technical replicates are also shown as a table. There were three animals in the CTL group, one in the Day 1, 3 and 5 groups and three in the Day 17 groups.

For *Ogg1*$^{+/+}$ mice we also included mice sacrificed 10 days after exposure. In the testis of *Ogg1*$^{+/+}$ mice similar relative levels of NADPH as in *Ogg1*$^{-/-}$ mice were observed. In general, the changes in NADP/NADPH-relationships after exposure to BaP in the *Ogg1*$^{+/+}$ followed

mainly the same patterns as did *Ogg1*$^{-/-}$ mice and at Day 10 the relationships between NADP and NADPH were almost one. One exception was the liver. The initial relative levels of NADPH were similar in *Ogg1*$^{+/+}$ and *Ogg1*$^{-/-}$ mice. The response following BaP-exposure was however significantly different between the two genotypes; instead of having the lowest relative amount of NADPH at Day 3, as in *Ogg1*$^{-/-}$ mice, the lowest and most pronounced reduction in the relative amount was observed at Day 1 (where we found no NADPH in the samples thus the NADP/NADPH ratio was close to ∞), followed by an increase at day 3 and another reduction at Day 5. At Day 10 and Day 17 the relative levels approached those of untreated CTL mice.

Ogg1+/+ NADP/NADPH			
Days after exposure	Liver	Lung	Testis
CTL	0.39 ± 0.02	0.80 ± 0.10	1.07 ± 0.11
1	∞	∞	0.88 ± 0.13
3	1.59 ± 0.75	3.22 ± 1.26	3.82 ± 2.55
5	3.49 ± 0.81	0.97 ± 0.40	0.50 ± 0.08
10	0.95	0.93	0.95
10 oil	1.30	1.09	0.95
17	0.94 ± 0.31	0.77	0.94 ± 0.15
17 oil	0.46 ± 0.09	1.13	0.96 ± 0.10

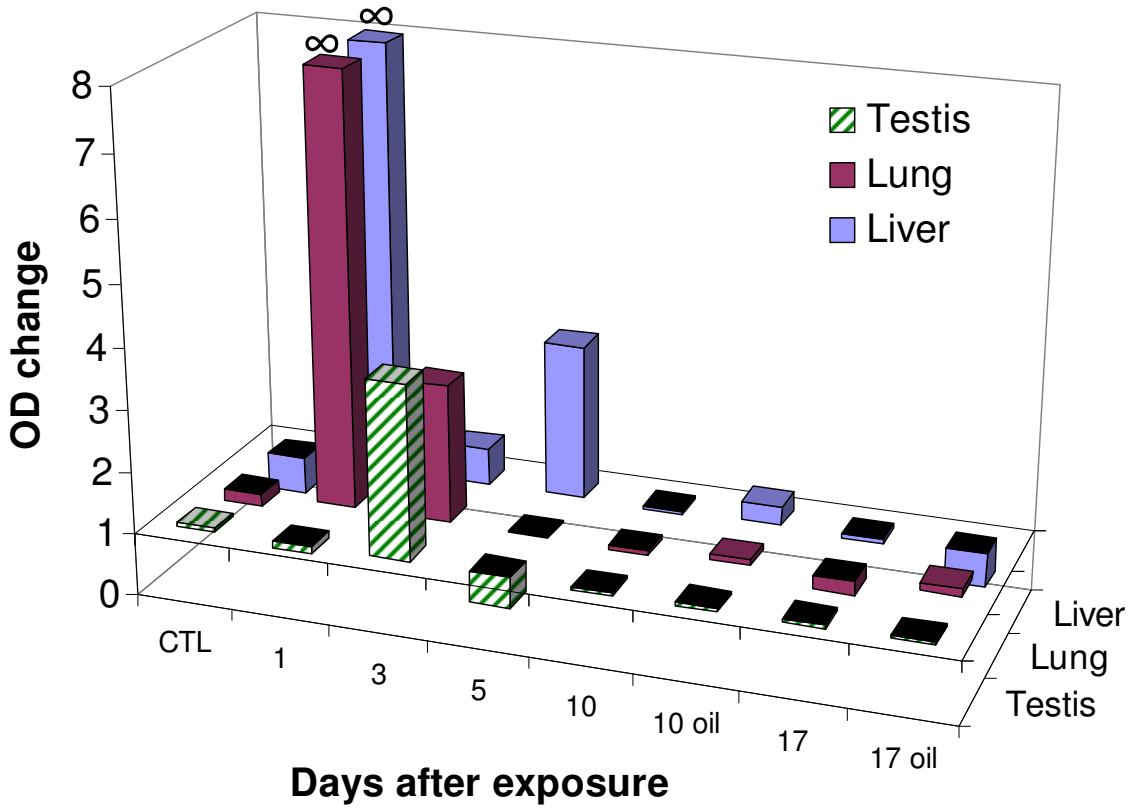

Figure 3.5: Ratios between NADP/NADPH in *Ogg1*$^{+/+}$ mice. The y-axis shows the ΔOD for NADP divided by the ΔOD for NADPH. The x-axis is categorical and shows the treatment and the day of sacrifice after treatment, single numbers represent mice exposed to BaP. The mean values and SD of technical replicates are also shown as a table There were three animals in the CTL group, one in the Day 1, 3, 5 and 10 groups and three in the Day 17 groups.

3.3 Gene expression pattern of two selected genes involved in BaP-metabolism

The final aim of this experiment was to see if there were any alterations in the gene expression.

3.3.1 RNA quality and quantity control

RNA quality (purity and integrity) and quantity were measured using a NanoDrop ND-1000 Spectrophotometer (Fisher Scientific, Norway). The total RNA concentration of the samples has been quantified with the NanoDrop-1000 software by measuring the extinction at 260 nm. Additionally, the OD260/280 and the OD260/230 ratio showing RNA purity were evaluated. An OD260/280 ratio of ~ 2.0 for RNA indicates pure samples, ratios lower than these values indicate the presence of protein, phenol or other contaminants that absorb light at 280 nm. An OD260/230 ratio above 2.0 indicates pure samples, and a ratio below 2.0 indicates contaminants such as carbohydrates, salts and phenols. Table 3.2A shows the average total RNA yields from testis, lung and liver. The total RNA yield ranged from a minimum of 1.16 µg (lung) to maximum of 195.8 µg (liver).

We have synthesised cDNA from 1 µg total RNA, and the quality of the generated cDNAs are acceptable (Table 3.2B). The average OD260/280 ratio ranged from 1.75 to 1.84. Pure DNA has an OD260/280 ratio ~ 1.8.

Table 3.2: RNA/cDNA quality and quantity*

A) RNA				
Tissue	Tissue (mg)	Amount RNA (µg)	260/280	260/230
Testis	32.8 ± 10.2	43.7 ± 21.8	2.21 ± 0.08	1.91 ± 0.26
Liver	57.9 ± 22.6	57.2 ± 44.6	2.12 ± 0.08	1.78 ± 0.34
Lung	40.6 ± 18.9	11.65 ± 18.6	2.18 ± 0.10	1.24 ± 0.48

B) cDNA				
Tissue	RNA (µg)	Amount cDNA (µg)	260/280	260/230
Testis	1	36.9 ± 6.3	1.84 ± 0.01	2.31 ± 0.02
Liver	1	66.4 ± 4.8	1.75 ± 0.06	2.14 ± 0.08
Lung	1	63.3 ± 5.8	1.76 ± 0.06	2.19 ± 0.08

*Mean values ± SD

3.3.2 Evaluation of housekeeping gene stability

Housekeeping genes, HKGs, or reference genes are considered as gold standard for normalization. They are used to even out variations in the expression of the target genes. However, up to now no general rules for which HKG is the right one to normalise the target genes is given. A good HKG should have a constant level of expression between individuals, among different tissues of an organism, at all stages of development, and should not be affected by the experiment treatment (Duale2010). It has been proposed to use several HKGs because the expression of one HKG might change slightly. It is recommended to use a reference gene index, i.e. a geometrical average of multiple HKGs. We have used the BestKeeper software (Pfaffl *et al.*, 2004b), to evaluate the stability of five HKGs (*18s rRNA, Actb, Gapdh, Hprt1* and *Rpl13a).* The software allows for an accurate normalization of qRT-PCR data by geometric averaging of multiple internal control genes, BestKeeper (BK). The major drawback of these methods is the need of many primer pairs and the complicated way to process the data. Figure 3.6 shows the stablitity of the five HKGs and their geometric mean (BK) for testis from *Ogg1*$^{-/-}$ mice (HKG stability for other tissues or genotype is shown in Appendix B).

For some samples we used only the geometric average of four HKGs because some single HKGs had a SD higher than 1.0 and these HKG were left out of the geometrical mean for the BK.

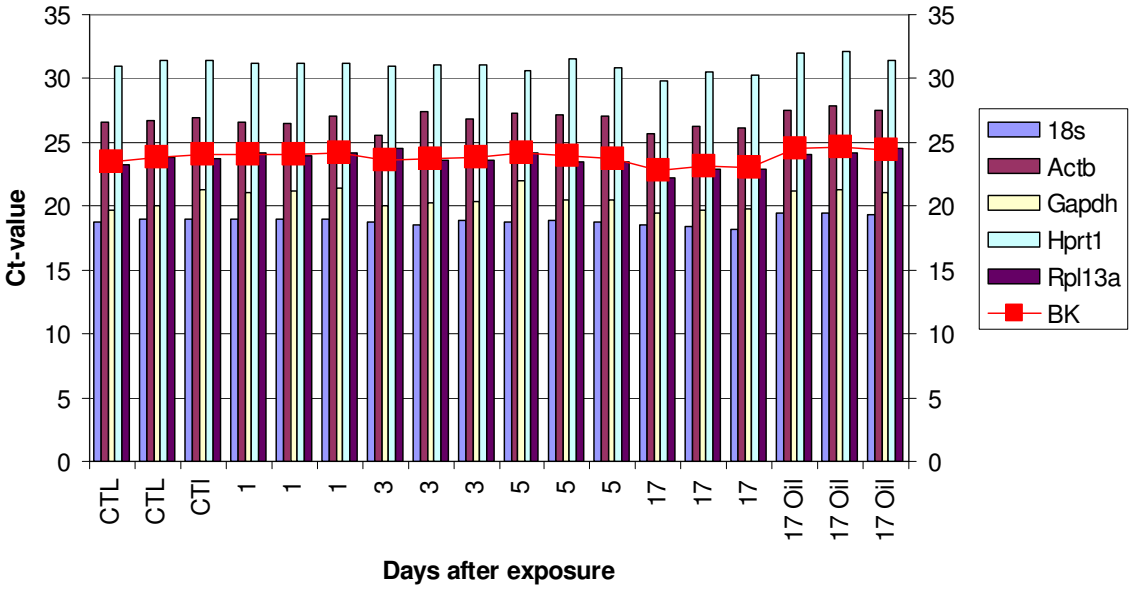

Figure 3.6: HKG stability in testis of *Ogg1*$^{-/-}$ mice. Evalution of five HKGs stability by BestKeeper software (Pfaffl *et al.*, 2004a). Bars (left axis) represent the CT-value of five HKGs and line (right axis, red) represents the geometric mean of the five HKGs (BK). For every group (CTL, Day 1, 3, 5, 17 and 17 oil) and for each HKG, three technical replicates were used. Results for the other organs and genotypes are shown in Appendix C.

3.3.3 Serial dilution curve analysis of cDNA standard

Each analysed sample generates an individual amplification history during real-time fluorescence analysis. Biological replicates, even technical replicates, result in significantly different amplification curves as a result of sample-to-sample variations. Constant amplification efficiency in all compared samples is one important criterion for reliable comparison between samples. A number of variables can affect the efficiency of the PCR, such as length of the amplicon, GC content of the amplicon, secondary structures and primer quality (Duale2010). The PCR efficiency can be calculated from the slope of the standard curve (Figure 3.7) as: Efficiency = $10^{(-1/\text{slope})} - 1$.

If the slope of the standard curve is -3.3 then the PCR is 100 % efficient. With 100 % efficiency, a 2-times dilution gives a ΔCt of 1 between each dilution (in each cycle the amount of amplification is doubled) (Duale2010). Equal efficiency is required for the ΔΔCT-method. Although valid data can be obtained that fall outside of the efficiency range, the RT-qPCR should be further optimized or alternative amplicons designed (Duale2010).

Serial dilution analysis was performed to find suitable dilution of cDNA and ensure that there are equal amplification efficiencies for all genes. The serial dilution analysis was done on the liver cDNA for both target genes (*Cyp1a1* and *Akr1a4*) used in this thesis and also for one HKG (*18s rRNA)* (Figure 3.7). There were about 200 ng/ul cDNA in the samples and we found the 1:10 dilution to be the best and this dilution was used for all samples for all tissues and genes.

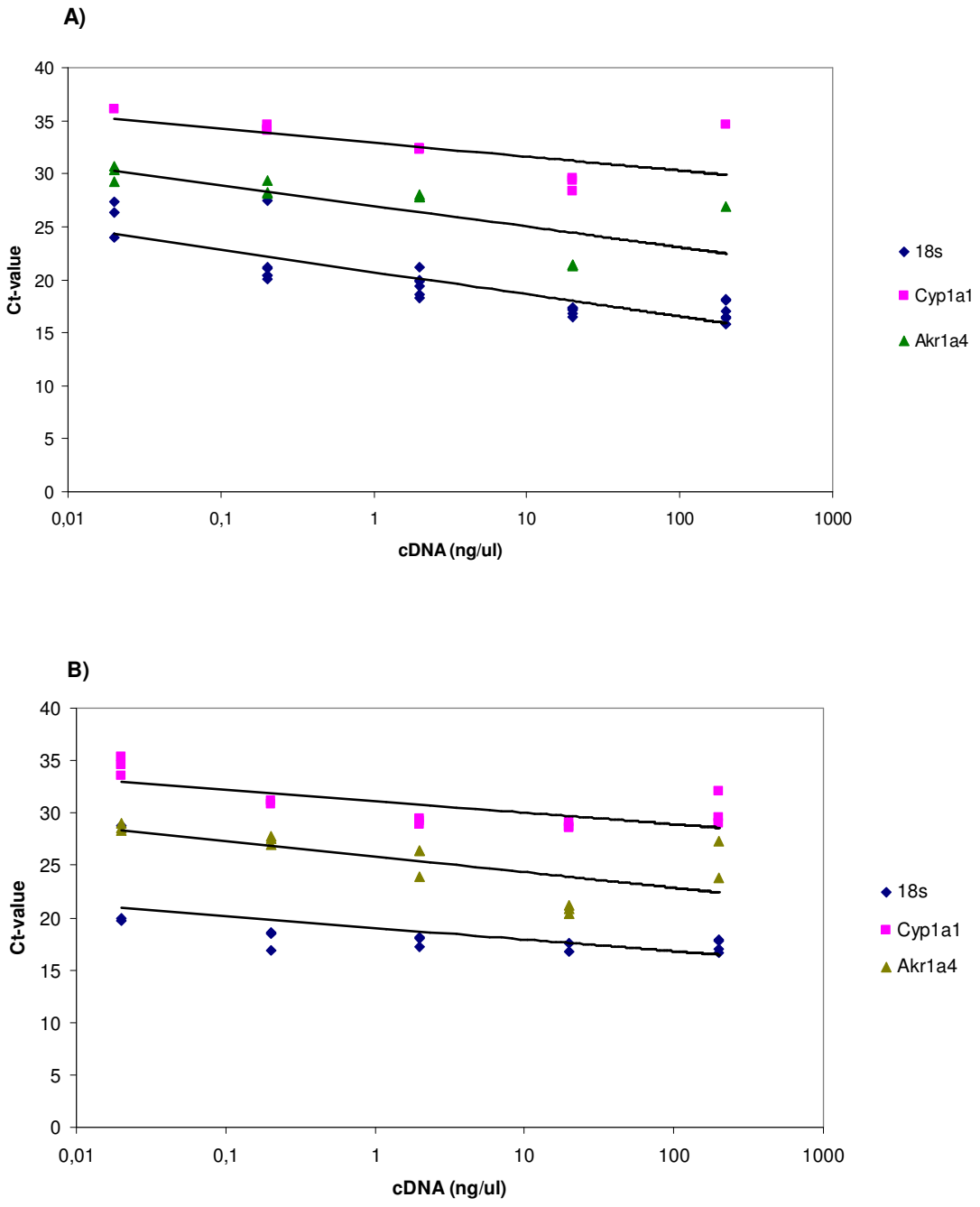

Figure 3.7: Serial dilution curve. cDNA standard for liver *Ogg1*$^{-/-}$ (A) and *Ogg1*$^{+/+}$(B) for *18s rRNA, Cyp1a1* and *Akr1a4*. R^2 for *Ogg1*$^{-/-}$ *18s rRNA* is 0.33, for *Cyp1a1* 0.51 and for *Akr1a4* it is 0.48. For *Ogg1*$^{+/+}$ R^2 is *18s rRNA 0.72, Cyp 1a1* 0.39 and *Akr1a4* 0.59.

3.3.4 Gene expression analysis

The relative gene expression of two genes (*Cyp1a1* and *Akr1a4)*, which are involved in the BaP-metabolism, were studied in testis, liver and lung from mice exposed to BaP, corn oil and unexposed controls (CTL). Animals were sacrificed at Day 1, 3, 5 or 17 after exposure. There are three mice that were sacrificed at Day 17 after corn oil treatment. For every treatment group there are three mice, and for every mouse there are three technical replicates. Four CTL mice were used. For every CTL there are two technical replicates. All samples are normalised to the geometric average of five (or four) HKGs, BK-value (see section 3.3.2). The average of CTL mice was used as calibrators. i.e. each normalised gene (ΔCT -target gene) was subtracted by average unexposed controls (CTL) (ΔCT-control) in the $2^{-\Delta\Delta CT}$ – method to find fold differences. The relative expression of a target gene (fold change) in BaP or corn oil exposed sample compared with unexposed controls (CTL) is given as: fold change = $2^{-\Delta\Delta CT}$. The log2-transformed fold change values were used to construct Figure 3.7 and 3.8.

3.3.4.1 The effect of BaP on Cyp1a1 gene expression

In the testis $Ogg1^{-/-}$ and $Ogg1^{+/+}$ samples had significant different ($p < 0.01$) expression patterns with maximum induction at Day 1 for $Ogg1^{+/+}$, while $Ogg1^{-/-}$ samples reached maximum level at Day 5 (Figure 3.8A), at Day 17 the *Cyp1a1* gene expression reached baseline level for both $Ogg1^{+/+}$ and $Ogg1^{-/-}$ samples. In liver there was time-dependent statistical significant ($p < 0.05$) induction of *Cyp1a1* in both $Ogg1^{-/-}$ and $Ogg1^{+/+}$ compared to untreated controls (Figure 3.8B). Both $Ogg1^{-/-}$ and $Ogg1^{+/+}$ had similar expression pattern between the genotypes, with maximum induction at Day 1. Then the *Cyp1a1* gene expression declines to the baseline level at seventeen days after exposure (Figure 3.8B). In the lung there was induction of *Cyp1a1* both in $Ogg1^{+/+}$ and $Ogg1^{-/-}$ but the expression pattern was somehow different ($p = 0.01$) (Figure 3.8C). The *Cyp1a1* gene expression level reached maximum induction at Day 1 for both samples.

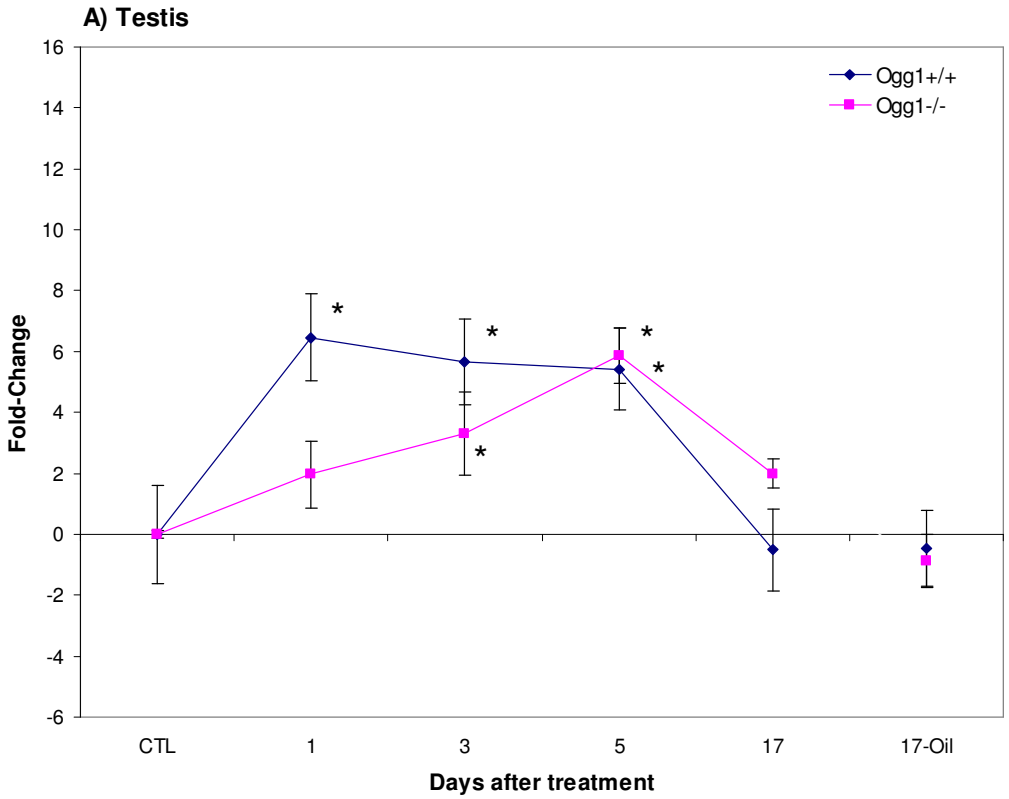
A) Testis
Ogg1+/+
Ogg1-/-
Fold-Change
16
14
12
10
8
6
4
2
0
-2
-4
-6
CTL
1
3
5
17
17-Oil
Days after treatment

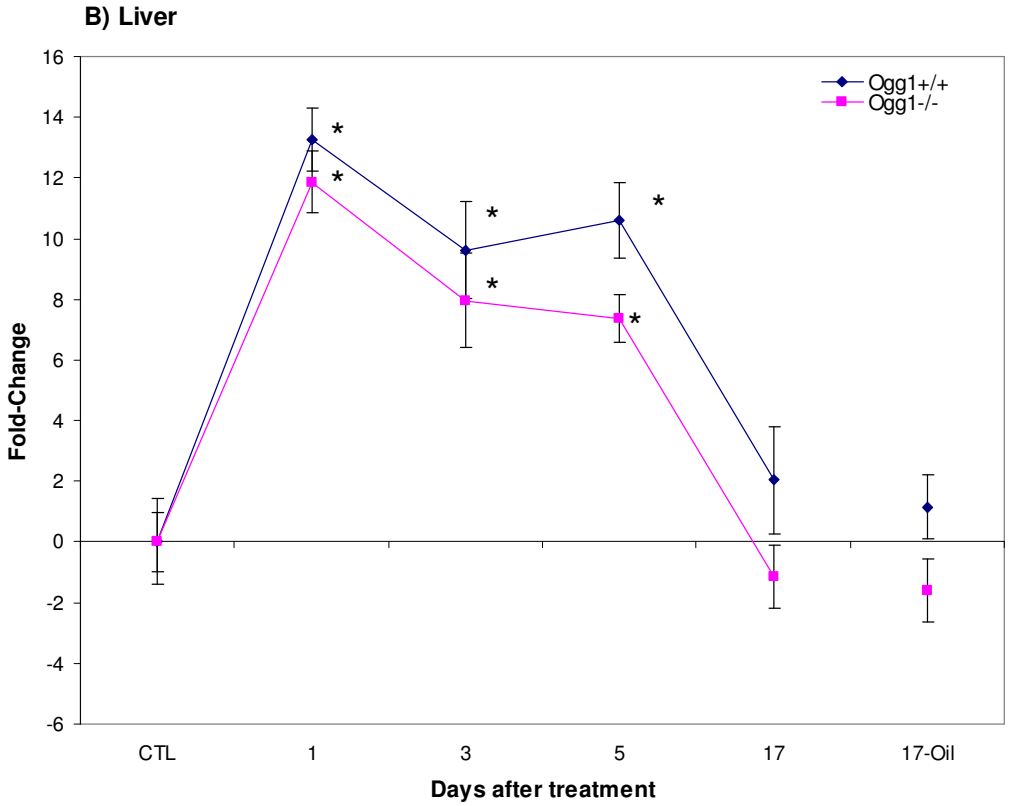
B) Liver
Ogg1+/+
Ogg1-/-
Fold-Change
16
14
12
10
8
6
4
2
0
-2
-4
-6
CTL
1
3
5
17
17-Oil
Days after treatment

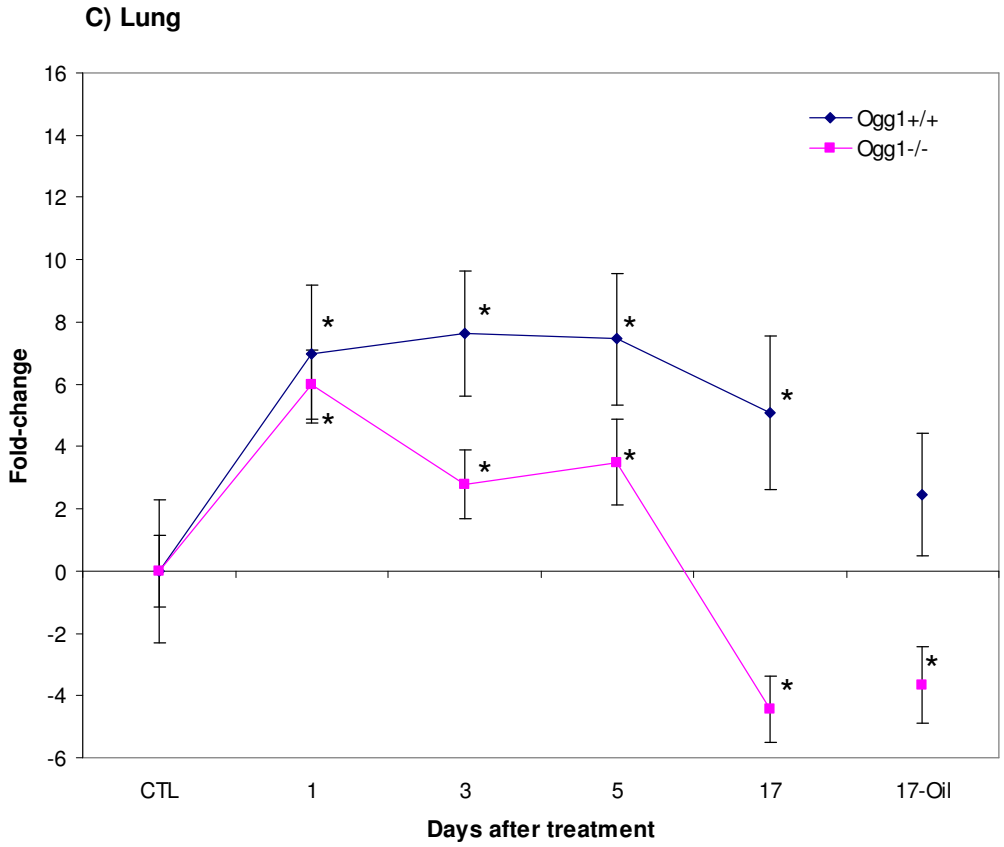

Figure 3.8: Relative gene expression. *Cyp1a1* gene expression in testis (A), liver (B) and lung (C) of mice treated with BaP. There are three mice at every group and three technical replicates for each of them. The mean of all the results using the ΔΔCT method ± SE is shown for the different days after exposure. A: Statistical significant increase at Day 1,3 and 5 for both genotypes (except $Ogg1^{-/-}$ Day 1) compared to CTL value. B: Statistical significant increase at Day 1,3 and 5 compared to CTL value for both genotypes ($p < 0.05$). C: Statistical increase (and decrease) for all results for both genotypes, except WT Day 17-oil. * Statistical significant different from CTL ($p < 0.05$)

3.3.4.2 The effect of BaP on Akr1a4 gene expression

In the testis the *Akr1a4* gene expression pattern of $Ogg1^{-/-}$ mice was significantly different from the expression pattern of $Ogg1^{+/+}$ ($p < 0.001$), with no induction of *Akr1a4* gene in $Ogg1^{-/-}$ mice and a maximum induction in $Ogg1^{+/+}$ mice at Day 17 (Figure 3.9A). In the liver the *Akr1a4* gene expression pattern was similar ($p > 0.05$) for both $Ogg1^{-/-}$ and $Ogg1^{+/+}$ mice and no induction of the *Akr1a4* gene was observed (Figure 3.9B). In the lung there was a time dependent induction of the *Akr1a1* gene in both $Ogg1^{-/-}$ and $Ogg1^{+/+}$ mice (Figure 3.9C). The *Akr1a4* gene expression pattern of $Ogg1^{-/-}$ mice was significantly different from

the expression pattern of *Ogg1*$^{+/+}$ ($p < 0.001$), with a maximum induction at Day 5 for *Ogg1*$^{+/+}$ mice and Day 17 for *Ogg1*$^{-/-}$ mice (Figure 3.9C).

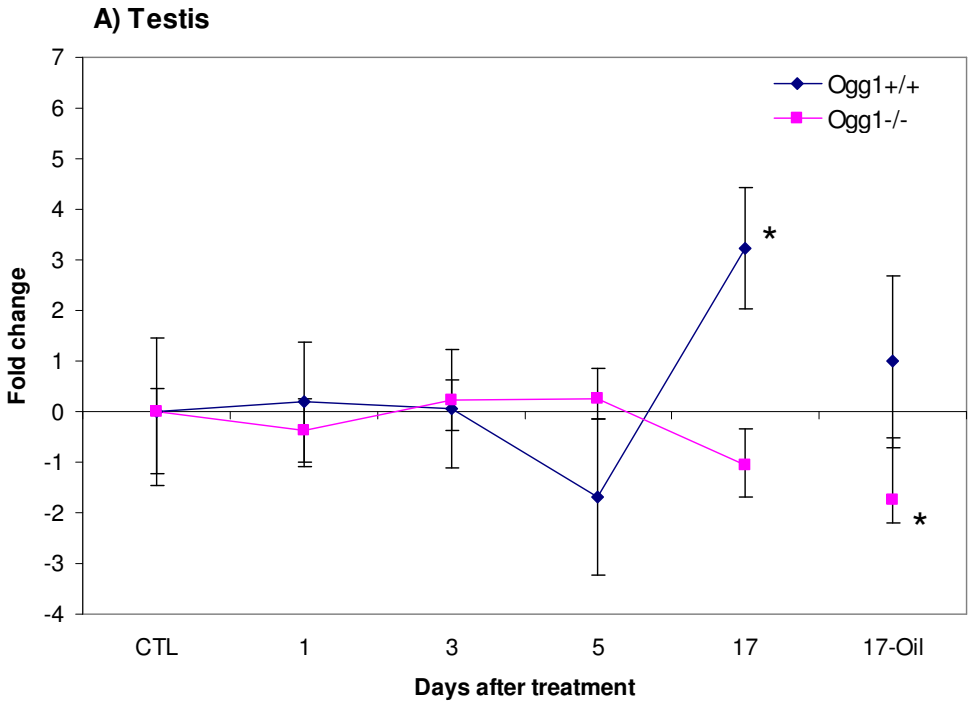

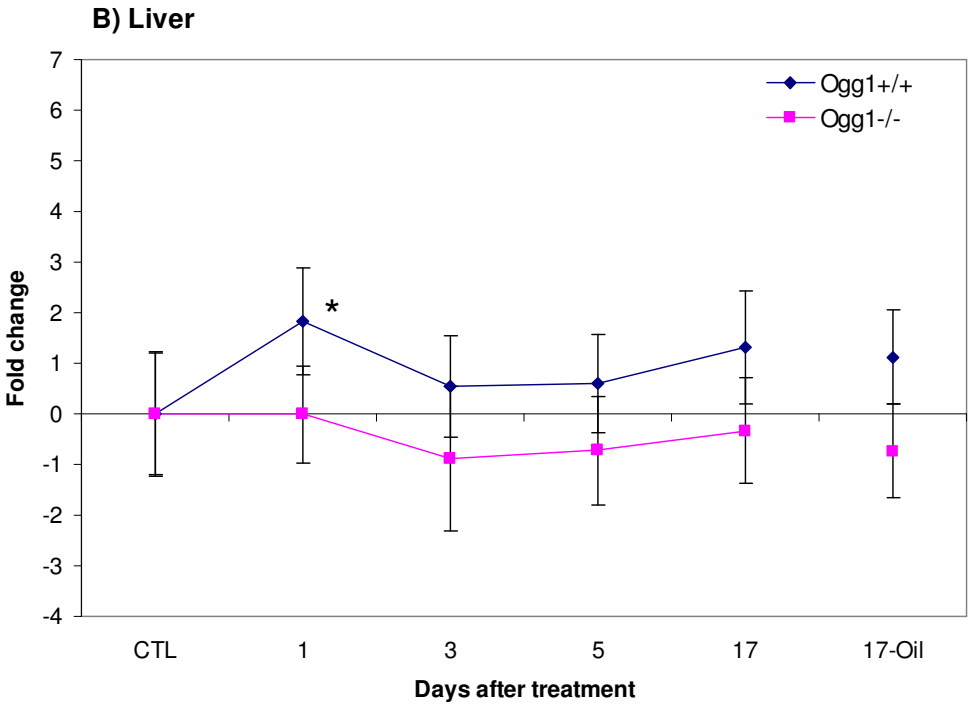

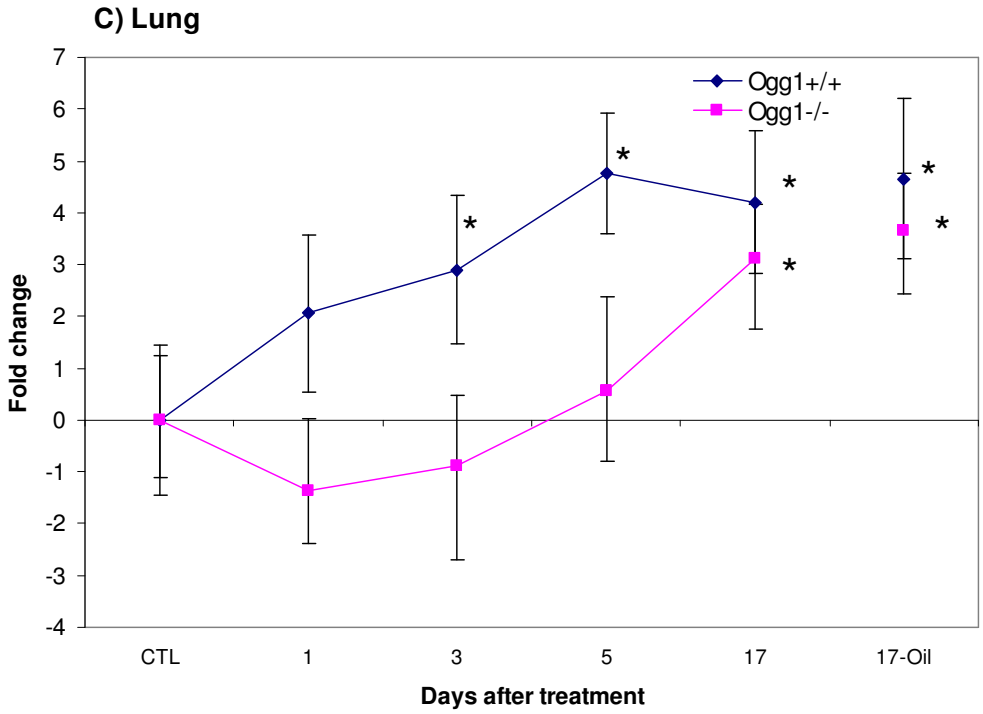

Figure 3.9: Relative gene expression of *Akr1a4*. *Akr1a4* gene expression in testis (A), liver (B) and lung (C) of mice treated with BaP. There are three mice in every group and three technical replicates for each of them. The mean of the results after using the ΔΔCT method ± SE are shown. A: Statistical significant increase at Day 17 for $Ogg1^{+/+}$ compared to CTL value, and significant decrease for $Ogg1^{-/-}$ Day 17-oil compared to CTL. B: Statistical significant increase at Day 1 for $Ogg1^{+/+}$ compared to CTL value. C: Statistical significant increase at Day 17 and Day 17-oil for both genotypes and also for Day 3 and 5 for $Ogg1^{+/+}$ compared to CTL. * Statistical significant different from CTL ($p < 0.05$)

3.3.4.3 Constitutive levels of gene expression

The constitutive levels of gene expression were evaluated (Figure 3.10). The relative quantities are derived from the normalised $2^{-\Delta CT}$ values of unexposed CTL mice were used. The figure shows a higher constitutive expression level of *Akr1a4* gene in all tissues compared to the *Cyp1a1*gene expression level, with the highest difference in testis, medium difference in liver and the lowest difference in lung. From the figure (Figure 3.10) we also see that the *Akr1a4* gene expression clearly is higher in $Ogg1^{-/-}$ mice for both testis and liver tissue.

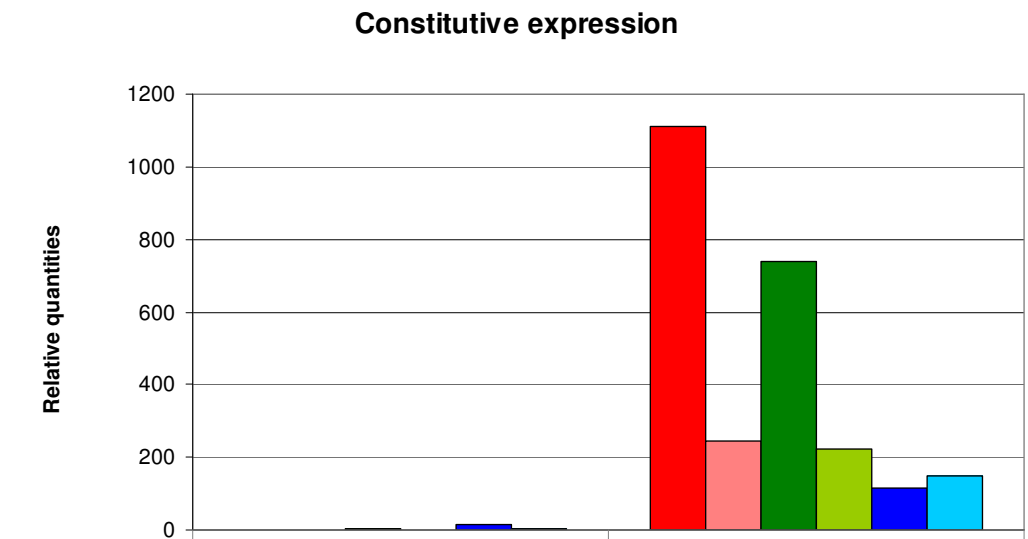

	Cyp1a1	Akr1a4
Testis Ogg1-/-	0.02	1110
Testis Ogg1+/+	0.06	247
Liver Ogg1-/-	2.7	738
Liver Ogg1+/+	0.9	221
Lung Ogg1-/-	14	117
Lung Ogg1+/+	3	148

Figure 3.10: The constitutive expression of *Cyp1a1* and *Akr1a4*. The relative quantities are derived from the normalised $2^{-\Delta CT}$ values for CTL mice for *Cyp1a1* and *Akr1a4* in all tissues for both $Ogg1^{-/-}$ and $Ogg1^{+/+}$ mice.

4. Discussion

On a daily basis, we are exposed to PAHs such as BaP from food, burning of fossil fuels, forest fire, tobacco smoke and diesel exhaust which qualifies for extensive studies to achieve a thorough understanding of the possible negative effects of exposure of humans. Knowing that smoking men have more DNA damage than non-smokers in their sperm (Sipinen *et al.*, 2010), and that DNA damage in the sperm is correlated with reduced sperm quality and disturbed embryo development (Aitken *et al.*, 2009) give rise for concern for the possible negative effects on male germ cells of human exposure to environmental agents. Moreover smoking men have lower success rates in assisted reproduction procedures (Zitzmann *et al.*, 2003) and paternal exposure to PAHs via cigarette smoke increase the risk of childhood cancer in the offspring (Boffetta *et al.*, 2000; Cordier *et al.*, 1997; Lee *et al.*, 2009).

BaP-exposure leads to induction of DNA damage that may be removed via DNA repair. We have previously shown that human testicular cells exhibit poor repair of oxidative damage such as 8-oxoG, compared to rodents (Olsen *et al.*, 2003). We, and others, have also shown that male germ cells exhibit a low NER function for several bulky DNA adducts, including BPDE-adducts (Brunborg *et al.*, 1995; Jansen *et al.*, 2001; (Olsen *et al.*, 2010; Verhofstad *et al.*, 2010b) . These findings indicate that male germ cells, particularly human, may be very sensitive for exposure to certain environmental agents and that care should be taken in extrapolating results from rodents to man. The use of repair deficient mice, such as *Ogg1*$^{-/-}$ mice, thus mimics the repair capacity of human male germ cells and allows more relevant analyses of genotoxicity of exposure to environmental agents.

In this study a small increase in oxidative damage was observed in the testis at Day 31 following BaP-exposure of *Ogg1*$^{-/-}$ mice (Figure 3.1), which was most evident in haploid round spermatids (Figure 3.2). Oxidative damage was also induced in the somatic tissues investigated; we observed a small increase at Day 31 in the liver and a more pronounced induction in the lung at both Day 17 and Day 31 (Figure 3.1) in *Ogg1*$^{-/-}$ mice. The analyses of NADP/NADPH-ratios (Figures 3.4 and 3.5) along with expression analyses of *Cyp1a1* (Figures 3.8 and 3.10) and *Akr1a4* (Figures 3.9 and 3.10) in the different tissues corroborated the DNA damage levels observed.

4.1 Testis

BaP is found in high levels in cigarette smoke and has been shown to induce increased levels of 8-oxoG lesions and DNA adducts in sperm, as well as abnormal sperm and reduced fecundity (Fraga *et al.*, 1996; Zenzes *et al.*, 1999a; Zitzmann *et al.*, 2003). BaP gives rise to bulky DNA lesions in sperm and testicular cells at all stages of spermatogenesis (Verhofstad *et al.*, 2010a; Verhofstad *et al.*, 2010b; Zenzes *et al.*, 1999a). Recently, we reported a temporal pattern of genotoxic consequences following exposure to BaP (Olsen *et al*. 2010); exposure to stem cell spermatogonia gave de novo mutations in the resulting sperm whereas exposure late during spermatogenesis gave sperm containing high levels of bulky BPDE-adducts (Olsen *et al*. 2010).

In Study 1, a marginal, but statistically significant increase in Fpg-ss at 17 days after BaP exposure in male germ cells from *Ogg1*$^{-/-}$ mice, using the comet assay (Meier2008). In this work we aim to reproduce this experiment. The increase in Fpg-ss at Day 17 after BaP-exposure was not verified in this experiment. Anyhow at Day 31 we do observe a small increase in net Fpg-ss (Figure 3.1) is observed, and we can ascribe this damage to the haploid rohund spermatids (Figure 3.2). These data are however based on one single animal for each genotype. The haploid round spermatides scored in the comet assay originated from spermatogonial stem cells at the time of exposure. This suggests that the stem cell stage may be susceptible to accumulation of Fpg-ss following BaP-exposure. Stem cell spermatogonia are located at the outside of the blood-testis barrier and may therefore be more exposed to agents via the blood. Spermatogonia are rapidly dividing making the DNA less tight and prone for damage. Although BaP-exposed samples had higher DNA damage levels than corn oil treated samples at Day 31, the damage levels recorded were not higher than the spontaneous background damage level (Appendix B). We thus suggest that exposure to BaP give rise to limited oxidative damage in male germ cells certain stages of spermatogenesis, assuming that the oxidative damage induced have not been removed by back-up repair.

The amount of NADP and NADPH in the testis was low compared to liver or lung. NADPH needs to be present, as the reducing cofactor of the quinone, for the formation of ROS (Figure 1.8). A decrease in the amount of NADPH will give an indication of the amount of ROS formed. A low amount of NADP and NADPH in testis indicates that there may be

limited reduction to catechol of the quinones formed and hence limited formation of ROS in the testis (Park *et al.*, 2006a). The somatic tissues had higher initial levels of NADPH, which may be one of the reasons why testicular cells differ in accumulation of oxidative DNA damage. We observed a marked increase in NADP/NADPH ratio at Day 3 showing that the level of NADPH is indeed reduced compared to NADP, and the observed increased ratios were not statistically different between *Ogg1*$^{-/-}$ and *Ogg1*$^{+/+}$ mice. Deficiency in repair of oxidative damage due to Ogg1 thus did not influence the dynamics of NADP or NADPH. These are indications for at least some futile redox cycling do occur in testicular cells forming ROS, but at levels that are undetectable as oxidative DNA damage in the comet assay during time frame investigated, with exception for the damage observed at Day 31 following exposure.

The expression of *Cyp1a1* in *Ogg1*$^{+/+}$ and *Ogg1*$^{-/-}$ mice was greatly increased in all tissues (Figure 3.8), with the lowest increase in testis. The temporal expression pattern in the testis differed significant ($p < 0.01$) between *Ogg1*$^{-/-}$ and *Ogg1*$^{+/+}$ mice; in the *Ogg1*$^{-/-}$ testis there was a gradual increase with a maximum at Day 5, whereas in *Ogg1*$^{+/+}$ testis there was maximal increase at Day 1 that was equally high at Day 3 and 5, followed by a decrease at Day 17 in both genotypes with *Ogg1*$^{+/+}$ showing baseline levels and *Ogg1*$^{-/-}$ approaching baseline levels. The *Cyp1a1* gene expression pattern observed in this study was largely similar (with minor discrepancies) to that observed in Study 1;(Meier et al. 2008). The reproducibility of these results in two studies with two different operators indicates that the experimental approaches used are reliable and robust. It has also been reported a low constitutive and highly induced expression of *Cyp1a1* in the testis, even higher than in the liver, following a single i.p. exposure to PAH (100 mg/kg bw) of C57BL/6J mice, sacrificed after 72 hours (Shimada *et al.*, 2003) and this report correspondence well with our results.

Akr1a4 is a mouse homologue of the human AKR1A1 (Barski *et al.*, 1999), which is one of several AKR-enzymes involved in BaP metabolism (AKR1A1, and AKR1C1-1C4) (Penning *et al.*, 1996). The constitutive expression of *Akr1a4* gene is markedly higher than *Cyp1a1* gene in testis (Figure 3.10), and this differences is more pronounced in testis than in the other tissues investigated. High constitutive expression was observed in Study 1;(Meier *et al.* 2008), and also reported by others (Allan and Lohnes 2000). In humans AKR1A1 gene is expressed in the testis (Barski *et al.*, 1999). The high constitutive expression level of *Akr1a4*

gene may favour metabolism of BaP via the AKR-route in the testis, which facilitate ROS generation. However, this requires the availability of reducing agents and oxygen within the cell. The high constitutive *Akr1a4* mRNA level is probably associated with the stable *Akr1a4* expression observed after BaP-exposure in the testis. Similar *Akr1a4* gene expression pattern was observed for *Ogg1*$^{-/-}$ mice in Study 1, but the expression magnitude was somehow lower than our result. The BaP exposure induced *Akr1a4* expression at Day 17 in *Ogg1*$^{+/+}$ mice, which was not apparent in *Ogg1*$^{-/-}$ mice (Figure 3.9A). The AKR enzymes can efficiently compete with CYPs for metabolising BaP, and the dominant pathway depends on the redox state of the cell (Quinn and Penning2008). When quinones are formed they lead directly to induction of CYP enzymes through the AhR-pathway (Burczynski and Penning 2000; Park *et al.*, 2006a). Testis cells exhibit a lower amount of NADPH and a lower oxygen pressure than liver and lung, implying that the AKR pathway might not dominate.

Several *in vitro* studies with BaP in different cell types have found 8-oxoG damage following BaP exposure (Briede *et al.*, 2004; Park *et al.*, 2006a; Park *et al.*, 2008a; Park *et al.*, 2009; Park *et al.*, 2006b; Quinn and Penning2008; Sipinen *et al.*, 2010),. Only few *in vivo* studies of BaP have been conducted, and to our knowledge none of these have reported on oxidative damage in testis.

In human sperm, using the comet assay plus Fpg our group observed DNA damage irrespective of BaP and BPDE exposure (Sipinen *et al*. 2010), showing that this method is suitable for measuring oxidative damage.

BaP-induced oxidative damage may theoretically arise in male germ cells in several ways; (i) futile redox cycling of quinones arising via the AKR-pathway in nuclei after AhR translocation, (ii) indirect induction due to the presence of BPDE (maybe through extensive damage to mitochondria) or (iii) via a general inflammatory process after acute dosing to BaP. The appearance of detectable levels of oxidative DNA lesions may thus not be expected immediately after BaP exposure. The small induction of oxidative damage observed at Day 31, may thus be ascribed to one or several of the above mentioned options.

Mitochondrial DNA plays a vital role in sperm, for processes such as sperm motility. Mitochondrial DNA is more susceptible for ROS-attack due to the essentially unprotected nature (Sawyer *et al.*, 2001). Genes regarding mitochondrial functions, such as energy

metabolism is required to propel the flagellum (Kao *et al.*, 1998), has been reported to be down regulated in BaP-exposed mice (Verhofstad *et al.*, 2010a). BaP-exposure is thus likely to impair sperm motility and fertilisation capacity, and may contribute to explain the low *in vitro* fertilisation rates for smoking fathers (Zitzmann *et al.*, 2003). Chromatin anomalies in human spermatozoa in general give a lower fertilization rate (Sakkas *et al.*, 1998). This may however act as a selective mechanism, not making offspring from damaged sperm. Female mice fertilised by BaP-exposed *Xpc*$^{-/-}$ males were indeed found to have smaller litters (Verhofstad *et al.*, 2010a).

4.2 Liver

In the liver of BaP-exposed *Ogg1*$^{-/-}$ mice a small decrease in net Fpg-ss was observed at Day 17 followed by an increase at Day 31 (Figure 3.1). In *Ogg1*$^{+/+}$ mice there were a modest increase in net Fpg-ss at Day 17 that decreased to baseline levels at Day 31, but this increase at Day 17 might as well be due to really few Fpg-ss in the oil treated samples than an actual increase in Fpg-ss in the BaP treated samples, because it is still lower than CTL values (Figure 7.2, Appendix B). Comparing the genotypes, we found a significant difference between net Fpg-ss at Day 17 ($p = 0.049$), with *Ogg1*$^{-/-}$ liver showing lower levels than *Ogg1*$^{+/+}$ liver. These findings suggest that Fpg-ss sites are transiently reduced followed by an induction after BaP-exposure, and that the use of *Ogg1*$^{-/-}$ mice facilitated their detection. Our findings correlate well with the previous experiment conducted (Study 1;(Meier2008)), observing no significant increases in oxidative DNA damage for the time points up to Day 17 after exposure to BaP.

The liver had the highest initial level of NADPH compared with testis and lung (Table 3.1) and the relative NADPH amount declined in both genotypes following BaP-exposure with *Ogg1*$^{-/-}$ mice showing a maximum reduction at later time points than the *Ogg1*$^{+/+}$ mice (Figures 3.4 and 3.5). However, the NADPH/NADP-ratios were changed considerably in *Ogg1*$^{+/+}$ mice compared to *Ogg1*$^{-/-}$ mice, and the *Ogg1*$^{+/+}$ mice showed another peak at a later time point (Day 5). These data (Day 1, Day 3 and Day 5) are however based on single animal in each group, and must therefore be interpreted with care. At Day 17 three mice were included in each group. The reduced relative amounts of NADPH after BaP exposure suggest

that the quinones formed in the liver are reduced to catechols, implying that ROS are most likely formed in liver cells, which is in compliance with the induced Fpg-ss detected at Day 31.

Similarly, and as expected, the fold change of *Cyp1a1* was highest in the liver compared to the other tissues. The temporal expression patterns were however similar in $Ogg1^{-/-}$ and $Ogg1^{+/+}$ mice, with a maximum at Day 1 (Figure 3.8B). In line with this, a significant increase in *Cyp1a1* at Day 1 after exposure followed by a gradual decrease to base levels at Day 17, both for $Ogg1^{-/-}$ and $Ogg1^{+/+}$ mice were observed in Study 1;(Meier2008).

The expression of *Akr1a4* was not altered in any of the genotypes (Figure 3.9B). This may be associated with the high constitutive level of *Akr1a4*, compared to *Cyp1A1* (Figure 3.10). Alternatively *Cyp1A1* is more important than *Akr1a4* for BaP-metabolism in the liver, consistent with high levels of BPDE-adducts compared to the levels of oxidative damage in liver cells. The liver can indeed express the highest amount of CYP-enzymes of all tissues (Casarett *et al.*, 2008). Anyhow, the mutagenicity of a compound is not always determined by the most prevalent DNA-lesion, but more to the occurrence of DNA lesion with the high mutagenic potential.

The levels of Fpg-ss sites observed in the $Ogg1^{-/-}$ mice observed may be underestimated compared to the actual level of oxidative damage induced due to back-up DNA repair. The liver most probably do express backup DNA repair systems (see chapter 4.1.4) since the liver is the most important organ for metabolising exogenous agents (Casarett *et al.*, 2008), agents that in many cases will lead to induction of oxidative damage.

4.3 Lung

BaP lead to cancer in several organs, including the lung (Melendez-Colon *et al.*, 1999; Yeh and Wu 2006)(chapter 1.3.3). BPDE-DNA adducts are believed to be involved in the development of lung cancer, but also metabolism of BaP through the AKR-pathway giving rise to *o*-quinones is shown to cause G to T transversions in *p53* cDNA, in the presence of NADPH and $CuCl_2$ (Hollstein *et al.*, 1991; Park *et al.*, 2008a). G-T transversions in *p53* is the most unambiguous signature of lung cancer. One important question to address in this

context is whether exposure to BaP *in vivo* gives rise to DNA lesions, with potential to give G to T transversions, via the AKR-pathway.

Indeed, we provide evidence that BaP-exposure do give rise to oxidative damage in the lung *in vivo.* The most pronounced induction of oxidative DNA damage among the tissues investigated was in the lung of *Ogg1*$^{-/-}$ mice (Figure 3.1). We thereby confirm the findings in Study 1;(Meier *et al*. 2008) of significant increase in Fpg-sensitive sites in lung tissue at Day 17 after BaP-exposure. Supporting evidence is provided by the consumption of NADPH (Figures 3.4 and 3.5) and induction of *Akr1a4* (Figure 3.9) irrespective of genotype following BaP-exposure, even if the expression levels of *Akr1a4* differed between the genotypes. The findings suggest that BaP-metabolism through the AKR-pathway is important in the lung. Furthermore the induced oxidative damage may contribute to give rise to G to T transversions in genes like *p53* and thereby maybe adding to the risk of lung cancer.

Others have investigated ROS and DNA adduct formation in rat lung finding a transient decrease in 8-oxoG after oral administration of BaP exposure (10 mg BaP in tricapryline/kg bw), this study lasted for 20 days (Briede *et al.*, 2004).

Stedeford et al. (2001) studied effects of BaP given to rats by measuring 8-oxoG levels and activity of *Ogg1* in lung, kidney and liver tissue. The rats were given 20 mg/kg body weight BaP in corn oil i.p. twice a day for up to five days, giving a maximum dose of 200 mg/kg body weight. The relative amount of 8-oxoG was 7-fold increased at day three and returned back to basal levels at day five. They measured 8-oxoG using a HPLC method, which have been compared to results obtained with the comet assay by Gedik and Collins *et al.* (2005). HPLC-methods were found to be less sensitive that the comet assay, and during the isolation of non-related DNA oxidative damage is easily introduced to the DNA. In the comet assay, we isolate cells or nuclei circumventing this challenge (Gedik and Collins2005). Stedeford further reported that the *Ogg1* activity was initially inhibited in lung tissue measured by cleavage of double-stranded oligonucleotides carrying a DNA lesion by tissue extracts. They found an initial decrease at three days and increased activity at five days in the lung whereas the activity was unchanged in the other organs tested. The *in vitro* assay used is however linear only at low levels of oligonucleotide cleavage, giving possibility for non-accurate conclusions.

Further, we showed elevated expression of *Cyp1a1* in both genotypes, with a maximum at Day 1 (≈ 8-fold) after exposure (Figure 3.8). The expression levels were approximately 50% lower than that observed in the liver and comparable to the induction in the testis. This is consistent with others reporting lower amounts of CYP enzymes in the lung compared to liver (Cavalieri and Rogan1995; Stedeford *et al.*, 2001). The expression in *Ogg1*$^{-/-}$ mice differed from the wild type with the *Ogg1*$^{-/-}$ mice expressing lower levels of *Cyp1a1* than the wild type at the subsequent time-points after Day 1 eventually expressing *Cyp1a1* at levels below the level of untreated mice at Day 17. This indicate that the absence of Ogg1 influence the metabolism of BaP. Moreover, and supporting the induction of oxidative damage in the lung, it was the only organ investigated where *Akr1a4* was induced, in both genotypes (figure 3.8), with increasing expression levels with time, suggesting that AKR plays a central role in the lung for the metabolism of BaP. Induction of oxidative damage in the lung is further supported by the complete consumption of the existing NADPH already at Day 1 after exposure in both genotypes. Active AKR-pathway leading to generation of ROS is consistent with the oxidative damage we observed in the lung (Figure 3.1).

Our findings also correlate well with *in vitro* studies showing that lung tissue has a high capacity to form quinones (Figure 1.2) (Bevan and Weyand1988; Cavalieri and Rogan1995). The decreasing NADPH suggest that the quinones are formed also *in vivo* and are likely to be reduced to catechols giving rise to futile redox cycles forming ROS (Figures 1.2 and 1.8, (Penning2004)).

Relative to the induction of bulky BPDE-adducts, Verhofstad *et al.* (2009) exposed mice to BaP (oral dose of 13 mg/kg bw) and measured bulky BPDE-adducts in lung, testis and sperm. They observed increased BPDE-adduct levels at day one for lung, with a gradual decline until 14 days after treatment. This corresponds with our findings with expression of *Cyp1a1*, which is maintained at high levels the first five days and decline at Day 17 (Figure 3.8).

In the absence of Ogg1 it is evident that oxidative damage detectable by Fpg accumulates in the mouse lung at Day 17 following exposure, suggesting that BaP gives rise to ROS in the lung. Such induction is not apparent in wild type mice, probably due to efficient removal of oxidative damage via base excision repair. The damage levels were detectable in the lung of *Ogg1*$^{-/-}$-mice despite the existence of back-up repair, possibly explaining why oxidative

damage was not evident at earlier time points after BaP-exposure. The actual level of oxidative damage induced by BaP is therefore probably underestimated.

4.4 Backup repair mechanisms

The limited amounts of oxidative DNA damage observed in the testis and liver in *Ogg1*$^{-/-}$ mice suggests that ROS are not formed in marked amounts or that or that oxidative DNA damage is removed via back-up, or redundant, DNA repair. Findings by Klungland *et al.* (1999) suggest that in the absence of Ogg1 an alternative repair pathway exist, to minimize the effects of an increased load of 8-oxoG in the genome. This has also been suggested after observing a transient reduction, that can be because of induction of repair enzymes, of oxidative DNA damage of testis, liver and lung of mice deficient in Ogg1 (Briede *et al.*, 2004; Meier2008). NER is an important repair pathway for DNA adducts, reviewed by (Rechkunova and Lavrik2010), and has been suggested to be a backup repair pathway for oxidative damage (Lin and Sancar 1989; Sunesen *et al.*, 2002). Alternatively, other DNA glycosylases may excise oxidative DNA lesions, such as NTH1, NEIL1 and NEIL2, with variable efficiency. Mammalian hNTH1 and hNEIL1 recognise several common oxidative base lesions and have been proposed to have redundant repair roles in cells (Katafuchi *et al.*, 2004), a role that probably becomes more evident for 8-oxoG in cells lacking hOGG1. NEIL1 is ubiquitous expressed in most tissues and is found to have properties similar to mammalian OGG1, with preferred removal of 8-oxoG basepared with C (Morland *et al.*, 2002). NEIL2 on the other hand have marginal or negligible lyase activity when it was tested on oxidative base lesions (Katafuchi *et al.*, 2004), but it needs further investigation. MYH removes adenine basepared with 8-oxoG (Aburatani *et al.*, 1997), whereas OGG1 removes 8-oxoG basepared with G, so MYH will still remove some of the 8-oxoG in the cells.

Another interesting characteristic of NEIL1 as backup repair are its ability to excise hydantoins from DNA (Krishnamurthy *et al.*, 2008). Oxidation of 8-oxoG leads to the formation of hydantoins, a class of oxidative damage that have recently been getting more attention due to their unusual structure and high mutagenic potential (David *et al.*, 2007; Neeley and Essigmann 2006). Hydantions are suggested to be the best substrate known for NEIL1 so far (Krishnamurthy *et al.*, 2008; Zhao *et al.*, 2010). Cells of the *Ogg1*$^{-/-}$ mice that

exhibit significant levels of spontaneous oxidative damage may be susceptible for the generation of hydantoins via oxidation, with subsequent efficient removal via NEIL1. Oxidation leading to hydantoins *in vivo* will therefore probably be efficiently removed (within hours) in *Ogg1*$^{-/-}$ mice instead of being measured as oxidative damage in the comet assay. Hydantions are also excised by Fpg giving rise to Fpg-ss in the comet assay. The role of DNA backup repair needs to be further investigated.

If there is an induction of oxidative damage in testis and liver, it is only a small induction, and the backup repair mechanism might be able to remove the damage before we are able to se anything.

The oxidative damage observed was delayed compared with the induction of metabolic enzymes and reduction in NADPH. In the cells of all tissues examined there are initially higher levels (Figure 3.10) of *Akr1a4*, favouring the formation of quinones. The quinones as well as BaP itself are ligands for AhR, thereby inducing *Cyp1a1* (Park *et al.*, 2009), which translocates BaP into the nuclei thereby facilitating ROS generation within the nuclei. If AhR is an important pathway in testis for human is unsure, because there have been reported an extremely high AhRR gene expression in testis, compared to lung and liver (Yamamoto *et al.*, 2004). In mice the expression pattern of AhRR mRNA varies from tissue to tissue, both in untreated mice, and BaP treated mice (Bernshausen *et al.*, 2006).

4.5 Methodological consideration

4.5.1 Design and conduction of experiment

This work was divided into two parts; the first part was to confirm the findings in a previous master degree (Study 1; (Meier2008)) whereas part two was to further understand the effects of BaP-exposure by including more animals and new analyses. This study is denoted Study 2.

These studies are large, time- and labour-consuming mouse studies. The numbers of mice at selected time points as well as untreated control mice were increased in Study 2 compared to the Study 1 to obtain more robust results, and other time points of sacrifice after exposure

were included (10 and 31 days). In Study 1 a small but significant increase in oxidative DNA lesions was observed in testicular cells from *Ogg1*$^{-/-}$-mice at Day 17 following BaP-exposure. This finding warranted confirmation. In this study sacrifice of mice prior to and also after Day 17 following exposure were included to further explore the possible induction of oxidative DNA damage in mice exposed to BaP. In Study 1 expression of genes involved in BaP-metabolism were measured in the testis and liver and were normalised to only one untreated mice, whereas in Study 2 analyses of the lung were included since BaP is a lung carcinogen and the results were normalised to a higher number of untreated control mice.

The mice in our studies were given one acute dose of BaP of 150 mg/kg body weight. This is a high dose given as one single exposure compared with the level and manner of exposure of humans (3 mg/day in USA, according to Environmental Protection Agency (Stedeford *et al.*, 2001)). Higher exposure to humans might be expected in cases where chronically exposure occurs through cigarette smoke, occupation or living in the vicinity of contaminated sites. It is common practise to use high exposure in animal experiments for effects to be evident. For BaP we used a dose that is below LD_{50} dose of 232 mg/kg for mice (Salamone M.F. 1981). Corn oil was used as vehicle, and we observed unexpected high oxidative damage in some mice treated with corn oil only (both old and new corn oil; see appendix B), and the reason for the high corn oil induced oxidative damage is unknown.

The genotypes of the mice used were *Ogg1*$^{-/-}$ and *Ogg1*$^{+/+}$. Several oxidatively modified DNA bases are removed by *Ogg1* (Aburatani *et al.*, 1997; Boiteux and Radicella 1999). *Ogg1* deficient mice serve two purposes: First, the *Ogg1*$^{-/-}$ mouse line functions as a model for human testicular cells mimicking the low repair capacity for oxidative DNA lesions (Olsen et al., 2003). Second, the repair of oxidative DNA damage in cells of *Ogg1*$^{-/-}$ mice is reduced and leading to a possible accumulation in any tissue, depending on the activity of back-up repair systems, thereby increasing the potential for detecting such DNA lesions. In wild type mice such lesions are rapidly repaired and may therefore not be detected.

4.5.2 The comet assay

The single-cell gel electrophoresis technique or comet assay is widely regarded as a quick and reliable method of analysing DNA damage in individual cells and has been used for over 20 years (McArt *et al.*, 2009). It is a sensitive tool and has ability to detect a wide range of

DNA damage (McArt *et al.*, 2009; Moller 2006; Ostling and Johanson 1984), and it is a central method in our lab. The method is easy and quick, but there are still challenges to resolve. One limitation is the ability to detect very low or very high levels of DNA damage with precision. The sensitivity is best when the assay is calibrated then from as low as one hundred breaks and up to several thousand breaks per cell can be determined, and by adding enzyme treatment (like Fpg) the range and sensitivity is greatly increased (Collins *et al.*, 2008). Thus even small increase in Fpg-ss should be detected in our comet assay.

There are different aspects to the comet assay techniques that might give difference in results; solution molarity, pH, wash times, unwinding times, electrophoresis time, staining and microscope settings all which contribute to the scoring value, making it important to include some kind of calibration in the assays Also the person scoring (the operator) may introduce bias since the cells/nuclei to be scored are chosen by the operator. Ideally, the operator should be "blind", not knowing if the sample is treated or not, to avoid bias. The scoring is preferably done without personal interference, but sometimes the operator has to manually set the middle of the comet head due to software limitations

Due to the unexpected and unexplainable high damage level in samples from mice sacrificed at Day 10 after oil exposure, we decided to expose more mice to repeat this finding. We observed that the exposure to oil itself might give some oxidative damage in all the tissues (Appendix B). We also observed lower levels of Fgp-sensitive sites in the untreated CTL mice than observed in previous untreated CTL mice, which is likely to be due to operator skills getting better. The experiment, from sacrifice, to squeezing of nuclei/cells from tissues, and moulding of cells into gels was faster for the later mice sacrificed. We know from previous experiments of this kind, that the time from sacrifice to the cells/nuclei are moulded in gels and subjected to lysis is important for keeping background damage levels low. Due to these issues some experiments were discarded due to high background damage levels.

4.5.3 NADP/NADPH ratios

The procedure was conducted according to the recommendations of the manufacturer and pilot studies showed that the measurements were stabile. The amount of tissue required for each organ and initial steady state ratios were established in pilot studies. We used ~20 µg for each organ and since the amount of tissue was not identical in every reaction the total

quantity of NADP and NADPH could not be detected, but the ratios were established. Using approximately similar amounts of tissue from each organ it was evident that the liver exhibited the highest level of NADPH, with lower levels in the lung and little in the testis. Few biological or technical replicates exist for these results, which might be a source of error.

4.5.4 Real time PCR

Following the example of the microarray community and the MIAME guidelines (Brazma and Vilo 2001), the Real-Time PCR Data Markup Language (RDML) consortium has recently proposed the Minimum Information for Publication of Quantitative Real-Time PCR Experiments (MIQE) guidelines that describe the minimum information necessary for evaluating RT-qPCR experiments (Bustin *et al.*, 2009). In Study 2, we tried to follow the MIQE-guideline in the RT-qPCR experiments and our data are in compliance with the guideline. We set up the experiments to have at least three mice (at least three biological replicates) in each group and three technical replicates to obtain robust results. For untreated control animals we included as many as four animals. This is more animals than was used in Study 1; (Meier2008). We also decided to include five reference genes to obtain more accurate results. In this way, we tried to control some of the technical aspects that may affect assay performance and result interpretation. Some of the technical aspects that must be controlled include: sample storage, preparation, and RNA quality (purity and integrity), reverse-transcription details, PCR efficiencies, and analysis parameters (statistical analyses), and finally, sample normalisation (against single or several reference genes, and justification of the choice of reference genes). We used the geometrical average of five reference genes and the BestKeeper software (Pfaffl *et al.,* 2004b) was used to evaluate the stability of these reference genes (Figure 3.6 and Appendix B).

4.6 Conclusions

Our first aim was to reproduce the results obtained in a previous study, Study 1;(Meier *et al*. 2008). In Study 1 a small but significant induction of Fpg-ss was observed in testicular cells of Ogg1-defective mice. We were unable to reproduce this small increase at Day 17, but we

found a possible increase at Day 31 after BaP exposure. The existence of potential backup DNA repair in the testis may have hampered the detection of such damage. In general, most of the findings in this study (Study 2) correlate well with the results in Study 1. The question of whether BaP-exposure leads to oxidative damage in male germ cells needs further investigation.

BaP exposure clearly gave rise to oxidative damage in lung, and from this thesis and work done by others, the lung seems as the most sensitive organ to BaP exposure with respect to induction of oxidative damage. Our results suggest that this is due to metabolism of BaP through the AKR-pathway creating ROS. Moreover, we also found induction of oxidative damage in liver after exposure to BaP at Day 31 after exposure

Investigating the ratio of NADP/NADPH gave results that were concurrent with the gene expression dat aand the damage levels observed. NADPH was present initially in all three tissues at various steady-state levels, enabling the reduction of quinones to catechol and thereby the futile cycle required for creating ROS. NADPH were clearly consumed and reformed in all tissues.

Cyp1a1 was induced in all tissues, with a maximum level at day one, for all except testis in *Ogg1*$^{-/-}$ that had a maximum level at Day 5 after exposure to BaP. *Akr1a4* gene expression was induced in liver for both genotypes and in WT testis at day 17 after exposure to BaP. Constitutively Akr1A4 was present at high constitutively levels whereas Cyp1A1 was almost absent in the tissues, allowing the BaP-metabolism to be routed into this pathway until Cyp1A1 was induced. This is favourable for ROS-generation and oxidative DNA damage.

Altogether our findings indicate that BaP is metabolised in all tissues investigated and clearly forming oxidative DNA damage in lung. The possibility of BaP inducing oxidative damage in male germ cells is still not resolved, and needs further investigation.

4.7 Future work

The possibility of BaP-induced oxidative DNA damage in male germ cells, and in lung, should be confirmed. This could be done by exposing more animals and sacrificing them at appropriate time points using the present methods and including alternative methods for

damage detection such as analytical methods. The use of mouse models with other repair defects would help outline the existence of possible back-up DNA repair of oxidative damage. In line with this, studying the regulation of other DNA repair proteins after BaP-exposure, would give indications on the importance of possible back-up repair and their role in the respective tissues studied. Further investigating of the NADP/NADPH ratios would strengthen the study, and also finding the total amount of NADP and NADPH. A inclusion of studies of inflammatory responses in the tissues, or in the blood, which also can induce ROS could be useful to deduce whether it is the high exposure levels of BaP that indirectly gives oxidative damage due to inflammation or it is due to metabolism of BaP. A study using lower exposure levels exposing for longer periods would also give indications on the relevance of the findings in this study to real-life exposure levels.

References

Reference List

Aburatani, H., Hippo, Y., Ishida, T., Takashima, R., Matsuba, C., Kodama, T., Takao, M., Yasui, A., Yamamoto, K., and Asano, M. (1997). Cloning and characterization of mammalian 8-hydroxyguanine-specific DNA glycosylase/apurinic, apyrimidinic lyase, a functional mutM homologue. *Cancer Res* **57,** 2151-2156.

Adami, H. O., Bergstrom, R., Mohner, M., Zatonski, W., Storm, H., Ekbom, A., Tretli, S., Teppo, L., Ziegler, H., Rahu, M., and . (1994). Testicular cancer in nine northern European countries. *Int J Cancer* **59,** 33-38.

Adler, I. D. (1996). Comparison of the duration of spermatogenesis between male rodents and humans. *Mutat. Res* **352,** 169-172.

Aitken, R. J., and De Iuliis, G. N. (2010). On the possible origins of DNA damage in human spermatozoa. *Mol Hum Reprod.* **16,** 3-13.

Aitken, R. J., De Iuliis, G. N., and McLachlan, R. I. (2009). Biological and clinical significance of DNA damage in the male germ line. *Int J Androl* **32,** 46-56.

Allan, D., and Lohnes, D. (2000). Cloning and developmental expression of mouse aldehyde reductase (AKR1A4). *Mech. Dev* **94,** 271-275.

Archibong, A. E., Ramesh, A., Niaz, M. S., Brooks, C. M., Roberson, S. I., and Lunstra, D. D. (2008). Effects of benzo(a)pyrene on intra-testicular function in F-344 rats. *Int J Environ Res Public Health* **5,** 32-40.

Barski, O. A., Gabbay, K. H., and Bohren, K. M. (1999). Characterization of the human aldehyde reductase gene and promoter. *Genomics* **60,** 188-198.

Bernshausen, T., Jux, B., Esser, C., Abel, J., and Fritsche, E. (2006). Tissue distribution and function of the Aryl hydrocarbon receptor repressor (AhRR) in C57BL/6 and Aryl hydrocarbon receptor deficient mice. *Arch Toxicol* **80,** 206-211.

Bevan, D. R., and Weyand, E. H. (1988). Compartmental analysis of the disposition of benzo[a]pyrene in rats. *Carcinogenesis* **9,** 2027-2032.

Bjorge, C., Brunborg, G., Wiger, R., Holme, J. A., Scholz, T., Dybing, E., and Soderlund, E. J. (1996). A comparative study of chemically induced DNA damage in isolated human and rat testicular cells. *Reprod. Toxicol* **10,** 509-519.

Boffetta, P., Tredaniel, J., and Greco, A. (2000). Risk of childhood cancer and adult lung cancer after childhood exposure to passive smoke: A meta-analysis. *Environ Health Perspect* **108,** 73-82.

Boiteux, S., and Radicella, J. P. (1999). Base excision repair of 8-hydroxyguanine protects DNA from endogenous oxidative stress. *Biochimie* **81,** 59-67.

Brazma, A., and Vilo, J. (2001). Gene expression data analysis. *Microbes. Infect* **3,** 823-829.

Briede, J. J., Godschalk, R. W., Emans, M. T., De Kok, T. M., Van, A. E., Van, M. J., Van Schooten, F. J., and Kleinjans, J. C. (2004). In vitro and in vivo studies on oxygen free radical and DNA adduct formation in rat lung and liver during benzo[a]pyrene metabolism. *Free Radic. Res* **38,** 995-1002.

Brunborg, G., Holme, J. A., and Hongslo, J. K. (1995). Inhibitory effects of paracetamol on DNA repair in mammalian cells. *Mutat. Res* **342,** 157-170.

Brunborg, G., Holme, J. A., Soderlund, E. J., Omichinski, J. G., and Dybing, E. (1988). An automated alkaline elution system: DNA damage induced by 1,2-dibromo-3-chloropropane in vivo and in vitro. *Anal. Biochem.* **174,** 522-536.

Burczynski, M. E., and Penning, T. M. (2000). Genotoxic polycyclic aromatic hydrocarbon ortho-quinones generated by aldo-keto reductases induce CYP1A1 via nuclear translocation of the aryl hydrocarbon receptor. *Cancer Res* **60,** 908-915.

Bustin, S. A., Benes, V., Garson, J. A., Hellemans, J., Huggett, J., Kubista, M., Mueller, R., Nolan, T., Pfaffl, M. W., Shipley, G. L., Vandesompele, J., and Wittwer, C. T. (2009). The MIQE guidelines: minimum information for publication of quantitative real-time PCR experiments. *Clin Chem* **55,** 611-622.

Casarett, L. J., Doull, J., and Klaassen C.D. (2008). Casarett and Doull's Toxicology: The Basic Science of Poisons, The McGraw-Hill.

Cavalieri, E. L., and Rogan, E. G. (1995). Central role of radical cations in metabolic activation of polycyclic aromatic hydrocarbons. *Xenobiotica* **25,** 677-688.

Cleaver, J. E. (1989). DNA repair in man. *Birth Defects Orig. Artic. Ser.* **25,** 61-82.

Collins, A. R. (2005). Assays for oxidative stress and antioxidant status: applications to research into the biological effectiveness of polyphenols. *Am J Clin Nutr* **81,** 261S-267S.

Collins, A. R., Oscoz, A. A., Brunborg, G., Gaivao, I., Giovannelli, L., Kruszewski, M., Smith, C. C., and Stetina, R. (2008). The comet assay: topical issues. *Mutagenesis* **23,** 143-151.

Cordier, S., Lefeuvre, B., Filippini, G., Peris-Bonet, R., Farinotti, M., Lovicu, G., and Mandereau, L. (1997). Parental occupation, occupational exposure to solvents and polycyclic aromatic hydrocarbons and risk of childhood brain tumors (Italy, France, Spain). *Cancer Causes Control* **8,** 688-697.

David, S. S., O'Shea, V. L., and Kundu, S. (2007). Base-excision repair of oxidative DNA damage. *Nature* **447,** 941-950.

David-Cordonnier, M. H., Laval, J., and O'Neill, P. (2001). Recognition and kinetics for excision of a base lesion within clustered DNA damage by the Escherichia coli proteins Fpg and Nth. *Biochemistry (Mosc).* **40,** 5738-5746.

De Iuliis, G. N., Thomson, L. K., Mitchell, L. A., Finnie, J. M., Koppers, A. J., Hedges, A., Nixon, B., and Aitken, R. J. (2009). DNA damage in human spermatozoa is highly correlated with the efficiency of chromatin remodeling and the formation of 8-hydroxy-2'-deoxyguanosine, a marker of oxidative stress. *Biol Reprod.* **81,** 517-524.

Devi, K. P., Kiruthiga, P. V., Pandian, S. K., Archunan, G., and Arun, S. (2008). Olive oil protects rat liver microsomes against benzo(a)pyrene-induced oxidative damages: an in vitro study. *Mol. Nutr. Food Res* **52 Suppl 1,** S95-102.

Duale, N. Causes and consequenses of cellular response to toxicants. 2010. Faculty of Medicine.
Ref Type: Thesis/Dissertation

Edwards, B. K., Brown, M. L., Wingo, P. A., Howe, H. L., Ward, E., Ries, L. A., Schrag, D., Jamison, P. M., Jemal, A., Wu, X. C., Friedman, C., Harlan, L., Warren, J., Anderson, R. N., and Pickle, L. W. (2005). Annual report to the nation on the status of cancer, 1975-2002, featuring population-based trends in cancer treatment. *J Natl. Cancer Inst.* **97,** 1407-1427.

Fraga, C. G., Motchnik, P. A., Wyrobek, A. J., Rempel, D. M., and Ames, B. N. (1996). Smoking and low antioxidant levels increase oxidative damage to sperm DNA. *Mutat. Res* **351,** 199-203.

Gallagher, J., George, M., Kohan, M., Thompson, C., Shank, T., and Lewtas, J. (1993). Detection and comparison of DNA adducts after in vitro and in vivo diesel emission exposures. *Environ Health Perspect* **99,** 225-228.

Gedik, C. M., and Collins, A. (2005). Establishing the background level of base oxidation in human lymphocyte DNA: results of an interlaboratory validation study. *FASEB J* **19,** 82-84.

Gelboin, H. V. (1980). Benzo[alpha]pyrene metabolism, activation and carcinogenesis: role and regulation of mixed-function oxidases and related enzymes. *Physiol Rev* **60,** 1107-1166.

Håland, J. T. Ogg1-defekte mus som modell for genotoksisitet i mannens kjønnsceller. 2005.
Ref Type: Thesis/Dissertation

Hankinson, O. (2005). Role of coactivators in transcriptional activation by the aryl hydrocarbon receptor. *Arch Biochem Biophys.* **433,** 379-386.

Hansen, S. H., Olsen, A. K., Soderlund, E. J., and Brunborg, G. (2010). In vitro investigations of glycidamide-induced DNA lesions in mouse male germ cells and in mouse and human lymphocytes. *Mutat. Res* **696,** 55-61.

Hollstein, M., Sidransky, D., Vogelstein, B., and Harris, C. C. (1991). p53 mutations in human cancers. *Science* **253,** 49-53.

Holstein, A. F., Schulze, W., and Davidoff, M. (2003). Understanding spermatogenesis is a prerequisite for treatment. *Reprod. Biol Endocrinol.* **1,** 107.

Hsu, G. W., Ober, M., Carell, T., and Beese, L. S. (2004). Error-prone replication of oxidatively damaged DNA by a high-fidelity DNA polymerase. *Nature* **431,** 217-221.

Hudder, A., and Novak, R. F. (2008). miRNAs: effectors of environmental influences on gene expression and disease. *Toxicol Sci* **103,** 228-240.

IARC. **Agents Classified by the *IARC Monographs***. 1-100. 2010.
Ref Type: Online Source

Ide, H., and Kotera, M. (2004). Human DNA glycosylases involved in the repair of oxidatively damaged DNA. *Biol Pharm Bull.* **27,** 480-485.

Jacobsen, R., Moller, H., Thoresen, S. O., Pukkala, E., Kjaer, S. K., and Johansen, C. (2006). Trends in testicular cancer incidence in the Nordic countries, focusing on the recent decrease in Denmark. *Int J Androl* **29,** 199-204.

Jarow, J. P., and Zirkin, B. R. (2005). The androgen microenvironment of the human testis and hormonal control of spermatogenesis. *Ann N Y. Acad. Sci* **1061,** 208-220.

Kao, S. H., Chao, H. T., and Wei, Y. H. (1998). Multiple deletions of mitochondrial DNA are associated with the decline of motility and fertility of human spermatozoa. *Mol Hum Reprod.* **4,** 657-666.

Katafuchi, A., Matsubara, M., Terato, H., Iwai, S., Hanaoka, F., and Ide, H. (2004). Damage specificity of human DNA glycosylases for oxidative pyrimidine lesions. *Nucleic Acids Symp. Ser. (Oxf)* 175-176.

Klungland, A., and Bjelland, S. (2007). Oxidative damage to purines in DNA: role of mammalian Ogg1. *DNA Repair (Amst)* **6,** 481-488.

Klungland, A., Rosewell, I., Hollenbach, S., Larsen, E., Daly, G., Epe, B., Seeberg, E., Lindahl, T., and Barnes, D. E. (1999). Accumulation of premutagenic DNA lesions in mice defective in removal of oxidative base damage. *Proc Natl. Acad. Sci U S A* **96,** 13300-13305.

Kodama, H., Yamaguchi, R., Fukuda, J., Kasai, H., and Tanaka, T. (1997). Increased oxidative deoxyribonucleic acid damage in the spermatozoa of infertile male patients. *Fertil. Steril.* **68,** 519-524.

Kovacic, P., and Wakelin, L. P. (2001). Review: DNA molecular electrostatic potential: novel perspectives for the mechanism of action of anticancer drugs involving electron transfer and oxidative stress. *Anticancer Drug Des* **16,** 175-184.

Krishnamurthy, N., Zhao, X., Burrows, C. J., and David, S. S. (2008). Superior removal of hydantoin lesions relative to other oxidized bases by the human DNA glycosylase hNEIL1. *Biochemistry (Mosc).* **47,** 7137-7146.

Kubista, M., Andrade, J. M., Bengtsson, M., Forootan, A., Jonak, J., Lind, K., Sindelka, R., Sjoback, R., Sjogreen, B., Strombom, L., Stahlberg, A., and Zoric, N. (2006). The real-time polymerase chain reaction. *Mol Aspects Med* **27,** 95-125.

Leadon, S. A., Stampfer, M. R., and Bartley, J. (1988). Production of oxidative DNA damage during the metabolic activation of benzo[a]pyrene in human mammary epithelial cells correlates with cell killing. *Proc Natl. Acad. Sci U S A* **85,** 4365-4368.

Lee, K. M., Ward, M. H., Han, S., Ahn, H. S., Kang, H. J., Choi, H. S., Shin, H. Y., Koo, H. H., Seo, J. J., Choi, J. E., Ahn, Y. O., and Kang, D. (2009). Paternal smoking, genetic polymorphisms in CYP1A1 and childhood leukemia risk. *Leuk. Res* **33,** 250-258.

Lin, J. J., and Sancar, A. (1989). A new mechanism for repairing oxidative damage to DNA: (A)BC excinuclease removes AP sites and thymine glycols from DNA. *Biochemistry (Mosc).* **28,** 7979-7984.

Lindahl, T. (1974). An N-glycosidase from Escherichia coli that releases free uracil from DNA containing deaminated cytosine residues. *Proc Natl. Acad. Sci U S A* **71,** 3649-3653.

Livak, K. J., and Schmittgen, T. D. (2001). Analysis of relative gene expression data using real-time quantitative PCR and the 2(-Delta Delta C(T)) Method. *Methods* **25,** 402-408.

Lu, R., Nash, H. M., and Verdine, G. L. (1997). A mammalian DNA repair enzyme that excises oxidatively damaged guanines maps to a locus frequently lost in lung cancer. *Curr Biol* **7,** 397-407.

Mangal, D., Vudathala, D., Park, J. H., Lee, S. H., Penning, T. M., and Blair, I. A. (2009). Analysis of 7,8-dihydro-8-oxo-2'-deoxyguanosine in cellular DNA during oxidative stress. *Chem Res Toxicol* **22,** 788-797.

McArt, D. G., McKerr, G., Howard, C. V., Saetzler, K., and Wasson, G. R. (2009). Modelling the comet assay. *Biochem Soc Trans.* **37,** 914-917.

Meier, S. The fate of benzo(a)pyrene- inducted oxidative DNA damage in the testis of transgenic mice. 2008.
Ref Type: Thesis/Dissertation

Melendez-Colon, V. J., Luch, A., Seidel, A., and Baird, W. M. (1999). Cancer initiation by polycyclic aromatic hydrocarbons results from formation of stable DNA adducts rather than apurinic sites. *Carcinogenesis* **20,** 1885-1891.

Moline, J. M., Golden, A. L., Bar-Chama, N., Smith, E., Rauch, M. E., Chapin, R. E., Perreault, S. D., Schrader, S. M., Suk, W. A., and Landrigan, P. J. (2000). Exposure to hazardous substances and male reproductive health: a research framework. *Environ Health Perspect* **108,** 803-813.

Moller, P. (2006). The alkaline comet assay: towards validation in biomonitoring of DNA damaging exposures. *Basic Clin Pharmacol Toxicol* **98,** 336-345.

Morland, I., Rolseth, V., Luna, L., Rognes, T., Bjoras, M., and Seeberg, E. (2002). Human DNA glycosylases of the bacterial Fpg/MutM superfamily: an alternative pathway for the repair of 8-oxoguanine and other oxidation products in DNA. *Nucleic Acids Res* **30,** 4926-4936.

Neeley, W. L., and Essigmann, J. M. (2006). Mechanisms of formation, genotoxicity, and mutation of guanine oxidation products. *Chem Res Toxicol* **19,** 491-505.

Olsen, A. K., Andreassen, A., Singh, R., Wiger, R., Duale, N., Farmer, P. B., and Brunborg, G. (2010). Environmental Exposure of the Mouse Germ Line: DNA Adducts in Spermatozoa and Formation of De Novo Mutations during Spermatogenesis. *PLoS One* **5,** e11349.

Olsen, A. K., Bjortuft, H., Wiger, R., Holme, J., Seeberg, E., Bjoras, M., and Brunborg, G. (2001). Highly efficient base excision repair (BER) in human and rat male germ cells. *Nucleic Acids Res* **29,** 1781-1790.

Olsen, A. K., Duale, N., Bjoras, M., Larsen, C. T., Wiger, R., Holme, J. A., Seeberg, E. C., and Brunborg, G. (2003). Limited repair of 8-hydroxy-7,8-dihydroguanine residues in human testicular cells. *Nucleic Acids Res* **31,** 1351-1363.

Olsen, A. K., Lindeman, B., Wiger, R., Duale, N., and Brunborg, G. (2005). How do male germ cells handle DNA damage? *Toxicol Appl. Pharmacol* **207,** 521-531.

Osterod, M., Larsen, E., Le, P. F., Hengstler, J. G., Van Der Horst, G. T., Boiteux, S., Klungland, A., and Epe, B. (2002). A global DNA repair mechanism involving the Cockayne syndrome B (CSB) gene product can prevent the in vivo accumulation of endogenous oxidative DNA base damage. *Oncogene* **21,** 8232-8239.

Ostling, O., and Johanson, K. J. (1984). Microelectrophoretic study of radiation-induced DNA damages in individual mammalian cells. *Biochem Biophys. Res Commun.* **123,** 291-298.

Park, J. H., Gelhaus, S., Vedantam, S., Oliva, A. L., Batra, A., Blair, I. A., Troxel, A. B., Field, J., and Penning, T. M. (2008a). The pattern of p53 mutations caused by PAH o-quinones is driven by 8-oxo-dGuo formation while the spectrum of mutations is determined by biological selection for dominance. *Chem Res Toxicol* **21,** 1039-1049.

Park, J. H., Mangal, D., Frey, A. J., Harvey, R. G., Blair, I. A., and Penning, T. M. (2009). Aryl hydrocarbon receptor facilitates DNA strand breaks and 8-oxo-2'-deoxyguanosine formation by the aldo-keto reductase product benzo[a]pyrene-7,8-dione. *J Biol Chem* **284,** 29725-29734.

Park, J. H., Mangal, D., Tacka, K. A., Quinn, A. M., Harvey, R. G., Blair, I. A., and Penning, T. M. (2008b). Evidence for the aldo-keto reductase pathway of polycyclic aromatic trans-dihydrodiol activation in human lung A549 cells. *Proc Natl. Acad. Sci U S A* **105,** 6846-6851.

Park, J. H., Troxel, A. B., Harvey, R. G., and Penning, T. M. (2006a). Polycyclic aromatic hydrocarbon (PAH) o-quinones produced by the aldo-keto-reductases (AKRs) generate abasic sites, oxidized pyrimidines, and 8-oxo-dGuo via reactive oxygen species. *Chem Res Toxicol* **19,** 719-728.

Park, S. Y., Lee, S. M., Ye, S. K., Yoon, S. H., Chung, M. H., and Choi, J. (2006b). Benzo[a]pyrene-induced DNA damage and p53 modulation in human hepatoma HepG2 cells for the identification of potential biomarkers for PAH monitoring and risk assessment. *Toxicol Lett.* **167,** 27-33.

Penning, T. M. (2004). Aldo-keto reductases and formation of polycyclic aromatic hydrocarbon o-quinones. *Methods Enzymol.* **378,** 31-67.

Penning, T. M., Ohnishi, S. T., Ohnishi, T., and Harvey, R. G. (1996). Generation of reactive oxygen species during the enzymatic oxidation of polycyclic aromatic hydrocarbon trans-dihydrodiols catalyzed by dihydrodiol dehydrogenase. *Chem Res Toxicol* **9,** 84-92.

Pfaffl, M. W., Tichopad, A., Prgomet, C., and Neuvians, T. P. (2004a). Determination of stable housekeeping genes, differentially regulated target genes and sample integrity: BestKeeper - Excel-based tool using pair-wise correlations. *Biotechnology Letters* **26,** 509-515.

Pfaffl, M. W., Tichopad, A., Prgomet, C., and Neuvians, T. P. (2004b). Determination of stable housekeeping genes, differentially regulated target genes and sample integrity: BestKeeper--Excel-based tool using pair-wise correlations. *Biotechnol. Lett.* **26,** 509-515.

Quinn, A. M., and Penning, T. M. (2008). Comparisons of (+/-)-benzo[a]pyrene-trans-7,8-dihydrodiol activation by human cytochrome P450 and aldo-keto reductase enzymes: effect of redox state and expression levels. *Chem Res Toxicol* **21,** 1086-1094.

Radicella, J. P., Dherin, C., Desmaze, C., Fox, M. S., and Boiteux, S. (1997). Cloning and characterization of hOGG1, a human homolog of the OGG1 gene of Saccharomyces cerevisiae. *Proc Natl. Acad. Sci U S A* **94,** 8010-8015.

Ramesh, A., Inyang, F., Lunstra, D. D., Niaz, M. S., Kopsombut, P., Jones, K. M., Hood, D. B., Hills, E. R., and Archibong, A. E. (2008). Alteration of fertility endpoints in adult male F-344 rats by subchronic exposure to inhaled benzo(a)pyrene. *Exp Toxicol Pathol.* **60,** 269-280.

Ramesh, A., Walker, S. A., Hood, D. B., Guillen, M. D., Schneider, K., and Weyand, E. H. (2004). Bioavailability and risk assessment of orally ingested polycyclic aromatic hydrocarbons. *Int J Toxicol* **23,** 301-333.

Rechkunova, N. I., and Lavrik, O. I. (2010). Nucleotide excision repair in higher eukaryotes: mechanism of primary damage recognition in global genome repair. *Subcell. Biochem* **50,** 251-277.

Richiardi, L., Bellocco, R., Adami, H. O., Torrang, A., Barlow, L., Hakulinen, T., Rahu, M., Stengrevics, A., Storm, H., Tretli, S., Kurtinaitis, J., Tyczynski, J. E., and Akre, O. (2004). Testicular cancer incidence in eight northern European countries: secular and recent trends. *Cancer Epidemiol Biomarkers Prev* **13,** 2157-2166.

Roman, B. L., Pollenz, R. S., and Peterson, R. E. (1998). Responsiveness of the adult male rat reproductive tract to 2,3,7,8-tetrachlorodibenzo-p-dioxin exposure: Ah receptor and ARNT expression, CYP1A1 induction, and Ah receptor down-regulation. *Toxicol Appl. Pharmacol* **150,** 228-239.

Rosenquist, T. A., Zharkov, D. O., and Grollman, A. P. (1997). Cloning and characterization of a mammalian 8-oxoguanine DNA glycosylase. *Proc Natl. Acad. Sci U S A* **94,** 7429-7434.

Russel, L. D., Ettlin, R. A., Hikim, A. P., and Clegg, E. C. (1990). Histological and histopathological evaluation of the testis, Catche river press.

Sadowski, I. J., Wright, J. A., and Israels, L. G. (1985). A permeabilized cell system for studying regulation of aryl hydrocarbon hydroxylase: NADPH as rate limiting factor in benzo(a)pyrene metabolism. *Int J Biochem* **17,** 1023-1025.

Saiki, R. K., Scharf, S., Faloona, F., Mullis, K. B., Horn, G. T., Erlich, H. A., and Arnheim, N. (1992). Enzymatic amplification of beta-globin genomic sequences and restriction site analysis for diagnosis of sickle cell anemia. 1985. *Biotechnology* **24,** 476-480.

Sakkas, D., Urner, F., Bizzaro, D., Manicardi, G., Bianchi, P. G., Shoukir, Y., and Campana, A. (1998). Sperm nuclear DNA damage and altered chromatin structure: effect on fertilization and embryo development. *Hum Reprod.* **13 Suppl 4,** 11-19.

Salamone M.F. (1981). Toxicity of 41 carcinogens and noncarcinogenic analogs. *Evaluation of short-term tests for carcinogens: report of the international collaborative program* 682-687.

Sawyer, D. E., Roman, S. D., and Aitken, R. J. (2001). Relative susceptibilities of mitochondrial and nuclear DNA to damage induced by hydrogen peroxide in two mouse germ cell lines. *Redox. Rep* **6,** 182-184.

Shaposhnikov, S., Azqueta, A., Henriksson, S., Meier, S., Gaivao, I., Huskisson, N. H., Smart, A., Brunborg, G., Nilsson, M., and Collins, A. R. (2010). Twelve-gel slide format optimised for comet assay and fluorescent in situ hybridisation. *Toxicol Lett.* **195,** 31-34.

Shimada, T., Sugie, A., Shindo, M., Nakajima, T., Azuma, E., Hashimoto, M., and Inoue, K. (2003). Tissue-specific induction of cytochromes P450 1A1 and 1B1 by polycyclic aromatic hydrocarbons and polychlorinated biphenyls in engineered C57BL/6J mice of arylhydrocarbon receptor gene. *Toxicol Appl. Pharmacol* **187,** 1-10.

Sims, P., Grover, P. L., Swaisland, A., Pal, K., and Hewer, A. (1974). Metabolic activation of benzo(a)pyrene proceeds by a diol-epoxide. *Nature* **252,** 326-328.

Sipinen, V., Laubenthal, J., Baumgartner, A., Cemeli, E., Linschooten, J. O., Godschalk, R. W., Van Schooten, F. J., Anderson, D., and Brunborg, G. (2010). In vitro evaluation of baseline and induced DNA damage in human sperm exposed to benzo[a]pyrene or its metabolite benzo[a]pyrene-7,8-diol-9,10-epoxide, using the comet assay. *Mutagenesis*.

Stedeford, T., Cardozo-Pelaez, F., Hover, C., Harbison, R. D., and Sanchez-Ramos, J. (2001). Organ-specific differences in 8-oxoguanosine glycosylase (OGG1) repair following acute treatment with benzo[a]pyrene. *Res Commun. Mol. Pathol. Pharmacol.* **109,** 73-85.

Sunesen, M., Stevnsner, T., Brosh, R. M., Jr., Dianov, G. L., and Bohr, V. A. (2002). Global genome repair of 8-oxoG in hamster cells requires a functional CSB gene product. *Oncogene* **21,** 3571-3578.

Verhofstad, N., Pennings, J. L., van Oostrom, C. T., van, B. J., Van Schooten, F. J., van, S. H., and Godschalk, R. W. (2010a). Benzo(a)pyrene induces similar gene expression changes in testis of DNA repair proficient and deficient mice. *BMC Genomics* **11,** 333.

Verhofstad, N., van Oostrom, C. T., van, B. J., Van Schooten, F. J., van, S. H., and Godschalk, R. W. (2010b). DNA adduct kinetics in reproductive tissues of DNA repair proficient and deficient male mice after oral exposure to benzo(a)pyrene. *Environ Mol Mutagen.* **51,** 123-129.

Weyand, E. H., and Bevan, D. R. (1986). Benzo(a)pyrene disposition and metabolism in rats following intratracheal instillation. *Cancer Res* **46,** 5655-5661.

Xue, W., and Warshawsky, D. (2005). Metabolic activation of polycyclic and heterocyclic aromatic hydrocarbons and DNA damage: a review. *Toxicol Appl. Pharmacol* **206,** 73-93.

Yamamoto, J., Ihara, K., Nakayama, H., Hikino, S., Satoh, K., Kubo, N., Iida, T., Fujii, Y., and Hara, T. (2004). Characteristic expression of aryl hydrocarbon receptor repressor gene in human tissues: organ-specific distribution and variable induction patterns in mononuclear cells. *Life Sci* **74,** 1039-1049.

Yauk, C. L., Jackson, K., Malowany, M., and Williams, A. (2010). Lack of change in microRNA expression in adult mouse liver following treatment with benzo(a)pyrene despite robust mRNA transcriptional response. *Mutat. Res*.

Yeh, S. L., and Wu, S. H. (2006). Effects of quercetin on beta-apo-8'-carotenal-induced DNA damage and cytochrome P1A2 expression in A549 cells. *Chem Biol Interact.* **163,** 199-206.

Zenzes, M. T., Bielecki, R., and Reed, T. E. (1999a). Detection of benzo(a)pyrene diol epoxide-DNA adducts in sperm of men exposed to cigarette smoke. *Fertil. Steril.* **72,** 330-335.

Zenzes, M. T., Puy, L. A., Bielecki, R., and Reed, T. E. (1999b). Detection of benzo[a]pyrene diol epoxide-DNA adducts in embryos from smoking couples: evidence for transmission by spermatozoa. *Mol Hum Reprod.* **5,** 125-131.

Zhao, X., Krishnamurthy, N., Burrows, C. J., and David, S. S. (2010). Mutation versus repair: NEIL1 removal of hydantoin lesions in single-stranded, bulge, bubble, and duplex DNA contexts. *Biochemistry (Mosc).* **49,** 1658-1666.

Zipper, H., Brunner, H., Bernhagen, J., and Vitzthum, F. (2004). Investigations on DNA intercalation and surface binding by SYBR Green I, its structure determination and methodological implications. *Nucleic Acids Res* **32,** e103.

Zitzmann, M., Rolf, C., Nordhoff, V., Schrader, G., Rickert-Fohring, M., Gassner, P., Behre, H. M., Greb, R. R., Kiesel, L., and Nieschlag, E. (2003). Male smokers have a decreased success rate for in vitro fertilization and intracytoplasmic sperm injection. *Fertil. Steril.* **79 Suppl 3,** 1550-1554.

Appendix A

6.1 Solutions

0.75% Agarose solution (low melting point)

Added 0.075 g NuSieve GTG Low melting agarose to 10 ml of 10 mM EDTA-solution, warmed up to boiling point until the Agarose is dissolved and held warm in a warming block at 37 C.

Merchant´s buffer

0.14 M NaCl

1.47 mM KH_2PO_4

2.7 mM KCl

8.1 mM Na_2HPO_4

10 mM EDTA

Dissolved in sterile H_2O, pH adjusted to 7.4, autoclaved and stored at 4 C.

Lysis fluid for Comet (stock)

2.5 M NaCl

100 mM EDTA

10 mM Tris-base

1% SLS

Dissolved in dH_2O, before SLS was added pH was adjusted to approximately 10 with NaOH solution. The stock was leaved to stir until everything was dissolved, and then pH was adjusted again to 10 with concentrated HCl or 10M NaOH.

Lysis fluid for Comet (for GelBond films)

300 ml Lysis fluid stock

10% DMSO (33.3 ml)

1% Triton-X (3.33 ml)

Mixing together and putting at 4C

Neutralising buffer for Comet

0.4 M Tris-base

Dissolved in dH_2O and pH adjusted to 7.5 with concentrated HCl.

Electrophoresis buffer for Comet

10 M NaOH

200 mM EDTA

Dissolved in dH_2O and pH adjusted to 13.2 with concentrated HCl.

Enzyme reaction buffer for Comet

40 mM Hepes

0.1 M KCl

0.5 mM EDTA

Dissolved in dH_2O and pH adjusted to 7.6 with 7M KOH.

TE-buffer

1 mM EDTA

10 mM Tris-HCl

Dissolved in dH_2O and pH adjusted to 8.0.

6.2 Products and producers

Product	Producer	Country
2-Mercaptoetanol	Sigma	France
Absolut alcohol prima	Arkus kjemi	Norway
Benzo(a)pyrene	Sigma	USA
Bovine serum albumine	Sigma	USA
Corn oil (old)	Coop	Norway
Corn oil (new)	Sigma	USA
DMSO	Merck	Germany
dH_2O	Bibco	USA
EDTA	Sigma	USA
EnzyChrom NADP/NADPH Assay Kit	BioAssay Systems	USA
Fpg	Locally produced	Norway
Gelbond® Film	Cambrex	USA
GeneElute Mammalian Total RNA Miniprep Kit	Sigma	USA
Glycerol	Sigma	USA
Glycine	Sigma	South Korea
Hepes	Sigma	USA
High-Capacity cDNA Reverse Transcription Kit	Applied Biosystems	USA
HCl	Merck	Germany
MicroAmp 96-well reaction plate	Applied Biosystems	Singapore

Primers	Quiagen	Germany
NuSieve GTG Low melting Agarose	Cambrex	USA
PBS	Locally produced	Norway
KCl	Merck	Germany
KH_2PO_4	Merck	Germany
KOH	Merck	Germany
Power SYBR® Green	Applied Biosystems	UK
NaCL	Merck	Germany
SDS	Fluka	Japan
Na_2HPO_4	Merck	Germany
NaOH	Merck	Germany
SLS	Sigma	UK
SYBR®Gold	Invitrogen	USA
SYBR®Green	Sigma	USA
Triton-X	Sigma	USA

Appendix B

As described in chapter 3.1 there were some problems with the mice receiving corn oil and sacrificed at Day 10 after exposure. Unexpected and unexplainable high levels of Fpg-sensitive DNA damage in the corn oil treated mice were observed for both *Ogg1*$^{-/-}$ and *Ogg1*$^{+/+}$ mice:

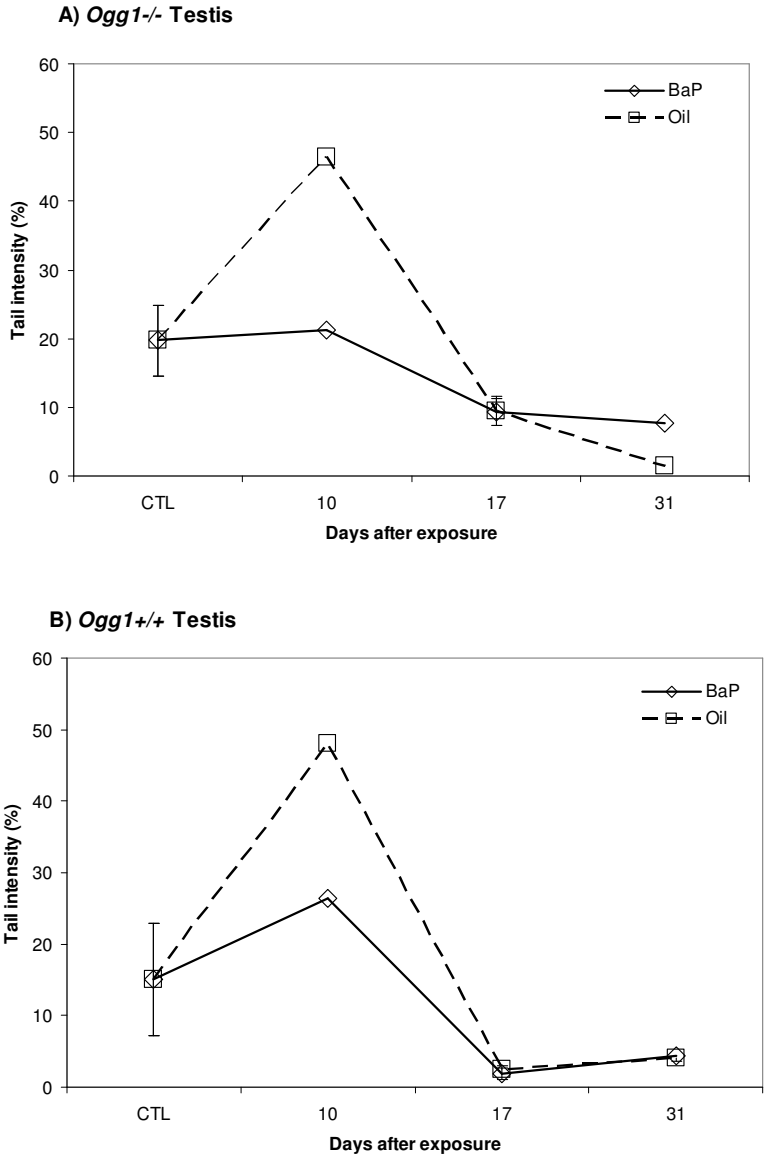

Fig 7.1: Testis, comet assay. % tail intensity in *Ogg1*$^{-/-}$ and *Ogg1*$^{+/+}$ mice at the different days after exposure.

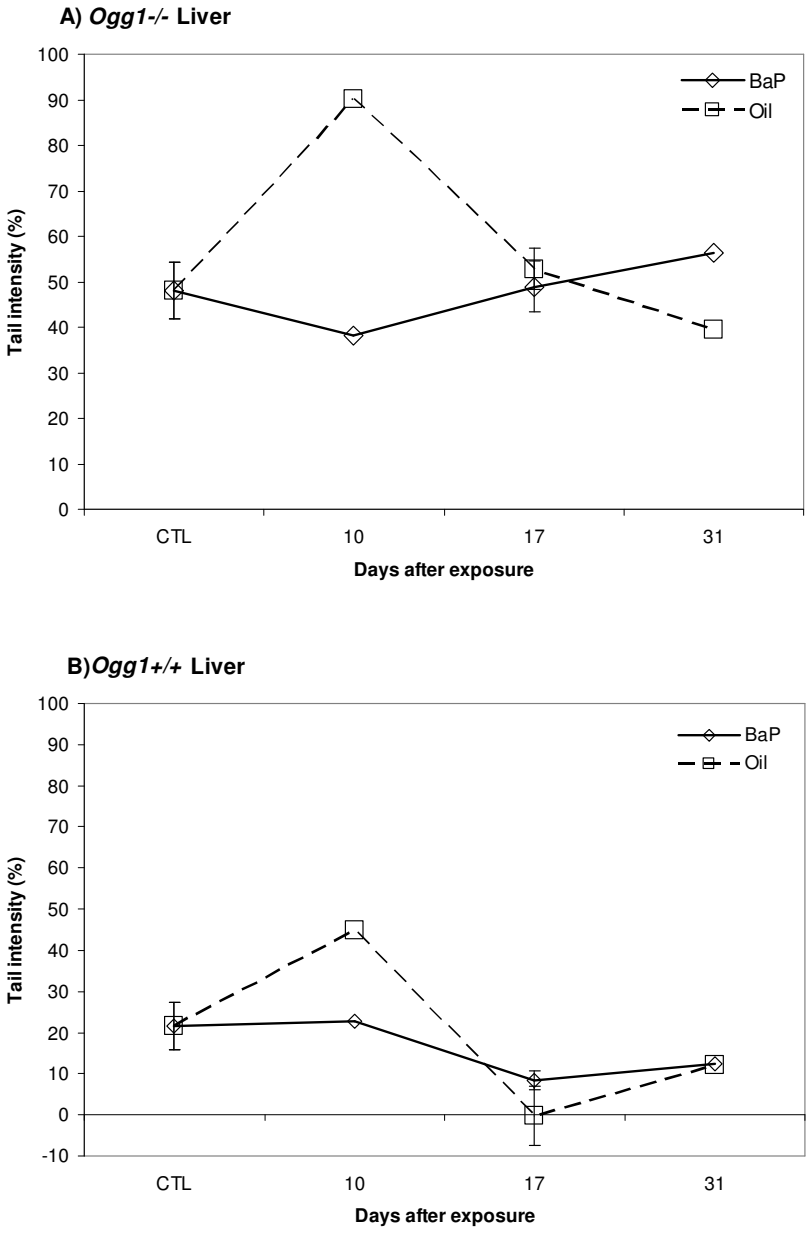

Fig 7.1: Liver, comet assay. % tail intensity in $Ogg1^{-/-}$ and $Ogg1^{+/+}$ mice at the different days after exposure.

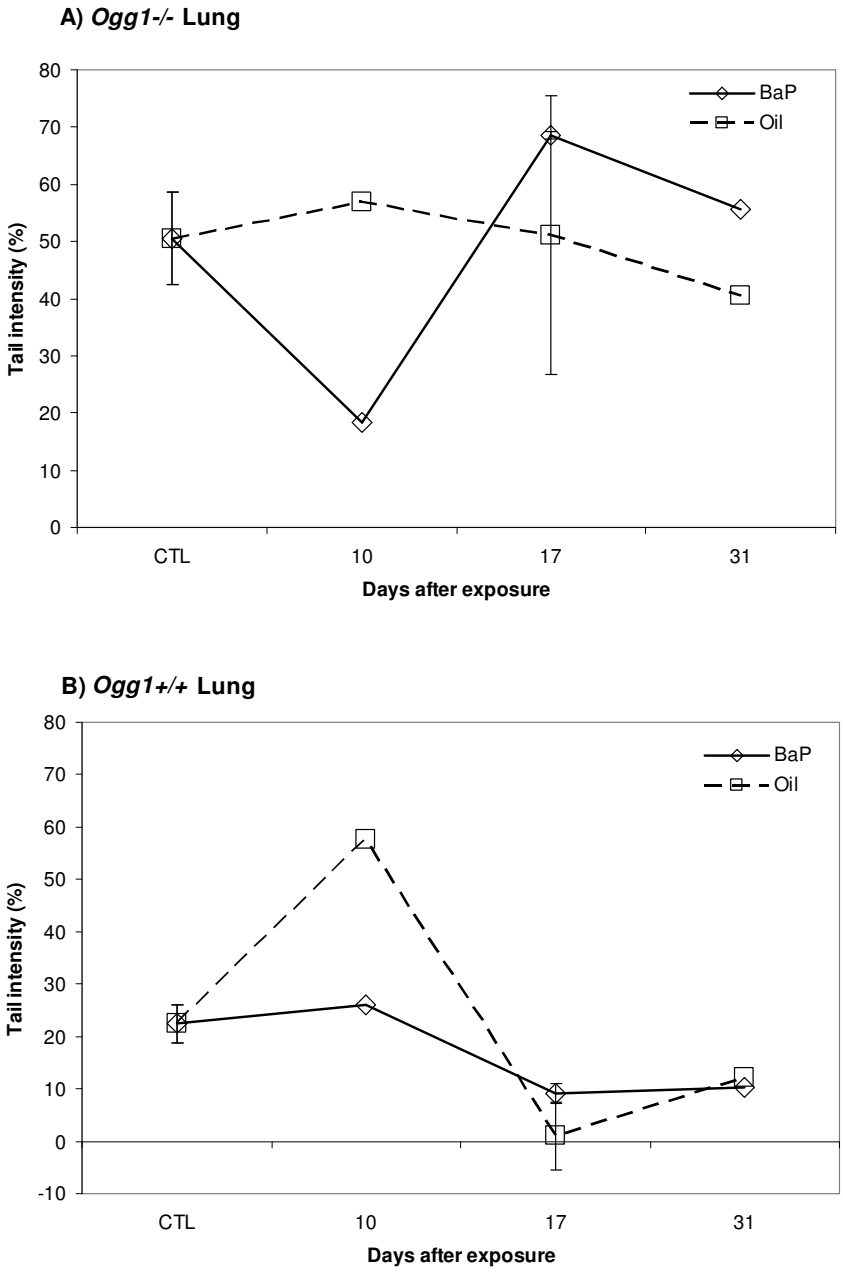

Fig 7.3: Lung, comet assay. % tail intensity in $Ogg1^{-/-}$ and $Ogg1^{+/+}$ mice at the different days after exposure.

Only one mouse was used of each genotype at Day 10, but we see the same pattern in both genotypes. We decided to repeat this part of the experiment, and also tested a new batch of corn oil (Sigma), to investigate whether corn oil alone would lead to such high DNA damage levels.

Experiment 2: Additional mice sacrificed at Day 10

Due to errors during genotyping, discovered after the experiment had been conducted, to verify the genotypes of the mice, only *Ogg1*$^{+/+}$ mice were used in experiment 2. . In the testis there were increased levels of oxidative damage following both the new and the old batch of corn oil compared to the untreated control, and BaP-exposure (using BaP dissolved in the first batch of corn oil used) did not give higher levels of oxidative damage than that observed with corn oil. Similarly, in the liver comparably increased levels of oxidative damage were observed in both corn oil- and BaP-treated mice compared to the untreated control. In the lung, on the other hand, there was no increase in the corn oil- or BaP-treated mice compared to the untreated control.

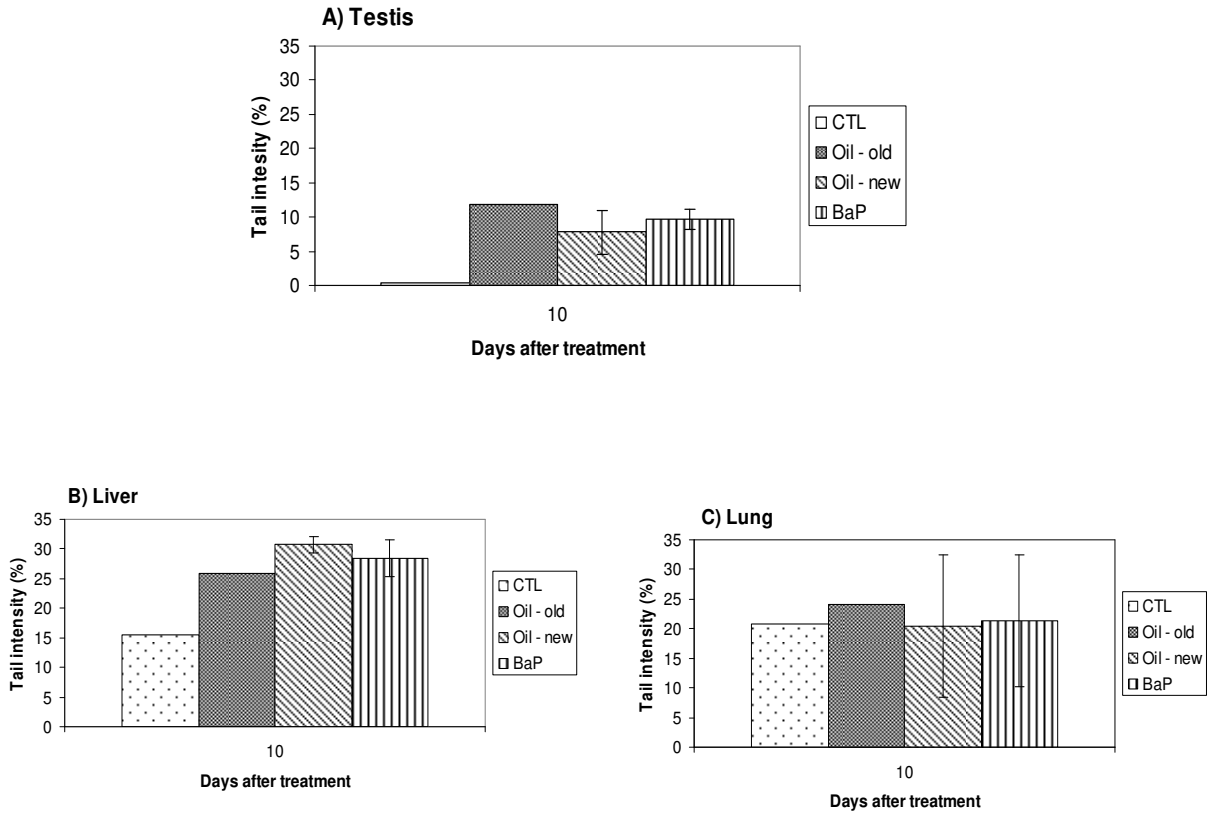

Fig 7.4: Day 10, comet assay. The % tail intensity in mice treated with oil, both old and new, and BaP, we also have one CTL mouse.

We conclude that no induction of oxidative damage occurred in *Ogg1*$^{+/+}$ mice sacrificed at Day 10 after BaP-exposure, but we do not know if this is true for *Ogg1*$^{-/-}$ mice. Corn oil

alone seems to induce some oxidative damage in the testis and liver. We cannot exclude that the mice were subjected to conditions that induced oxidative damage, such as inflammatory processes, or that errors made during the practical experiment led to these unexplainable results. We therefore chose to present the results from the mice sacrificed at Day 10 in Appendix B, and the damage levels presented (Figure 3.1) were calculated by subtracting the level of corn oil mice from that of BaP-exposed mice.

Appendix C

Evaluation of five housekeeping gene (HKG) stabilities using BestKeeper (BK) software.

A)

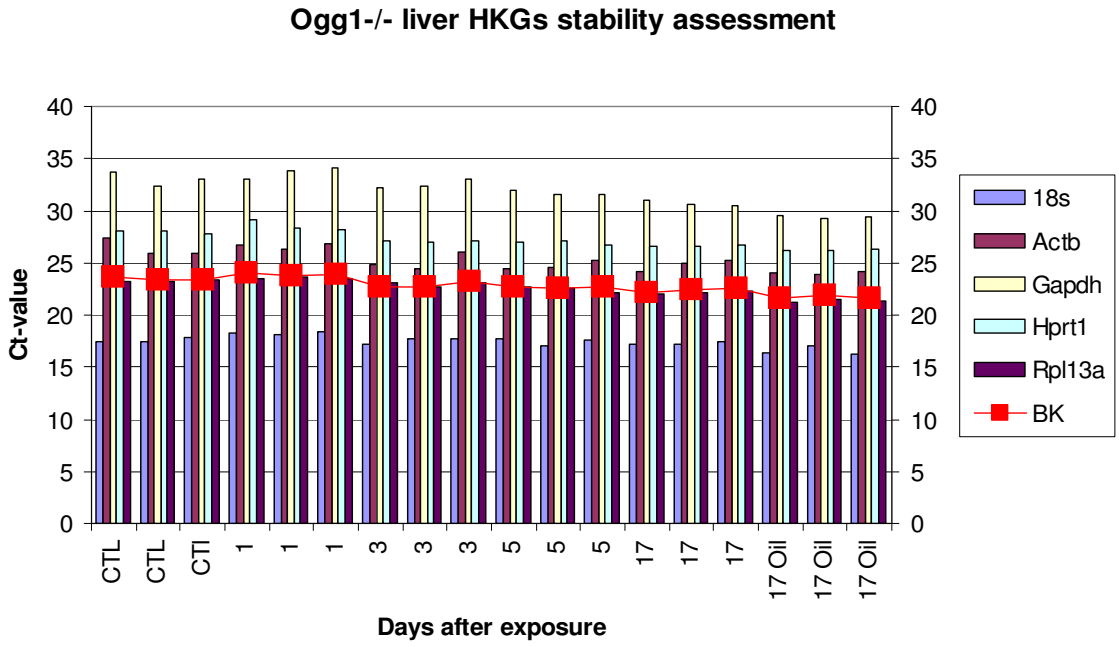

B)

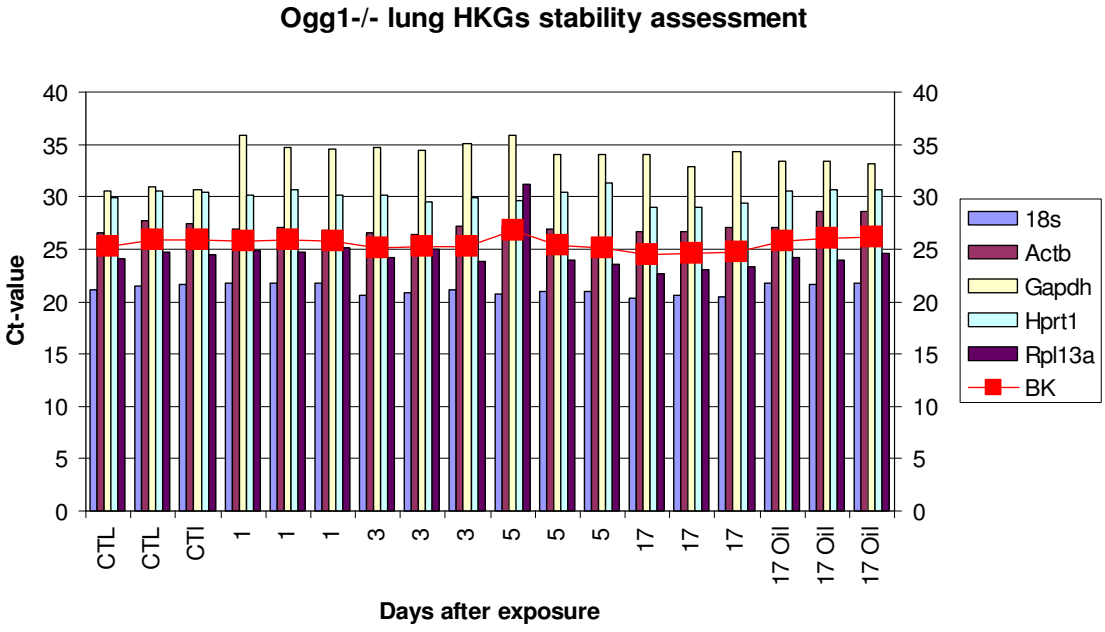

C)

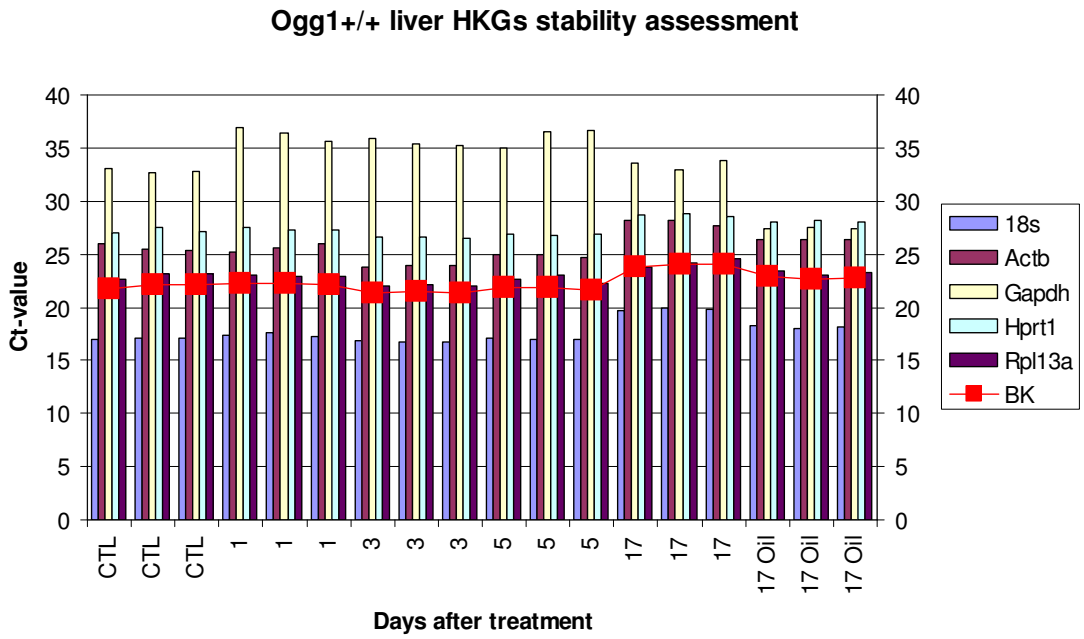
Ogg1+/+ liver HKGs stability assessment
Ct-value
Days after treatment
CTL
1
3
5
17
17 Oil
18s
Actb
Gapdh
Hprt1
Rpl13a
BK

D)

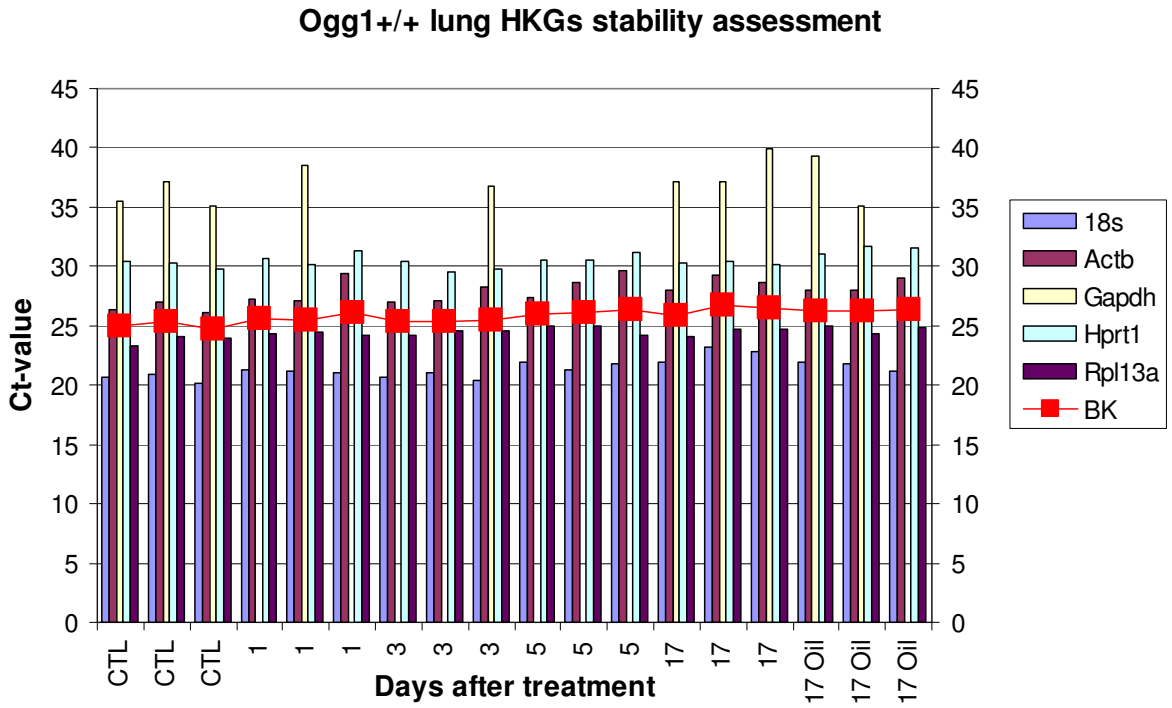
Ogg1+/+ lung HKGs stability assessment
Ct-value
Days after treatment
CTL
1
3
5
17
17 Oil
18s
Actb
Gapdh
Hprt1
Rpl13a
BK

E)

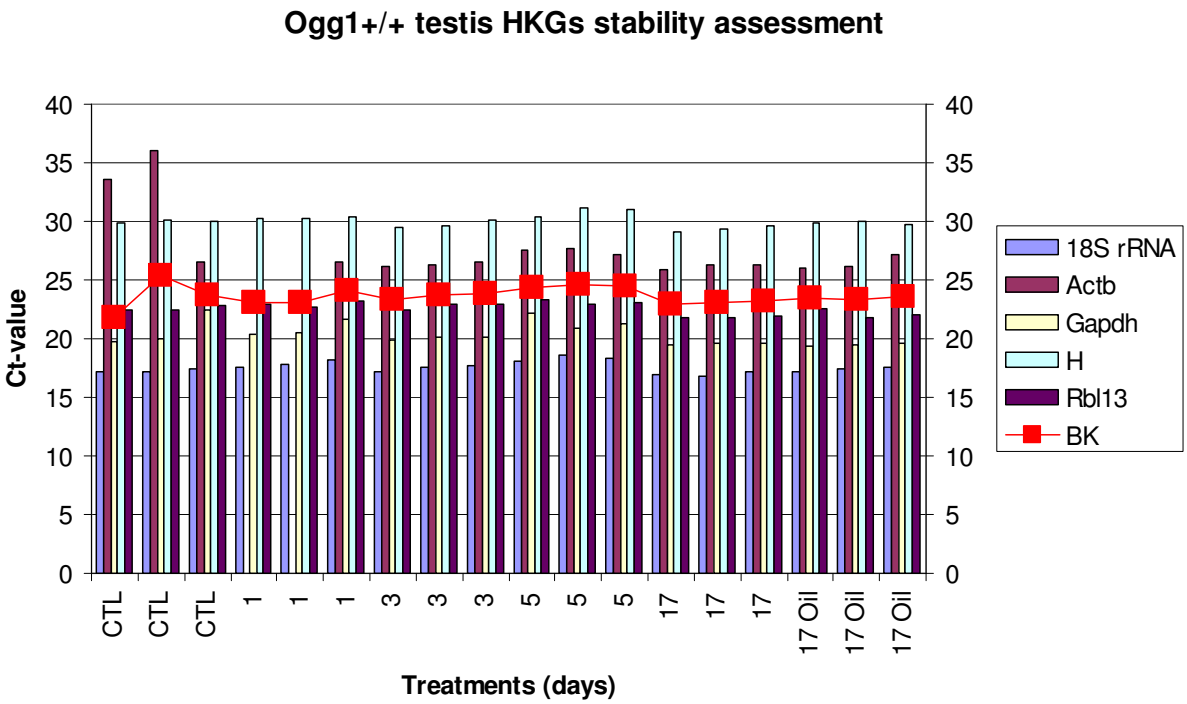
Ogg1+/+ testis HKGs stability assessment
Ct-value
40
35
30
25
20
15
10
5
0
CTL
CTL
CTL
1
1
1
3
3
3
5
5
5
17
17
17
17 Oil
17 Oil
17 Oil
Treatments (days)
18S rRNA
Actb
Gapdh
H
Rbl13
BK